

Modeling Soil Moisture Dynamics of Landscape Irrigation in Desert Cities

by

Thomas J. Volo

A Thesis Presented in Partial Fulfillment  
of the Requirements for the Degree  
Master of Science

Approved July 2013 by the  
Graduate Supervisory Committee:

Enrique R. Vivoni, Chair  
Zihua Wang  
Benjamin L. Ruddell

ARIZONA STATE UNIVERSITY

August 2013

## ABSTRACT

The history of outdoor water use in the Phoenix, Arizona metropolitan area has given rise to a general landscape aesthetic and pattern of residential irrigation that seem in discord with the natural desert environment. While xeric landscaping that incorporates native desert ecology has potential for reducing urban irrigation demand, there are societal and environmental factors that make mesic landscaping, including shade trees and grass lawns, a common choice for residential yards. In either case, there is potential for water savings through irrigation schedules based on fluxes affecting soil moisture in the active plant rooting zone.

In this thesis, a point-scale model of soil moisture dynamics was applied to two urban sites in the Phoenix area: one with xeric landscaping, and one with mesic. The model was calibrated to observed soil moisture data from irrigated and non-irrigated sensors, with local daily precipitation and potential evapotranspiration records as model forcing. Simulations were then conducted to investigate effects of irrigation scheduling, plant stress parameters, and precipitation variability on soil moisture dynamics, water balance partitioning, and plant water stress. Results indicated a substantial difference in soil water storage capacity at the two sites, which affected sensitivity to irrigation scenarios. Seasonal variation was critical in avoiding unproductive water losses at the xeric site, and allowed for small water savings at the mesic site by maintaining mild levels of plant stress.

The model was also used to determine minimum annual irrigation required to achieve specified levels of plant stress at each site using long-term meteorological records. While the xeric site showed greater potential for water savings, a bimodal

schedule consisting of low winter and summer irrigation was identified as a means to conserve water at both sites, with moderate levels of plant water stress. For lower stress levels, potential water savings were found by fixing irrigation depth and seasonally varying the irrigation interval, consistent with municipal recommendations in the Phoenix metropolitan area.

These results provide a deeper understanding of the ecohydrologic differences between the two types of landscape treatments, and can assist water and landscape managers in identifying opportunities for water savings in desert urban areas.

## ACKNOWLEDGMENTS

I would like to thank Dr. Enrique Vivoni for the opportunity to work on this research, and for his years of patience, guidance, and motivation as a truly inspiring advisor and educator. Thanks also go to my committee members Dr. Ben Ruddell and Dr. Zhihua Wang for providing their unique perspectives on this research and helping to guide me towards its completion. Funding is acknowledged from the National Science Foundation Grants EF1049251 “Assessing Decadal Climate Change Impacts on Urban Populations in the Southwestern United States” and BCS-1026865, DEB-0423704, and DEB-9714833 “Central Arizona-Phoenix Long-Term Ecological Research” (CAP-LTER). I would also like to acknowledge Dr. Chris Martin and Dr. Stevan Earl for their work at the North Desert Village study site, and thank them for their assistance obtaining and working with the soil moisture data therefrom. Finally, I would like to thank Dr. Vivoni’s entire hydrology research group, past and present, for all their assistance at various stages of this research, and for being part of a very positive learning and working environment.

# TABLE OF CONTENTS

	Page
LIST OF TABLES .....	vi
LIST OF FIGURES .....	viii
CHAPTER	
1 INTRODUCTION.....	1
1.1 Landscape Irrigation in Phoenix, Arizona: Background and Historical Context..	3
1.2 Landscape Irrigation in Phoenix, Arizona: Current State and Recent Research..	6
1.3 Research Motivation .....	15
2 METHODS .....	18
2.1 Soil Moisture Model.....	18
2.2 Study Area and Landscaping Treatments .....	23
2.3 Soil Moisture and Meteorological Data.....	26
2.4 Model Calibration and Testing .....	34
2.4.1 General Approach .....	34
2.4.2 Non-Irrigated Model Calibration.....	36
2.4.3 Irrigated Model Calibrations.....	38
2.5 Irrigation Simulations.....	40
2.6 Optimized Irrigation Schedules .....	41
3 RESULTS AND DISCUSSION .....	43
3.1 Model Calibration.....	43
3.1.1 Non-Irrigated Xeric Sensor.....	43
3.1.2 Irrigated Xeric Sensor .....	45

CHAPTER	Page
3.1.3 Irrigated Mesic Sensor .....	49
3.2 Irrigation Scenarios: Soil Moisture Dynamics and Water Balance Partitioning.... .....	51
3.3 Irrigation Scenarios: Plant Water Stress .....	58
3.4 Optimized Irrigation Schedules .....	62
3.4.1 Fixed Interval .....	64
3.4.2 Optimized Interval .....	67
4 CONCLUSIONS AND FUTURE WORK.....	76
REFERENCES .....	82
APPENDIX	
A NORTH DESERT VILLAGE IMAGES.....	86
B NORTH DESERT VILLAGE DATA .....	90
C PRECIPITATION AND POTENTIAL EVAPOTRANSPIRATION DATA .....	95
C.1 Arizona Meteorological Network .....	96
C.2 Phoenix Sky Harbor Airport.....	98
D GIS DATA .....	99
E SOIL MOISTURE BALANCE AND OPTIMIZATION SCRIPTS .....	101
E.1 Model Calibration and Testing.....	102
E.2 Idealized Irrigation Scenarios .....	106
E.3 Optimized Irrigation Schedules .....	107

## LIST OF TABLES

Table	Page
1. Table 1: Summary of precipitation at Phoenix Sky Harbor airport 1950-2010. ....	25
2. Table 2: Landscape and irrigation treatments of four neighborhoods at NDV. ....	26
3. Table 3: Summary of potential evapotranspiration data from the Queen Creek AZMET station, including years used for calibrations and simulations.....	32
4. Table 4: Summary of ten independent calibrations using data from the non-irrigated xeric sensor. ....	44
5. Table 5: Partial summarized results of initial 15 independent calibrations using data from the irrigated xeric site. Optimizations also included monthly depths of daily irrigation.....	46
6. Table 6: Summary of final 15 independent optimizations using data from the irrigated xeric sensor. ....	47
7. Table 7: Partial summarized results of initial 10 independent calibrations using data from the irrigated mesic site. Optimizations also included monthly depths of daily irrigation.....	50
8. Table 8: Summary of final 100 independent optimizations using data from the irrigated mesic sensor. ....	50
9. Table 9: Parameter values determined for the three model calibrations, with calibration range used for each. “+” indicates dependence on soil characteristics and applicability to all sites. “#” are dependent on soil and vegetation and applied only within one neighborhood (xeric or mesic).....	51

Table	Page
10. Table 10: Precipitation data for years depicted in Figure 17. Summer (April-September) is compared with winter (October-March) precipitation.....	62
11. Table 11: Intervals that minimize water use while maintaining an acceptable level of dynamic water stress for seasonally constant application. Results are from ten independent optimizations for each case with $q = 1$ and $k = 0.5$ . .....	69
12. Table 12: Conversion of recommendations from Water – Use It Wisely campaign (Figure 21) to annual totals. ....	72



## LIST OF FIGURES

Figure	Page
1. Figure 1: Conceptual schematic of modeled system. Solid lines show modeled interactions; dotted lines represent secondary interactions not directly considered.	19
2. Figure 2: Location of the NDV landscape experiment, with respect to: (a) the southwestern United States and the Sonoran Desert, and (b) the Phoenix metropolitan area. (c) Four instrumented neighborhoods at NDV. Images of the mesic (d) and xeric (e) sites.....	24
3. Figure 3: Installation of CS616 soil moisture sensor at xeric site.....	27
4. Figure 4: Image from the SSURGO database showing NDV as mohall loam (“Mv”). The boundary with Contine clay loam (Co) is north of the portions of NDV used for this study (compare with Figure 2c). .....	28
5. Figure 5: Unprocessed soil moisture data from the xeric site. ....	29
6. Figure 6: Unprocessed soil moisture data from the mesic site.....	29
7. Figure 7: Soil moisture observations from August 1, 2008 to August 1, 2009 for three sensors at NDV with precipitation and PET forcing from the Queen Creek AZMET station.....	33
8. Figure 8: Example of first-order set of calibration runs, showing convergence for only some of the estimated parameters.....	36
9. Figure 9: Irrigation input for four scenarios expressed as a percentage of the annual total for: (a) daily constant, (b) seasonal daily, (c) monthly constant pulses, and (d) monthly seasonal pulses. ....	41

Figure	Page
10. Figure 10: Time series and frequency diagram of modeled and observed relative soil moisture at the non-irrigated xeric site. Inset shows frequency distribution in which ordinate values represent frequency of $s$ within a bin interval of 0.02, relative to the total number of soil moisture values.....	45
11. Figure 11: Time series and frequency diagram of modeled and observed relative soil moisture at the irrigated xeric site. Inset shows frequency distribution with bin interval of 0.02. Water input reflects precipitation and calibrated irrigation.....	48
12. Figure 12: Time series and frequency diagram of modeled and observed relative soil moisture at the irrigated mesic site. Inset shows frequency distribution with bin interval of 0.02. Water input reflects precipitation and calibrated irrigation.....	52
13. Figure 13: Soil moisture frequency distributions for five-year simulations (January 2006-December 2010) for four irrigation scenarios at the irrigated xeric (a) and mesic (b) sites. Ordinate values represent frequency of $s$ with a bin interval of 0.02, relative to the total number of soil moisture data points. ....	53
14. Figure 14: Temporal average and standard deviation of relative soil moisture for varying total annual irrigation depths using calibrated model at xeric (a, c) and mesic (b, d) sites. Dotted vertical line indicates base input from calibrations.....	55

15. Figure 15: Water balance partitioning for varying annual irrigation at xeric (a, c, e, g) and mesic (b, d, f, h) sites.  $Q$  is runoff ( $s > 1$ ),  $L$  is leakage ( $s_{fc} < s \leq 1$ ),  $ET_u$  is unstressed evapotranspiration ( $s^* < s \leq s_{fc}$ ),  $ET_s$  is stressed evapotranspiration ( $s_w < s \leq s^*$ ), and  $E_b$  is bare soil evaporation below the wilting point ( $s \leq s_w$ ). Dotted vertical line indicates calibration input. .... 57
16. Figure 16: Plant water stress for xeric and mesic sites as the percentage of time with  $s_w < s \leq s^*$  (a, b), time-averaged dynamic water stress for  $q = 1$  and  $k = 0.5$  (c, d), and time-averaged dynamic water stress at different  $k$  and  $q$  for Scenario 2 (seasonal daily; e, f). Dotted vertical line indicated calibration irrigation. .... 59
17. Figure 17: Effects of inter- and intra-annual precipitation variability on dynamic water stress for varying irrigation input among years shown in Table 10 for Scenario 2,  $q = 1$ ,  $k = 0.5$  at xeric and mesic sites. (a, b) Varying annual total and constant seasonality. (c, d) Constant annual total and varying seasonality. .... 63
18. Figure 18: Minimized annual irrigation for several values of acceptable dynamic water stress at the xeric (a) and mesic (b) sites under Scenarios 1 and 2 (daily application,  $q = 1$ ,  $k = 0.5$ ). Schedules according to Scenario 2 (solid lines) and Scenario 1 (dashed lines) for  $\bar{\theta}_A = 0$  and 0.5 while minimizing annual input. Error bars show  $\pm$  one standard deviation from several independent optimizations for each case. .... 65

Figure	Page
19. Figure 19: Average minimized annual irrigation totals used to achieve various levels of acceptable dynamic water stress, using a constant and seasonally varying irrigation interval ( $q = 1, k = 0.5$ ). Error bars show $\pm$ one standard deviation from several independent optimizations for each case.....	69
20. Figure 20: Schedule of irrigation intervals that minimize water input for acceptable levels of dynamic water stress. Error bars show $\pm$ one standard deviation. ....	71
21. Figure 21: Landscape watering guidelines from the Water – Use It Wisely campaign website, referenced by several municipal websites in the Phoenix metropolitan area. ....	72
22. Figure 22: Results of sensitivity analysis on plant stress parameters $q$ and $k$ . Annual total (a and b) is determined by both event depth (c and d) and irrigation interval (not presented). ....	73
23. Figure 23: Annual water saved with seasonal irrigation compared to seasonally constant for the same plant stress parameters and level of dynamic water stress. Error bars show $\pm$ one standard deviation. ....	75

## 1 INTRODUCTION

As global populations continue to grow, securing an adequate water supply for municipal, agricultural, industrial, and environmental purposes is an increasing challenge requiring a robust portfolio of solutions at the national, regional, local, and individual levels. While municipal water accounts for a relatively small portion of total water withdrawals (approximately 13% worldwide, Coates *et al.*, 2012), there are many simple yet effective low- or no-cost opportunities for everyday water savings among urban populations, including proper maintenance of water lines and fixtures, reuse of washwater for landscaping purposes, and turning off faucets when not in immediate use. Such promotion of everyday water consciousness has the potential to engender a sense of responsibility and stewardship among future generations of the urban populace, which may help shape policy in coming decades towards enhanced water security.

While there are many worthwhile opportunities for water conservation inside the home, a greater portion of residential water in many United States homes is consumed outdoors (Mayer and DeOreo, 1999), much of which is used for landscape irrigation. Native and exotic tree, shrub, and grass species in urban areas provide a variety of services, including recreation, a sense of space, and wildlife habitat (Sadler *et al.*, 2010), but are often highly dependent on water input beyond precipitation and local groundwater stores (Martin and Stabler, 2002). In desert cities, the value of these benefits, when considered against the potentially high economic and environmental costs of large supply-side infrastructure projects, creates an incentive for demand management. For example, with water supply largely fixed by the Colorado River Compact of 1922, Las

Vegas, Nevada has enacted ordinances to restrict and reduce water use for maintaining commercial and residential landscaping, including the promotion of low water-use desert (“xeric”) landscaping over high water-use turf grass lawns (“mesic” landscaping). In Phoenix, Arizona, however, the growth of the city has been characterized and even fueled by indulgent water use, especially outdoors. Success in acquiring abundant water supplies allowed the metropolis to grow rapidly throughout the twentieth century, which only led to higher water demand, and eventually a need to further increase supplies. The demand has been met by an “acquisitive” water policy of increasingly large supply-side infrastructure development along the Salt, Verde, and distant Colorado Rivers, as well as by groundwater pumping, rather than through a more sustainable realization of the natural restrictions the region imposes on growth (Hirt, Gustafson, and Larson, 2008). This long-standing culture of unrestricted water use, cultivated by a century of relatively abundant water despite desert conditions, may hamper the feasibility and effectiveness of initiatives designed to limit residential outdoor water use. However, there is evidence that a top-down shift in landscape design and maintenance can result in decreased water demand, especially if water application schedules are derived from a quantitative understanding of plant water needs within the context of local soil and climate conditions. This study examines irrigation of both xeric and mesic urban landscapes in such an ecohydrological context and, rather than arguing for the relative value of one over the other, investigates the effects of irrigation scheduling at both to draw conclusions about how to irrigate each better.

## **1.1 Landscape Irrigation in Phoenix, Arizona: Background and Historical Context**

Located in the American Southwest in an inland portion of the Sonoran Desert, the Phoenix area saw its first United States settlers arrive in the 1860's, though the beginnings of the irrigation network for the primarily agricultural early settlements were already established by previous cultures. The native Hohokam community flourished for centuries along the Salt River, surviving on water from higher land to the east and northeast. The civilization declined in the 14<sup>th</sup> century, but left over 300 km (180 mi) of large canals, up to 10 m across and 3 m deep, plus hundreds of kilometers more in smaller irrigation ditches (Martin, 2008). Many of the large canals currently supplying water to the greater Phoenix metropolitan area run through these same channels used by the Hohokam. Beginning in 1868 with what remained of the Hohokam system, settlers created private companies to build irrigation ditches, supporting a rapidly growing agricultural population, and the nascent town of Phoenix (Logan, 2006).

However, the growth and prosperity in the region were threatened by both drought conditions and floods in the 1890's. In Phoenix, the response was to buffer irrigation supplies against drought by building a system of dams and reservoirs along the Salt River, with assistance from the 1902 National Reclamation Act. In 1912, Roosevelt Dam was completed, securing Phoenix's water supply for decades through the Salt River Valley Water Users' Association ("SRP: Canal origins", 2013). For comparison, nearby Tucson, which did not have the extensive Hohokam network to build from and received flows from the much smaller Santa Cruz River, relied more heavily on groundwater pumping to supplement surface water flows and develop an agricultural base. In times of

drought, Tucson was faced with restrictions on water use and a need for increased pumping, while the canal system in Phoenix kept the city in relative water abundance. This resulted in quadrupled agricultural production in Phoenix from 1890 to 1920 while Tucson's production remained fairly constant (Logan, 2006).

While there were many reasons that Phoenix quickly outgrew Tucson in the early 20<sup>th</sup> century, the superior water supply and related agricultural dominance were necessary components. Tourism grew in the area, punctuated by the opening of the Arizona Biltmore in 1929, designed by a student of Frank Lloyd Wright, and attracting investors among industrial elites from the East Coast and Midwest. Phoenix was marketed as a "winter playground" of golf courses and swimming pools, as the Valley Beautiful Committee launched a national ad campaign entitled "Let's Do Away with the Desert". Residents were encouraged to plant non-native trees, shrubs, and grasses, relegating the desert to areas beyond their immediate locale. Phoenix earned a reputation as a desert oasis, quenched by the dammed waters of the Salt and Verde Rivers.

Growth accelerated mid-century as major corporations ( notably Goodyear and Motorola) built facilities in the Phoenix metropolitan area during and after World War II. The population quadrupled from 1950 to 1960, with Maryvale, Deer Valley, Glendale, and other newly built areas consisting almost entirely of single-family homes with residents escaping densely developed and much colder cities on the coasts and in the mid-west (Logan, 2006). Consistent with the paradigm established by the Valley Beautiful Committee, the new homes were built with landscape designs that emulated the aesthetic of the eastern United States (Walker *et al.*, 2009). Water was supplied by additional infrastructure projects along the Verde River, and provided through irrigation ditches to



the new subdivisions built on converted farmland. Lawn irrigation was thus provided in “flood-style” pulses directly from the Salt River Project, as opposed to standard residential water lines. Yards included turf grass and shade trees, replacing the native desert landscape of trees and bushes adapted to low-water environments among predominantly bare soil. While the shift was certainly driven both by a desire for environs familiar to eastern transplants, and by the propagation of the oasis ethos established by the high society visitors of the previous decades, there were practical reasons for the foreign mesic landscaping as well. In a time before air conditioning, the cooling and shading effects of turf grass and large, broad-leaved trees were essential to making the desert heat of the region habitable. After all, those purchasing land were no longer merely coming to visit and escape winter freezes elsewhere, but now were younger families coming to work for new businesses year-round.

Fortunately, the advent of air conditioning in the 1960’s reduced the need for mesic yards, as Phoenix locals were able to drive air-conditioned cars from their air-conditioned homes to air-conditioned jobs, shopping malls, restaurants, and recreational facilities. However, a sustained conservation movement for xeriscaped yards that reflected the native desert landscape would not occur until the 1990’s, and so residential outdoor water use continued to rise in the Phoenix area, supplied in part by additional groundwater pumping. The Groundwater Management Act (GMA) of 1980 attempted to resolve legal disputes among farmers, Native Americans, and other water users, while also establishing programs to reduce overpumping, requiring municipalities to gradually reduce per capita consumption, and supporting completion of the Central Arizona Project (CAP), a 530 km (330 mile) canal to bring water from the Colorado

River to Phoenix and Tucson (Jacobs and Holway, 2004). While the overall effectiveness, environmental costs, and long-term sustainability of the GMA may be debated (see the response to Jacobs and Holway, 2004 in Hirt, Gustafson, and Larson, 2008), the additional water brought by CAP and the regulatory framework established by the GMA allowed continued population and economic growth in the area (for better or worse) without requiring real water use restrictions on Phoenix area residents.

## **1.2 Landscape Irrigation in Phoenix, Arizona: Current State and Recent Research**

Now with over 4 million residents in the metropolitan area that includes Phoenix, Tempe, Scottsdale, Mesa, Chandler, Gilbert, and the surrounding municipalities (Phoenix-Mesa-Glendale Metropolitan Statistical Area; U.S. Census Bureau, 2010), this region of the Sonoran Desert has clearly overcome challenges of local water supply. In terms of residential outdoor water use, however, the history of water supply in the Phoenix area has resulted in a general landscape that surprises many visitors and newcomers. Whereas 80 years ago, domestic immigrants were told to “Do away with the desert,” many are now left wondering “What happened to the desert?”. Drought conditions and water supply issues have resulted in shortages and restrictions even in water-rich portions of the country, while an area with far less precipitation and no large bodies of water sits in an apparent glut of sprinkler systems, fountains, and open-hose car washes. Even in nearby Tucson, restrictions on watering lawns date back as far as 1903 (Logan, 2006). Phoenix, however, seems to pride itself on its lack of any restrictions, as stated on its website:

Long-range planning, investments in water supply alternatives, and a history of successes in water conservation have allowed the city of Phoenix to weather this drought without resorting to mandatory water use restrictions or prohibitions. However, the city is prepared to establish such restrictions in future years if necessary (“Drought in Perspective,” 2013, para. 2).

Indeed, a century of long-term investments made in Phoenix’s water supply afford its citizens the luxury of not having to worry about water security, removing one potential impetus for water conservation through reduced landscape irrigation, in yards of both mesic and xeric design.

Nonetheless, conservation efforts in Phoenix have been reported as having successfully reduced per capita water use by 15% from 1980 to 2005, though residential outdoor water use in Phoenix far surpasses per capita volumes in other cities, with 60-75% used for landscapes and swimming pools (Balling and Gober, 2007). This represents an opportunity to reduce water demand through improved planning and management, thereby contributing to overall water security while developing a culture of responsible use and environmental stewardship, as opposed to one of misplaced excess.

Residential outdoor water use is obviously tied very closely with choices in landscape design, so in order to effectively manage demand, the benefits and drawbacks of different landscape designs, both real and perceived, must also be understood. A series of publications have studied landscape choices in the Phoenix metropolitan area, primarily by quantitative surveys and qualitative interviews of inhabitants of single-family homes. Distinctions are made between “xeric” yards that contain low water-use plants and gravel or bare soil, “mesic” yards that contain high water-use turf grass and

shade trees, and “oasis” yards that contain turf grass as islands among an otherwise dry, native landscape.

Yabiku *et al.* (2008) showed that while residents find xeriscaped yards aesthetically pleasing, they preferred mesic yards for their own homes. Women were less inclined towards desert landscapes, and those with young children had a larger tendency towards turf grass than those without. While the authors were unable to determine any reason for the gender difference, they cited safety concerns in play areas as a reason for the preference towards turf grass for homes with young children. It was also determined that a high level of environmental concern led to a preference for oasis landscapes, but not necessarily for xeric. Supported by other findings, this may suggest that residents find oasis treatments as a compromise between a personal preference for turf grass and environmental concerns that would favor a xeric landscape.

Larson *et al.* (2009) found similar results from a more qualitative study that included quotes from respondents regarding their preferences in landscape design. They found that long-standing cultural norms support landscapes with grass lawns. Respondents cited concern for cleanliness and safety as reasons to avoid xeric landscapes, while they found mesiscaping to be calming, cooling, and comfortable, evoking nostalgic positive feelings from their childhood, wherever that may have taken place. Xeriscaping, on the other hand, did prove valuable to residents in terms of ease of maintenance and as an appropriate design for the local climate and surrounding landscape. However, the authors take note of a dichotomous view of the desert and our place in it. Some respondents felt that xeriscaped yards felt as though we were encroaching on the desert, putting homes out in nature where they should not be; they

enjoyed and appreciated the desert, as long as they did not have to live in it. Interestingly, those that grew up in the Arizona desert region were more likely to have negative feelings towards xeriscaping. This is contrary to the common conception that preferences for mesic lawns are being imported from less arid parts of the country. Instead, this could show the legacy of the “Do away with the desert” mentality, deeply engrained in the cultural memory of the region. Respondents stated that homogeneous desert scenery is boring and, as they have lived here for so long, they can “get sick of it”. There is an attitude of “stewarding” nature by taming it through green landscapes at the home, and leaving the “real” desert out away from the home “where it belongs”.

Larsen and Harlan (2005) add an extra dimension to the discussion by looking at differences between front and back yards, and considered both landscape preference and landscape behavior (i.e. what residents would want in their yards and what they actually have). They found that income was the only significant predictor of front-yard landscaping behavior among four independent variables: income, length of residence in the Phoenix area, degree of environmental concern, and engagement in desert recreational activities. Low income residents preferred lawns, middle income preferred desert landscaping, while high income preferred a mix of desert and oasis landscapes. The authors suggest that if, as social class theory suggests, lower classes take preference cues from their perceptions of upper classes (a top-down perspective), the lower income class may be riding out the legacy of indulgent landscaping in the upper class that has since been curbed to merely oasis-style landscaping due to environmental concerns of the past few decades. This may prove beneficial to water conservation efforts in the future if lower classes do indeed follow higher income households to less turf lawns in the near

future. Income, however, was not a significant predictor in back yards. Front yard design was largely tied to both developer legacy and personal preference, while back yard design was related only to preference. They suggest that the front yard is the visible expression of the self, and so is closely tied to class association, in the same manner as type of home. The back yard, on the other hand, is a “personal pleasure ground” for recreational activity and “happy family events” despite the desert heat.

Martin, Peterson, and Stabler (2003) supported the idea of a top-down shift (here, from larger organizations to individuals) in landscape design by comparing residential landscaping between homes that were bound by the covenants, codes, and restrictions (CC&Rs) of community associations, and those that were not. They found that those with CC&Rs had fewer trees, more shrubs, less turf lawn, and were more likely to be identified as “desert” landscaping by homeowners. According to the authors, this suggests that the shift towards xeriscaping “is predominately a top-down social phenomenon directed by public and private interest groups” (p. 9). Other findings supported those described above, with 70% of homeowners preferring a yard with at least some lawn area (mesic or oasis style), and more Arizona natives than domestic immigrants preferring mesic landscapes. Ease of maintenance and aesthetics were cited as the primary drivers of personal preference. Homeowners who did prefer desert settings cited environmental concerns and a sense of desert place as their primary drivers for that preference.

Collectively, the findings of these studies suggest that the ethos embodied by the Valley Beautiful Committee may have a lasting legacy that still affects landscape preferences, and thus residential outdoor water use, today. If preferences do follow a top-

down pattern, and the promotion of green spaces decades ago still has a lasting effect, then it may be possible to shift those preferences through social and policy initiatives that support desert landscaping. To be successful, however, such programs would likely need to promote the desert as beautiful and fashionable, with little required maintenance, rather than simply focusing on water conservation (Larson *et al.*, 2009). Notwithstanding, if the attitude of keeping the desert at bay for reasons of safety and comfort is entrenched even deeper in the collective preferences of the citizenry than the mid-20<sup>th</sup> century movement towards green, single-family suburban homes, the best planned social programs may still gain little traction. There does seem to be hope though, in the higher preference rates for xeriscaping among domestic immigrants: there certainly is an appreciation for desert settings that may prove beneficial for residential outdoor water use rates in the future.

In the meantime, there are clearly long-standing historical, cultural, and personal reasons for the abundance of mesic yards found in the Phoenix area. It is thus insufficient to merely promote xeric yards, since water savings may also be achieved by improving irrigation in mesic yards for those who will nonetheless choose such landscaping for their homes. In addition, those with xeric yards will want to ensure that they are reaping the benefits in water savings afforded by their landscape design choice. After all, there is a large step between landscape preference, or even landscape choice, and actual water savings. Another set of studies examines actual water use rates around the Phoenix area, comparing them to various natural and social factors to determine the drivers of residential water use.

Balling and Gober (2007) found “clear evidence that water use is related to variations in weather and climate” (p. 1134), specifically controlled by the overall state of

drought, autumn temperatures, and summer-monsoon precipitation, though the relationship was so small as to be of limited consequence. By comparing annual per capita water use rates with meteorological records over several decades, they found that a 1% increase in evapotranspiration rates resulted in a 0.464% increase in residential water use, and a 1% increase in summer precipitation resulted in a 0.001% drop in water use. These relationships were statistically significant, and in the directions expected, but were much smaller than the authors anticipated, being dwarfed by changes in water use due to other causes. In a city where at least two-thirds of residential water use is outdoors for landscape irrigation and swimming pools, they expected that inter-annual climate fluctuations would have a larger impact on water use rates. They cite Phoenix's distant water supply as a cause for the small fluctuations in water demand:

Phoenix is so chronically short of precipitation that even sizable variation in local climatic conditions has a small effect on local water demand patterns because local demand is met by hydroclimate conditions in faraway places (e.g. the upper reaches of the Colorado River Basin). (Balling and Gober, 2007, p. 1130)

A similar study by Balling, Gober, and Jones (2008) examined water use rates by census tract to determine relationships between water use, climate, and such factors as lot size, swimming pool frequency, income, and proportion of irrigated mesic landscaping. Among their results, they found greater sensitivity to climate in parts of the city that had many pools or a high proportion of irrigated mesic landscaping. These results suggest the importance of what homeowners and landscape managers perceive or believe a landscape's water needs to be. Consider, for example, automatic sensors that add water to swimming pools to maintain a specified water level as water is lost to evaporation. These fairly common devices directly link evapotranspiration and precipitation rates to what is



for many homes the single greatest use of residential water, without any human interaction or consciousness of loss rates. A person who manually fills their pool may be more conscious of how much water is lost, and thereby more conscious of the true costs of pool ownership. The more conscious pool owner may then be more careful to avoid additional water losses through over-topping and carry-out during pool use. For landscape irrigation, the analogue would be automatic soil moisture sensors, but, while some are rather inexpensive, they are nevertheless rare for home use. Instead, changes in irrigation due to climate and weather fluctuations, like changes in pool input without a sensing device, are more likely the result of conscious decisions of homeowners to adjust irrigation system schedules in response to short-term differences in weather patterns. Unlike pools, however, it can be difficult for the average homeowner to determine how much water is necessary to maintain a certain status. Thus, as mentioned by Balling, Gober, and Jones (2007), the critical issue becomes the homeowner's perception of the landscape's needs and their ability to respond to that perception with appropriate adjustments to their water practices.

These perceptions can be very different than the actual need, and homeowners intent on maintaining and enjoying their investments are likely to err on the side of liberal water use. In xeric yards, Martin (2001) found that potential water savings from low water-use landscape design were often not realized due to similar misunderstandings of actual water needs of desert-adapted plants. Furthermore, residents with automated drip irrigation systems generally did not adjust their water applications in response to seasonal changes in evapotranspiration. This echoes the previous authors, who name irrigation systems that deliver water irrespective of temperature and precipitation conditions,

swimming pools, water features such as waterfalls and fountains, and low water prices as reasons for the relative insensitivity (i.e., less than expected) of urban water use to variations in climate conditions.

There thus appears to be an opportunity for water savings by informing homeowners of climate-dependent, seasonally varying rates of irrigation appropriate for their landscape design, such as those sought in this study. Indeed, Campbell *et al.* (2004) found that the addition of communication to engineering solutions can negate offsetting behavior. In other words, demand-side innovation, policy, or decision (such as installing low water-use xeriscaped yards) may develop a complacency that counteracts the goals of conservation, but this effect can be decreased with the dissemination of appropriate information concerning the conservation effort. Thus homeowners installing xeric landscapes should be adequately informed of the differences between xeric and mesic yards in terms of water requirements and optimal irrigation scheduling, which again is the focus of this study.

Martin (2008) gives several suggestions for sustainable landscape ecology for cities in the Sonoran Desert. These include the use of evapotranspiration- or soil moisture-based sensors for residential irrigation; a combination of water savings with ecosystem services in the form of more oasis-style landscaping; improved pruning practices to limit plant growth and biomass production, optimize water use, and maintain healthy soils; and the re-use of green waste on site, including composting, and harvesting biomass from residential landscapes for use as mulch. Many of these initiatives are mirrored by the city of Phoenix at their water services website, [phoenix.gov/waterservices](http://phoenix.gov/waterservices). The site also includes plans for landscaping and home

remodeling, tips on pool and sprinkler maintenance, and information on how to save water and energy with the use of patios, mulching, and shade trees as part of a landscape that combines design features native to the surrounding desert while taking into account personal preferences for a comfortable, safe, affordable home. The site also provides a link to the Water – Use it Wisely campaign ([wateruseitwisely.com](http://wateruseitwisely.com)), which has gained national recognition and cooperation in its quest to inform people of how to save water in a variety of ways both inside and outside the home. Features include a guide to xeriscaping that highlights the attractive qualities of the design style in addition to its water- and cost-saving advantages, and its natural place in the surrounding ecosystem. Guides on landscape watering and plant selection are also available, as well as step-by-step how-to guides on water system installation, xeriscaped design, and irrigation scheduling. Other cities in the Phoenix metropolitan area (e.g. Scottsdale, Chandler, and Gilbert) have similar resources for homeowners on their websites with recommendations for irrigating various types of yard landscapes, though the methods used for determining the prescribed values are not immediately clear. In this study, these irrigation recommendations are compared to schedules determined using a calibrated, quantitative model of ecohydrological fluxes, in order to evaluate their performance in relation to modeled plant water requirements based on rates of potential evapotranspiration.

### **1.3 Research Motivation**

The Phoenix, Arizona metropolitan area is clearly an example of a highly engineered urban water supply, with irrigation playing a substantial role on plant conditions. However, there is still a great need for a better understanding of the fate of

water used to maintain urban landscapes such as these (Pataki *et al.*, 2011). Also, the current demand for improved urban climate modeling (Grimmond *et al.*, 2010) is dependent upon the coupled relationship between water and energy balances, and thus the importance of quantifying urban water fluxes is further magnified. For example, assessing the potential for water-sensitive urban design elements to mitigate the environmental impacts of urban development on microclimates requires reliable evapotranspiration models (Mitchell *et al.*, 2010). Furthermore, while current ecohydrology literature is replete with physically-based models, it is comparatively lacking in studies that couple empirical approaches with modeling efforts, and those that include manipulative experimental design, where variables are controlled rather than just observed (King and Caylor, 2011). In response, this work is aimed at providing a more complete understanding of the water budget of landscaping treatments through the use of a set of modeling scenarios based upon deliberately designed xeric and mesic landscapes in a desert urban environment.

Plant-available soil moisture is clearly a major driver for the viability of desert urban landscapes, particularly for high water-use non-native plants (McCarthy and Pataki, 2010). However, as described above, irrigation schedules rarely respond to actual soil moisture levels, and irrigation is thus frequently in excess of plant demand. There is therefore potential for substantial water conservation through landscape irrigation with water budgets based on plant demands and the effects that rates of potential evapotranspiration have on soil moisture (White *et al.*, 2004). Additionally, though desert landscaping has the potential to reduce water use, mesic landscaping has been shown to reduce the urban heat island effect in Phoenix (Chow and Brazel, 2012). As a result,

choices in landscape designs can have environmental, economic, and social impacts (Grimm *et al.*, 2008), which underscore the need to understand the hydrological differences among design modes.

In this study, I apply a quantitative, physically-based model of soil moisture dynamics that includes variations in potential evapotranspiration to experimental sites in Mesa, Arizona that include irrigation of both mesic and xeric urban landscapes. After calibrating the model to observed soil moisture data, I analyze a series of idealized irrigation schedules in terms of relative soil moisture, water balance partitioning, and plant water stress. I also investigate the effects of inter- and intra-annual variability in precipitation on plant stress under irrigated conditions. I then utilize an automated optimization routine to determine irrigation schedules that minimize water input at each site, while maintaining prescribed levels of allowable plant water stress, considering the long-term climatology of the Phoenix metropolitan area. Results are compared to irrigation recommendations available from local municipalities to identify opportunities for water savings offered by alternative irrigation scheduling through a quantitative model based on experimental data. The goal is not to assess the hydrological (or other) benefit of one landscape design over the other (xeric or mesic), but instead, recognizing the historical and environmental reasons for each, to conduct a side-by-side analysis of the two to see what the differences between the two can teach about how to irrigate them both with less water input. The results are intended to assist homeowners and landscape managers to conserve water while providing adequate irrigation for urban landscapes in desert areas.

## 2 METHODS

In order to study urban landscape irrigation, a quantitative model of soil moisture dynamics was calibrated to soil moisture data from an experimental site that included irrigated xeric and mesic landscapes, with data from nearby meteorological stations as model forcing. This chapter discusses the model, site, data, and method of calibration, then describes a series of simulations conducted to first test the effects of irrigation scheduling on water balance partitioning and plant water stress, then determine schedules that minimize water input for a given value of plant water stress.

### **2.1 Soil Moisture Model**

As illustrated in Figure 1, the conceptual model used is centered on interactions affecting the soil water balance. Soil and vegetative characteristics control the impact of meteorological forcing on water fluxes, then factor into the determination of plant water stress from the resultant soil moisture values. Irrigation is modeled as an additional forcing element, independent of, but supplemental to, precipitation input. Soil moisture dynamics are simulated mathematically, based on a point-scale model proposed by Laio *et al.* (2001b), but including an additional term to account for anthropogenic water input. Furthermore, historical precipitation data are used to test the model against soil moisture observations, as opposed to the stochastic rainfall input included by the model's original authors to facilitate their probabilistic approach.

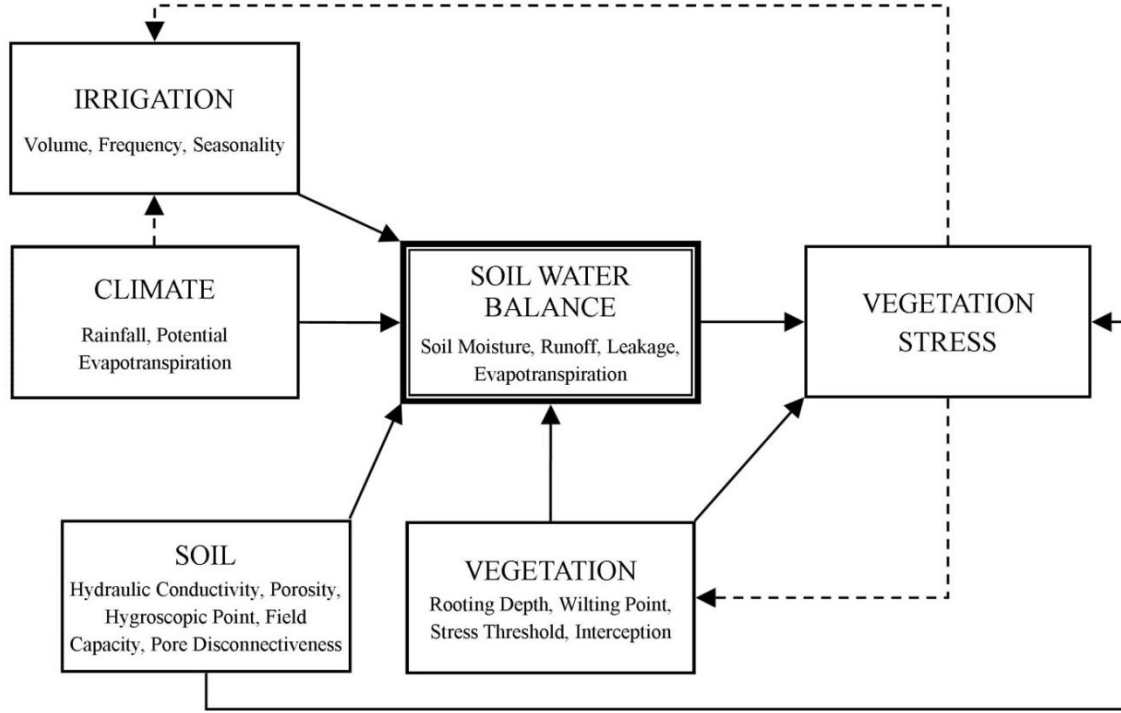


**Figure 1:** Conceptual schematic of modeled system. Solid lines show modeled interactions; dotted lines represent secondary interactions not directly considered.

In the following equation, the change in time of relative soil moisture  $s$  (0 for perfectly dry soil and 1 at saturation) is expressed as the result of applicable water fluxes, averaged over a rooting depth  $Z_r$  [L]:

$$nZ_r \frac{ds}{dt} = P + I - Q(s) - L(s) - ET(s), \quad (1)$$

with soil porosity  $n$  [ $L^3_{\text{voids}} / L^3_{\text{total}}$ ], precipitation  $P$ , irrigation  $I$ , evapotranspiration  $ET$ , leakage  $L$ , and runoff  $Q$  (all [ $L T^{-1}$ ]). Relative soil moisture  $s$  is defined as the fraction of porosity  $n$  that is occupied by the volumetric soil moisture  $\theta$  [ $L^3_{\text{water}} / L^3_{\text{total}}$ ]:

$$s = \frac{\theta}{n}. \quad (2)$$

A numerical approach is applied, discretizing the above differential equation at a daily time scale. For each time step, water inputs ( $P + I$ ) are added to the soil moisture value from the previous time step, resulting in an intermediate  $s$  value used for the determination of the loss function, partitioned into  $Q$ ,  $L$ , and  $ET$ . The daily time scale was chosen to match available data for potential evapotranspiration. While many hydrological processes, such as irrigation and precipitation, often occur at sub-daily time scales, to model them as such would require a loss function of similar resolution, perhaps based on actual, rather than potential, evapotranspiration. Such an analysis could investigate the effects of variations in time of day of water input (both precipitation and irrigation), but is beyond the scope of the current work.

Runoff  $Q$  is modeled as being generated through a saturation excess mechanism when the application of water inputs ( $P + I$ ) results in values of  $s$  greater than 1. In these cases, runoff is calculated as  $nZ_r(s - 1)$ , thereby returning  $s$  to the level of saturation for subsequent calculations of  $ET$  and  $L$ . While Manfreda *et al.* (2010) investigated the impact of including infiltration excess runoff, preliminary results indicated that soil hydraulic conductivity in this study was sufficiently high to allow for the exclusion of such effects without significant change to modeled soil moisture, water balance partitioning, or plant water stress.

Leakage, or deep infiltration beyond the active rooting zone, is assumed to only occur when relative soil moisture  $s$  surpasses the field capacity of the soil  $s_{fc}$ . The leakage rate  $L$  is modeled as a fraction of the saturated hydraulic conductivity  $K_s$  [ $L T^{-1}$ ], and is a function of  $s$ , dependent on only soil (i.e. not vegetative) parameters:



$$L(s) = K_s \frac{e^{\beta(s-s_{fc})} - 1}{e^{\beta(1-s_{fc})} - 1}, \quad (3)$$

where  $\beta = 2b + 4$  and  $b$  [-] is the pore size distribution index. Thus the hydraulic conductivity decays exponentially from a maximum ( $K_s$ ) at the saturated value when  $s = 1$ , to zero when  $s = s_{fc}$ .

Evapotranspiration is treated as a multi-stage function of relative soil moisture, with boundaries between behaviors delineated by threshold values determined by soil and vegetation properties:

$$ET(s) = \begin{cases} 0 & s \leq s_h \\ \frac{s - s_h}{s_w - s_h} E_w & s_h \leq s \leq s_w \\ E_w + \frac{s - s_w}{s^* - s_w} (ET_{max} - E_w) & s_w \leq s \leq s^* \\ ET_{max} & s \geq s^* \end{cases} \quad (4)$$

The hygroscopic point  $s_h$  and field capacity  $s_{fc}$  are related to matric potentials through a soil's water retention curve and are dependent only on soil characteristics (Clapp and Hornberger, 1978).  $E_w$ , the rate of evaporation from bare soil below the wilting point is similarly dependent only on soil characteristics, though the wilting point  $s_w$  and stress threshold  $s^*$  are additionally dependent on vegetation (Laio *et al.*, 2001b). Potential evapotranspiration (PET) as determined by the Penman-Monteith equation is used as the maximum rate of evapotranspiration  $ET_{max}$ . However, to more accurately reflect soil moisture dynamics, daily meteorological records are used, as opposed to the temporally invariant or seasonal estimates used by Caylor *et al.* (2005), Laio *et al.* (2002), and other studies. The calculation of the daily PET values used is discussed by Brown (2005), and

includes several factors that drive plant transpiration, including vapor pressure deficit, net radiation, mean daily air temperature, and mean daily wind speed.

Plant water stress  $\zeta(s)$  is calculated in relation to  $s^*$ , at which stomatal closure is induced ( $\zeta = 0$ ), and the wilting point  $s_w$ , at which transpiration ceases ( $\zeta = 1$ ).

$$\zeta(s) = \left( \frac{s^* - s}{s^* - s_w} \right)^q. \quad (5)$$

In this static water stress function proposed by Porporato *et al.* (2001),  $q$  represents the ability of a plant to withstand low levels of water stress with minimal physiological response while reserving more drastic and potentially inelastic response for periods of greater water stress (Rodriguez-Iturbe and Porporato, 2004). The mean dynamic water stress  $\bar{\theta}$  totaled over a growing season  $T_{seas}$  is used to quantify the effects of prolonged exposure to moisture conditions below the stress threshold:

$$\bar{\theta} = \begin{cases} \left( \frac{\bar{\zeta}' \bar{T}_{s^*}}{k T_{seas}} \right)^{1/\sqrt{\bar{n}_{s^*}}} & \text{if } \bar{\zeta}' \bar{T}_{s^*} < k T_{seas}, \\ 1 & \text{otherwise.} \end{cases} \quad (6)$$

Here,  $\bar{n}_{s^*}$  is the average number of periods in a growing season with  $s < s^*$ , and  $\bar{T}_{s^*}$  and  $\bar{\zeta}'$  are, respectively, the average duration and intensity of these periods.  $k$  represents the ability of a plant to withstand prolonged water stress; it can be seen as the maximum average  $\zeta$  value a plant can endure for an entire growing season without permanent damage. Due to the year-round warm temperatures of the region, a growing season of 1 year was assumed in this study. While plant water stress is quantified based on the soil moisture time series, it does not impact either irrigation or vegetation, as shown by the dashed lines in Figure 1. Plant growth dynamics, including seasonally varying vegetation

parameters and growth cycles, plant mortality, and increased water uptake due to increased biomass, are not modeled.

## **2.2 Study Area and Landscaping Treatments**

The North Desert Village landscape experiment (NDV) is located on the Arizona State University Polytechnic Campus in Mesa, Arizona (33.31° N, 111.68° W, elevation 406 m). The campus lies near the eastern edge of the greater Phoenix metropolitan area, at the intersection of urban, agricultural, and natural desert land cover types (Figure 2a-c). Average daily maximum temperatures in the area range from 19° C (66° F) in December to 42° C (104° F) in July, with an average 175 days per year above 32° C (90° F), occasionally surpassing 46° C (115° F) in the summer months. As summarized in Table 1, rainfall averages ~200 mm annually, arriving predominantly by winter storms (December-March, 45% of total annual rainfall) and late summer monsoon and thunderstorm activity (July-September, 30%), with little to no precipitation in spring and early summer months (April-May, 5%; June, <2%). (Climate statistics compiled from the National Climatic Data Center, [www.ncdc.noaa.gov](http://www.ncdc.noaa.gov), Phoenix Sky Harbor Airport, 1950-2010.) Annual PET rates in the area average ~2000 mm (Balling *et al.*, 2008), which are sufficiently high compared to precipitation rates to classify the area as desert conditions (code BW) under the Köppen climate classification system.

In 2005, four small “neighborhoods” were fitted with differing vegetation and irrigation treatments as part of the Central Arizona Phoenix – Long-Term Ecological Research (CAP-LTER) project; a fifth was maintained without any particular treatment

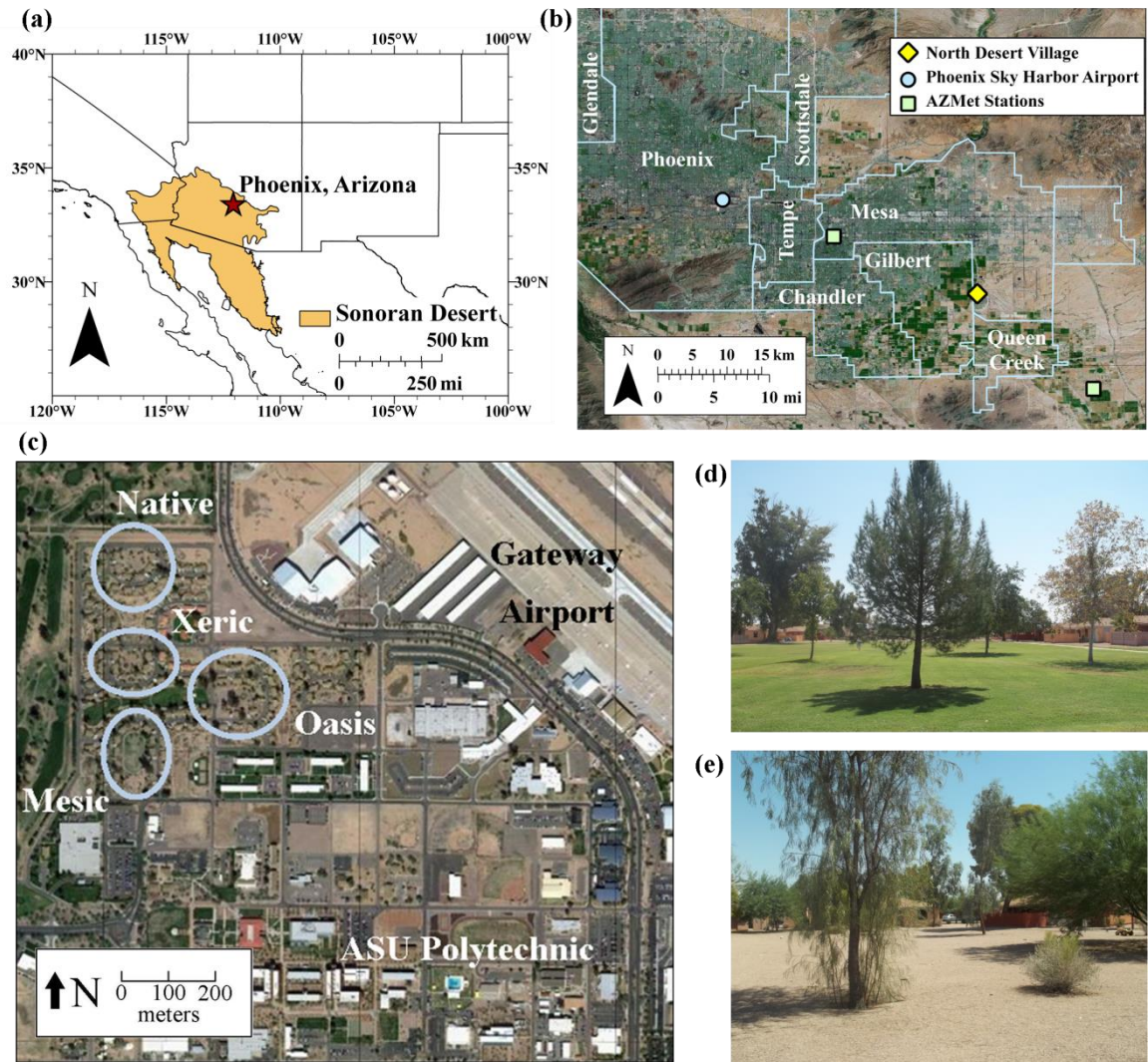


**Figure 2:** Location of the NDV landscape experiment, with respect to: (a) the southwestern United States and the Sonoran Desert, and (b) the Phoenix metropolitan area. (c) Four instrumented neighborhoods at NDV. Images of the mesic (d) and xeric (e) sites.

as an experimental control (Martin *et al.*, 2007). Each neighborhood consists of six pre-existing single-story homes (100-200 m<sup>2</sup>) occupied by university faculty, staff, students, and their families, and arranged in a semi-circular configuration around a larger common area (Figure 2d, e). As detailed in Table 2, the “mesic” site includes turf grass and high water-use shade trees, while the “xeric” site features a decomposing granite base (~5 cm

**Table 1:** Summary of precipitation at Phoenix Sky Harbor Airport 1950-2010

<b>Month</b>	<b>Average Rainfall (mm)</b>	<b>% Annual</b>	<b>Season</b>	<b>Average Rainfall (mm)</b>	<b>% Annual</b>
<b>Jan</b>	20.74	10.89%			
<b>Feb</b>	19.30	10.13%	Winter	62.62	32.87%
<b>Mar</b>	22.58	11.85%			
<b>Apr</b>	6.78	3.56%			
<b>May</b>	3.18	1.67%	Spring	12.39	6.50%
<b>Jun</b>	2.43	1.28%			
<b>Jul</b>	22.67	11.90%			
<b>Aug</b>	25.41	13.33%	Summer	64.20	33.69%
<b>Sep</b>	16.12	8.46%			
<b>Oct</b>	15.12	7.94%			
<b>Nov</b>	14.80	7.77%	Fall	51.32	26.94%
<b>Dec</b>	21.40	11.23%			
<b>Total</b>	190.53	100%		190.53	100%

thickness) with a combination of native and exotic low water-use trees and shrubs.

Irrigation systems appropriate for each vegetative cover were also installed, including overhead sprinkler systems for turf grass, and individual drip irrigators at trees and shrubs for areas with predominantly decomposing granite surface mulch cover. The “oasis” and “native” sites were not used in this study, but are shown in Figure 2 and described in Table 2 as a reference.

At each neighborhood, volumetric water content was recorded at hourly intervals with two 30-cm long CS616 water content reflectometers (Campbell Sci., Logan, UT) that were installed horizontally and buried with native soil (Figure 3) within the active rooting zone of the surrounding vegetation at 30-cm depth (Martin *et al.*, 2007). Ambient air temperature and soil heat flux were also measured, though these data were not used in this study.

The Soil Survey Geographic (SSURGO) database (a product of the U.S. Department of Agriculture) classifies the entirety of the studied portion of NDV as

**Table 2:** Landscape and irrigation treatments of four neighborhoods at NDV

Treatment	Ground Cover	Plant Types and Examples	Irrigation	Sensor Cover
Mesic	Turf grass	High water-use shade trees, turf grass Turkish pine ( <i>Pinus brutia</i> ) Arizona sycamore ( <i>Platanus wrightii</i> ) Bermuda grass ( <i>Cynodon dactylon</i> )	Sprinkler	Turf grass (x2)
Xeric	Granitic gravel substrate	Low water-use native and exotic trees Eucalyptus ( <i>E. microtheca</i> ) Palo verde ( <i>Parkinsonia</i> hybrid) Mesquite ( <i>Prosopis</i> hybrid)	Individual drip emitters at each shrub and tree	Gravel, Palo verde
Oasis	Granitic gravel substrate with turf grass “islands”	High and low water use exotic trees and shrubs European fan palm ( <i>Chamaerops humilis</i> ) Desert petunia ( <i>Ruellia peninsularis</i> ) Bermuda grass ( <i>Cynodon dactylon</i> )	Sprinklers on turf grass, individual emitters in gravel areas	Turf grass, Gravel
Native	Gravel	Native Sonoran Desert plants Agave ( <i>A. Americana</i> ) Saguaro cactus ( <i>Carnegiea gigantea</i> ) Creosote bush ( <i>Larrea tridentata</i> )	None	Gravel, Saguaro cactus

Mohall loam (“Mv” in Figure 4). While this study does not use soil properties or characteristics from SSURGO, the single soil classification for the entire area is used to justify the use of soil parameters calibrated at one NDV site to others within the area. The site also exhibits low relief, with variations in altitude <1 m throughout NDV. This allows an assumption of generally negligible lateral fluxes, and thus the applicability of a spatially non-distributed model of soil moisture dynamics.

### 2.3 Soil Moisture and Meteorological Data

Two sensors recorded volumetric soil moisture hourly at each of the four NDV landscape experiment sites (“neighborhoods”) over the period from April 10, 2006 to June 15, 2010. Where applicable, the two sensors for each neighborhood were buried



**Figure 3:** Installation of CS616 soil moisture sensor at xeric site.

under areas of differing ground cover, as shown in Table 2. At the xeric site, one sensor was placed beneath a Palo verde tree with drip-style irrigation emitters. Another sensor was placed away from any vegetation (and thus irrigation) in an area covered only by a layer of decomposing granitic gravel. At the mesic site, both sensors were placed under turf grass, away from any trees or shrubs, irrigated by a sprinkler system.

Figures 5 and 6 show unprocessed soil moisture data from the full 50-month duration of the experiment at the xeric and mesic sites, respectively. Figure 5 shows behavior at the non-irrigated sensor in the first year that is unexpected for a site without any additional water input beyond precipitation. A maintenance issue followed by a data gap in December 2007 created further unreliable data. It is not until after the decline of the elevated recession limb in early 2008 that the data assumes an expected pattern of punctual precipitation inputs followed by recession limbs from gradual extractions from evapotranspiration demands, in the shape of an exponential decay. This pattern continues





**Figure 4:** Image from the SSURGO database showing NDV within the cyan box as Mohall loam (“Mv”). The boundary with Contine clay loam (Co) is north of the portions of NDV used for this study (compare with Figure 2c).

into the fall of 2009, until another data gap at the end of that year. When the data resumes in early 2010, the irrigated mesic sensor shows abnormally high values. Previously, the irrigated sensor showed a sinusoidal pattern following irrigation patterns of higher water input in the summer months, interrupted by precipitation events in the winter months (most notably in December 2009). In order to utilize a full year of continuous data free from the effects of dysfunctional irrigation and sensing equipment, the twelve-month period from August 1, 2008 to August 1, 2009 was chosen for model testing. This period includes three large, clear precipitation events at the non-irrigated xeric site, with recession limbs as would be expected. At the irrigated site, this period includes a full year of the pattern expected from increased irrigation in the summer.



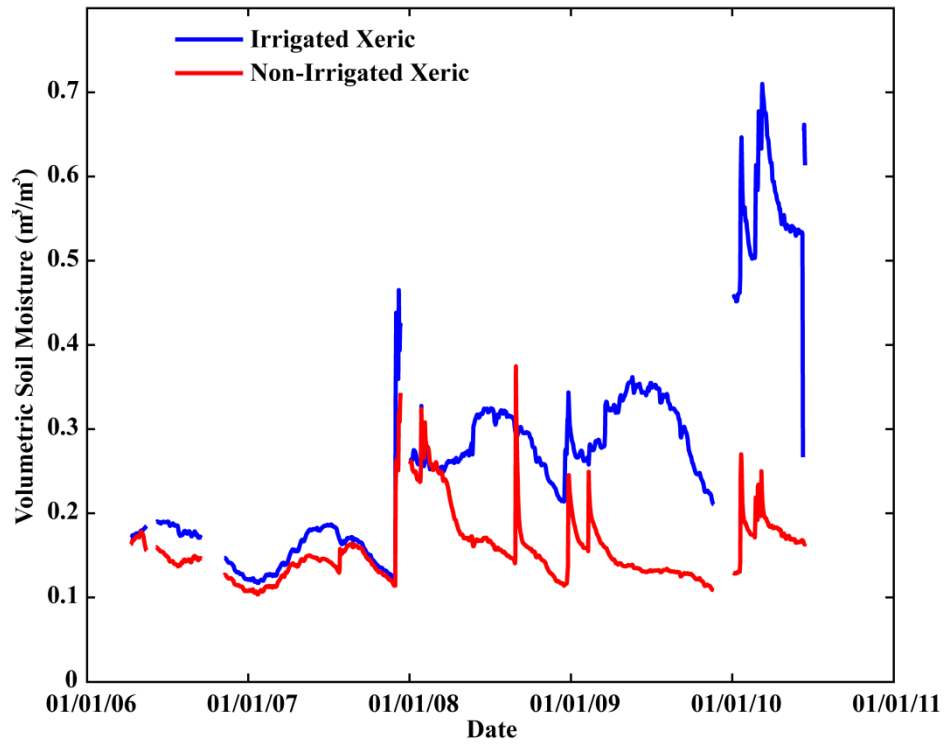


**Figure 5:** Unprocessed soil moisture data from the xeric site.

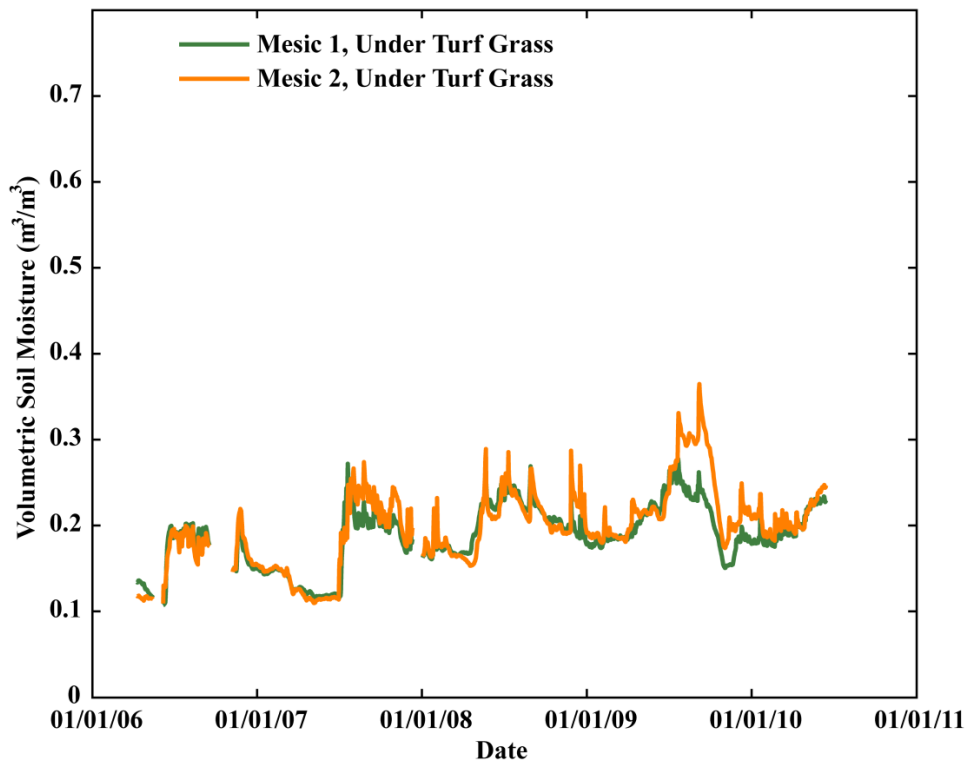


**Figure 6:** Unprocessed soil moisture data from the mesic site.

Figure 6 shows that the two sensors at the mesic site had similar soil moisture observations for the full duration of the experiment, as would be expected since the two were located in close proximity to each other, and both were buried under open turf grass away from any trees or shrubs. One however, labeled “Mesic 2” in Figure 6, exhibited greater displacements from a base soil moisture value during wetting events (i.e. a “peakier” response curve). The difference between the two could be due to a number of factors, including slight differences in elevation creating extremely localized areas of ponding, preferential flowpaths in the disturbed soil following sensor deployment, or the effects of surrounding vegetation, either by intercepting and redirecting irrigation from the sprinkler system, or by creating preferential flowpaths through their root systems. Regardless, without records of the irrigation schedule during the experiment, the more punctuated soil moisture series resulting from greater response to irrigation events were more difficult for the model to reproduce in preliminary tests. (See section 2.4.3 for further explanation of modeling the irrigated sites.) Thus the series labeled “Mesic 1” was used for model testing, over the same one-year period used at the xeric site, in order to maintain consistency in the meteorological record throughout the analysis.

Unprocessed data from the site data loggers showed volumetric soil moisture ( $\theta$ ) as high as  $0.75 \text{ m}^3/\text{m}^3$ . These high values, on a scale where the maximum should equal porosity ( $n \sim 0.4$  to  $0.6 \text{ m}^3/\text{m}^3$ ) suggested that a sensor calibration was necessary. Since this maximum value occurred multiple times for different sensors in different neighborhoods, soil moisture observations were normalized to this value, thereby interpreting this sensor reading as a point of maximum saturation. Thus a sensor

calibration was achieved simultaneously with a conversion from volumetric soil moisture to the dimensionless relative soil moisture ( $s$ ) used in the model, ( $s = \theta/\theta_{max}$ ). This was done without requiring an estimate for porosity, which instead is included in a calibration parameter as described in section 2.4.2. After the conversion, daily soil moisture values were calculated as the arithmetic mean of hourly observations.

Daily precipitation and PET records were obtained from the Arizona Meteorological Network (AZMET) station at Queen Creek (see Figure 2b), approximately 20 km southeast of NDV, and supplemented by data from the AZMET station in Mesa, 20 km northwest of NDV ([ag.arizona.edu/azmet](http://ag.arizona.edu/azmet)). Hourly precipitation records were aggregated to daily data to match the resolution of PET data and maintain consistency in the model. Though spatial heterogeneity of precipitation is to be expected, particularly for summer thunderstorms, the magnitude and timing of rain events at the two stations were found to be sufficiently similar to allow an assumption of comparable rainfall at NDV between them. Unfortunately, annual precipitation totals from the Phoenix-Mesa Gateway Airport, adjacent to NDV (see Figure 2c), as provided by the National Climatic Data Center, were considered unreliable due to their significant inconsistency with other data sets in the area. A comparison of the two AZMET data sets shows little difference in PET between the stations, suggesting that either data set would be appropriate for use at NDV. The Queen Creek site was chosen as the primary source because the nearby farms and suburban development were deemed analogous to the adjacent golf course and campus housing at NDV, as compared to the more densely developed area surrounding the Mesa AZMET station. Calculated using a simplified version of the Penman-Monteith Equation recommended by the American Society of

**Table 3:** Summary of potential evapotranspiration data from the Queen Creek AZMET station, including years used for calibrations and simulations.

<b>Month</b>	<b>2006</b>	<b>2007</b>	<b>2008</b>	<b>2009</b>	<b>2010</b>	<b>Average</b>
<b>January</b>	89.4	60.3	62.5	65.5	62	67.94
<b>February</b>	106.2	83.7	68.7	79.7	64	80.46
<b>March</b>	118.4	154.9	144.7	148.1	115.4	136.3
<b>April</b>	167.4	179.5	202.6	193.2	169.6	182.46
<b>May</b>	218.8	212.1	203.5	234.6	225.9	218.98
<b>June</b>	215.6	200	221	243.4	241.2	224.24
<b>July</b>	224.8	203.6	211.7	262.4	231.4	226.78
<b>August</b>	207.3	207.2	227.8	241.3	215.1	219.74
<b>September</b>	165.4	171.8	195.2	198.3	191.1	184.36
<b>October</b>	110.7	129.9	151.6	149.4	125.2	133.36
<b>November</b>	87.7	77.9	90.1	94.1	88.3	87.62
<b>December</b>	64	47.9	50.6	52.9	59.6	55
<b>Total</b>	1775.7	1728.8	1830	1962.9	1788.8	1817.24

Civil Engineers, the AZMET PET value is an appropriate estimate for evaporative demand in ecosystems with high water supply such as urban irrigated landscapes (Brown, 2005). A summary of five years of PET data from the Queen Creek AZMET station is shown in Table 3.

Figure 7 shows data (after the conversion/normalization step) from the three sensors (two xeric, one mesic) used for model calibrations, with precipitation and PET records from the Queen Creek AZMET station. Precipitation occurred mostly in the winter and late summer, ranging from less than 5 to approximately 20 mm/d, with an annual total of 187 mm, similar to the annual trends shown over the 60-year history at Phoenix Sky Harbor Airport (Table 1). PET forcing exhibited both seasonal fluctuations and daily changes linked to weather conditions. The non-irrigated sensor showed the greatest soil moisture variation, ranging from  $s = 0.15$  to 0.50. As expected, the irrigated xeric sensor averaged higher soil moisture values than the non-irrigated sensor, with less

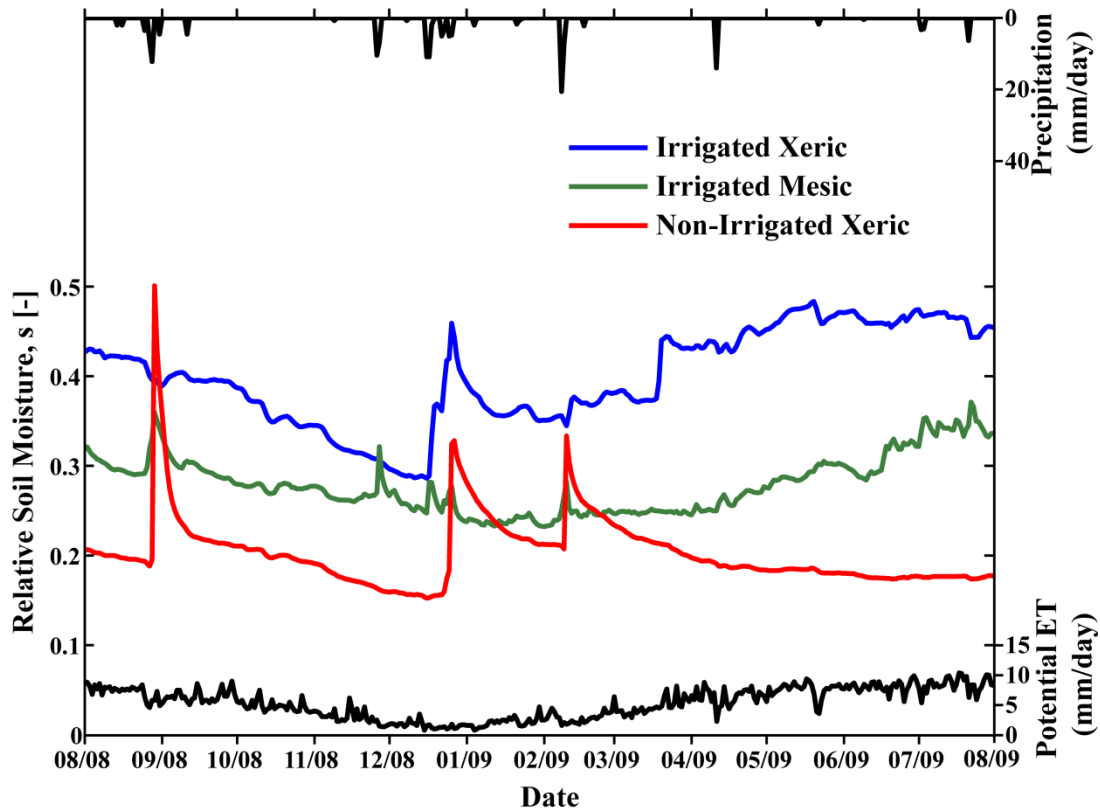


**Figure 7:** Soil moisture observations from August 1, 2008 to August 1, 2009 for three sensors at NDV with precipitation and PET forcing from the Queen Creek AZMET station.

variation. Interestingly, the irrigated sensor at the xeric site showed wetter conditions from concentrated drip irrigation as compared to the mesic sensor underneath the turf grass with the diffuse application from the overhead sprinkler system. Nevertheless, when averaged spatially over each neighborhood, a lower total volume of water was applied to the xeric site since it combined small areas of drip irrigation and large non-irrigated patches (e.g. Palo verde versus gravel areas).

It should be noted that while all three sensors recorded a response to large rain events in August, December, and February, the xeric sensors had no response to the November event. (The irrigated sensor at the xeric site showed a decrease in soil moisture

in response to the August event, which is not intuitive, but can be due to increased hydraulic conductivity under conditions of high soil moisture, as explained in Section 2.1 and reflected in Equation 3.) Additionally, the April event was not recorded at the non-irrigated sensor, and is difficult to discern at the irrigated sites. Finally, the relatively small August event appeared to have a disproportionately large effect at both sites when compared to the larger February event. These observations are the impetus for adjustments made to facilitate the calibration process as described in the following section.

## **2.4 Model Calibration and Testing**

### **2.4.1 General Approach**

With meteorological data from the Queen Creek AZMET station as model forcing, an automated optimization routine was used to estimate the soil and vegetative parameters that best represented the observations at NDV shown in Figure 7. The routine employed was the Shuffled Complex Evolution (SCE) method developed by Duan *et al.* (1993), which combines the optimization strategies of clustering, shuffled complexes, and competitive evolution to search multi-dimensional spaces for globally optimized parameter values. The objective function was the minimization of the root mean square error (RMSE) between the observed and modeled soil moisture time series over the one-year calibration period (August 1, 2008 to August 1, 2009). After preliminary analysis, the precipitation record was lagged by one day to account for the delayed response in the soil moisture record as water from precipitation events percolates through the soil to reach the 30 cm sensor depth.

The model was calibrated to each of the three time series sequentially to take advantage of parameters shared between locations with similar soils and thereby determine specific parameters under conditions best suited to their estimation. For example, the hygroscopic point was determined at the site with lowest soil moisture. This allowed for increased computational efficiency while returning results within a range of reasonable values culled from published literature (e.g. Caylor *et al.*, 2005; Laio *et al.*, 2001a, b; Manfreda *et al.*, 2010; Porporato *et al.*, 2003; Vico and Porporato, 2011).

In order to test for parameter convergence and determine the relative dependence of the objective function on each parameter, up to 100 independent calibrations were performed for each time series. Each of these independent calibrations began with the same parameter space and a different set of randomly chosen initial points, narrowing the parameter space through approximately 20,000 model runs until the RMSE converged to a minimum value. Figure 8 shows an example of final parameter values, normalized to their respective bounds in the initial parameter space, from a set of 100 independent calibrations, all seeking optimal values for the same sensor data, and returning similar values for the final RMSE. Clearly, achieving the optimal value was highly dependent on a precise value for parameters  $nZ_r$ ,  $s_w$ , and  $s_0$ , while parameters such as  $s^*$  and  $s_h$  were able to vary substantially while still achieving an optimal RMSE. If necessary, these results would then be used to set up a second set of optimization runs, with the parameters to which the RMSE was highly dependent now fixed to the values determined in the first set of optimizations, and the bounds for the others constrained to the range seen in the previous results. In this iterative manner, values were estimated for all

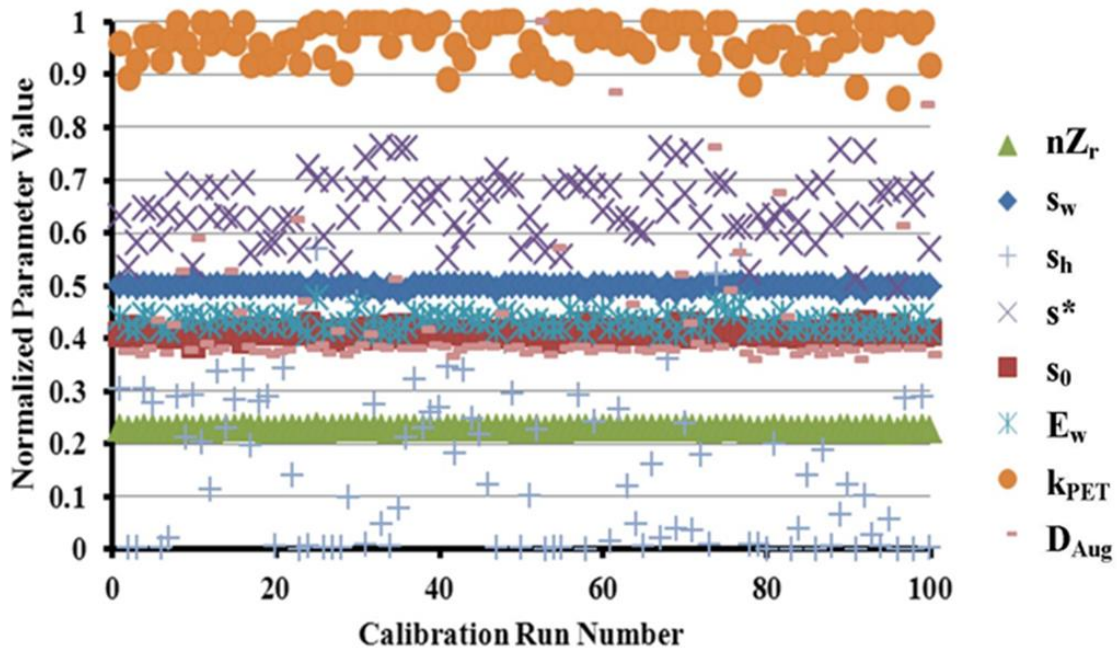


**Figure 8:** Example of first-order set of calibration runs, showing convergence for only some of the estimated parameters.

parameters appropriate for a given data set before advancing to the next soil moisture sensor.

Model testing was achieved using data from the same sensors during independent time periods, though the limited duration of reliable data (due to, for example, sensor malfunction, data gaps, or irrigation system maintenance) often necessitated shorter validation periods (7-10 months, as discussed in section 3.1) than desired.

#### 2.4.2 Non-Irrigated Model Calibration

Since irrigation input represents a relatively unknown model forcing (discussed below), and in order to build confidence in the model, the non-irrigated xeric sensor was chosen as the first calibration. Though this sensor is covered only by gravel, it was



assumed that the surrounding vegetation at the xeric site nonetheless had an impact on water dynamics through evapotranspiration of soil moisture. Preliminary tests indicated that soil moisture levels at the site were too low to induce significant leakage, so parameters used in the model only in the calculation of leakage ( $s_{fc}$ ,  $K_s$ , and  $b$ ) were unable to converge to viable calibrated values. Since the model does not use porosity or the rooting depth independently (Laio *et al.*, 2001a), their product  $nZ_r$  was used as a calibration parameter; it is not possible to separate the two to independently determine either using this method. Thus the set of model parameters determined from this calibration included  $nZ_r$ ,  $s_h$ ,  $s_w$ ,  $s^*$ , and  $E_w$ . It is assumed that  $s_h$  and  $E_w$  are dependent on only soil and are therefore applicable throughout NDV, all of which consists of Mohall loam by the SSURGO database. It is further assumed that  $nZ_r$ ,  $s_w$ , and  $s^*$  are dependent on both soil and vegetation and therefore cannot be applied to the mesic site, but can be used for the data from the other sensor at the xeric site. Antecedent moisture conditions were determined by calibrating a value for initial soil moisture  $s_0$ .

The final calibrated parameter was the depth of the late August 2008 rain event, since the recorded rainfall at the Queen Creek AZMET site was insufficient to elicit the observed soil moisture response. The soil moisture series shows a disproportionately large increase compared to later rain events with more rainfall recorded at the Queen Creek station. This is justified by the spatial heterogeneity of summer storms in the region. The Mesa AZMET station, for example, shows an event earlier that month consisting of several centimeters over three days, though no rainfall was reported at Queen Creek during that time. The August event thus lacks a reliably applicable rainfall depth, despite the importance of such a value due to the relative dominance of the effects

of the wetting event on the late summer moisture time series. It was therefore decided to use the magnitude of the storm as a calibration parameter, thereby allowing the calibration to prioritize the more spatially homogeneous winter events with more consistent rainfall data across the region, rather than the uncertain summer storm. Similarly, the large November and April events seen at the AZMET station were also removed from the precipitation record, as there was no record of them at the xeric site. In order for the model to achieve reasonable and reliable calibration results that accurately simulate the true soil moisture record, it was necessary to utilize a rainfall record where major events are seen as corresponding peaks in the soil moisture record. In this way, soil and vegetative parameters were determined that could be used to model soil moisture time series under different precipitation, irrigation, and PET forcing.

#### 2.4.3 Irrigated Model Calibrations

Although monthly water meter readings were kept for the irrigation systems in each of the neighborhoods, undocumented changes to the irrigation schedule disallow temporal resolution of irrigation input into a unit amenable to the current numerical simulation. Furthermore, heterogeneities in distribution mechanisms and irrigation frequencies and durations make conversion from volumetric readings to irrigation depths problematic. Therefore, without reliably precise data, irrigation was modeled as an average daily addition to the meteorological forcing, varying on a monthly schedule. Modeling irrigation application as a daily event allowed water movement to the sensor depth in a delayed and attenuated manner to mimic the observed soil moisture response. As seen in Figure 7, irrigation pulses are seen in the soil moisture record as small,

frequent increases in moisture levels, resulting in a relatively smooth curve when compared to data influenced only by rainfall. Additionally, these monthly irrigation parameters implicitly account for seasonally-dependent subtractions from water input due to interception.

The parameters determined from the non-irrigated xeric sensor were applied during the model calibration using data from the irrigated xeric sensor to determine drip irrigation depths for each month as well as the soil parameters related to leakage. This follows the assumption that soil and vegetative parameters remain constant throughout each neighborhood due to the extended root and canopy structures of the plants therein. Each neighborhood is thereby modeled as being homogenized, and vegetative parameters for individual plant species are undeterminable from the average effects of the overall landscape. This assumption disallows the consideration of spatial heterogeneities within a neighborhood, but allows for the calibration of the model under irrigated conditions with an unknown irrigation forcing. The same meteorological forcing was also used for both xeric sensors, though antecedent moisture  $s_0$  was again included as a calibration parameter for the second (irrigated xeric) data set. Finally, the model was calibrated to the irrigated mesic sensor data, using soil parameters determined previously, though vegetation- and site-dependent parameters  $nZ_r$ ,  $s_w$ ,  $s^*$ , and  $s_0$  were determined for the new neighborhood, with monthly irrigation values for the sprinkler application. The magnitude of the August storm was also determined for the mesic site to account for spatial heterogeneity in precipitation and emphasize the more reliable portions of the soil moisture time series.

## 2.5 Irrigation Simulations

To investigate the impact of varying irrigation schedules, the total annual irrigation inputs determined in the above calibrations were temporally redistributed according to four idealized irrigation scenarios representative of irrigation practices in the Phoenix metropolitan area (Figure 9; Martin and Stabler, 2002). Scenario 1 divides the annual total into equal daily inputs, representing daily irrigation without any seasonal variation. Scenario 2 varies daily irrigation based on the monthly factors determined in the site calibrations to capture seasonal variation of drip or sprinkler irrigation depth. Scenarios 3 and 4 are analogous to the first two in terms of representing constant and seasonally-varying inputs, but deliver water as monthly pulses on the first day of each month, simulating flood-style irrigation practices. Scenario 3 divides the annual input into twelve equal monthly pulses, while Scenario 4 varies the pulse volume according to the monthly ratios determined in the calibration. All four scenarios use the same annual total irrigation input, varying only the distribution schedule.

Simulations for all four scenarios were run for a five-year period (January 1, 2006 – December 31, 2010), using the calibrated model parameters from both the irrigated xeric and mesic sites, with meteorological forcing data (precipitation and PET) from the AZMET stations. Soil moisture statistics were observed for the base case, representing the total annual irrigation determined in the calibration for each site. The annual total was then varied for each scenario to investigate the impact on soil moisture dynamics, water balance partitioning, and plant stress at both sites. In these simulations, seasonality was maintained by keeping constant the percentage of annual irrigation applied during each month, effectively scaling water input by keeping month-to-month ratios the same.

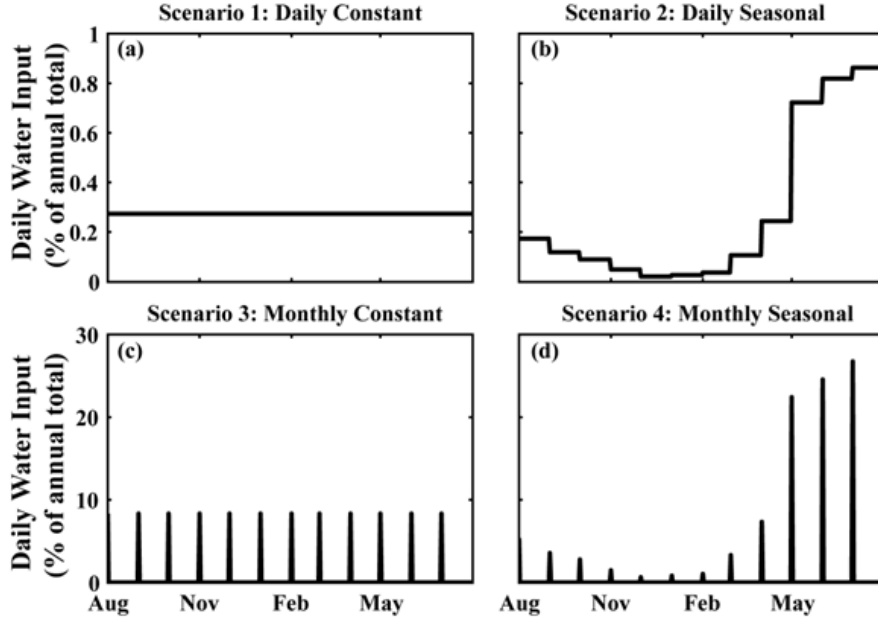


**Figure 9:** Irrigation input for four scenarios expressed as a percentage of the annual total for: (a) daily constant, (b) seasonal daily, (c) monthly constant pulses, and (d) monthly seasonal pulses.

Dynamic water stress was also determined for a range of plant stress parameters, and for cases of inter- and intra-annual precipitation variability.

## 2.6 Optimized Irrigation Schedules

The SCE optimization routine was then used to find irrigation schedules that achieved specified levels of dynamic water stress while minimizing irrigation. An optimization objective function  $f$  was used to simultaneously minimize total annual irrigation ( $I$ ) while maintaining a specified allowable plant water stress, denoted as  $\bar{\theta}_A$ :

$$f = |\bar{\theta} - \bar{\theta}_A| \times 10^m + I. \quad (7)$$

Here, the exponent  $m$  ( $\sim 5$ ) is used to make the difference between  $\bar{\theta}$  and  $\bar{\theta}_A$  (on the order of  $10^{-2}$ ) of a magnitude similar to the irrigation  $I$  (on the order of  $10^3$ ), allowing the

optimization routine to prioritize both approximately equally.  $m$  was varied to ensure that irrigation was minimized while achieving a dynamic stress value within 0.01 of  $\bar{\theta}_A$ .

Simulations were run for both sites using model parameters from the calibrations, precipitation data from Phoenix Sky Harbor Airport (1950-2010, acquired through the National Climatic Data Center) and averaged daily PET values from 10 years of data from the Queen Creek AZMET station. The long-term data was used to include decadal climate variability in determining optimized irrigation schedules appropriate for this specific region.

Optimizations were performed first using Scenario 1 (constant daily irrigation) to determine minimal irrigation for a range of  $\bar{\theta}_A$  values. The advantages of seasonal irrigation were then investigated by finding monthly irrigation depths, as in Scenario 2, that minimized irrigation with daily input. The difference between the daily irrigation interval of Scenario 1 and the monthly irrigation interval of Scenario 3 (as well as longer irrigation intervals) was then explored by finding an optimal interval at which to apply a seasonally constant irrigation depth for the entire year, again with several values of  $\bar{\theta}_A$ . Further optimizations were performed allowing the irrigation interval to vary among the precipitation seasons of the Phoenix area delineated in Table 1, while maintaining a constant irrigation depth throughout the year. These resulted in schedules with a structure similar to those recommended by local municipalities: a vegetation- and landscape-dependent, time-constant irrigation depth, applied at intervals that vary each season. A sensitivity analysis of plant stress parameters  $k$  and  $q$  was also performed to see how the ability of a plant to cope with water shortage can affect irrigation requirements.

## 3 RESULTS AND DISCUSSION

This chapter will begin with a discussion of the calibrations performed using data from each of the three soil moisture sensors used: the non-irrigated xeric sensor, the irrigated xeric sensor, and an irrigated mesic sensor. This is followed by a presentation of the results of simulations using the calibrated model, in terms of water balance partitioning and plant water stress. The simulations vary irrigation amount and scheduling, while also testing for sensitivity to plant stress parameters and intra- and inter-annual variability in precipitation. The calibrated model is then used with long-term meteorological forcing to determine irrigation schedules that minimize water input for specified values of plant water stress under several schedule structures, including daily irrigation with constant or monthly varying depth, and seasonally varying irrigation interval of constant, depth.

### 3.1 Model Calibrations

#### 3.1.1 Non-Irrigated Xeric Sensor

A summary of the results of calibrating the model to the data from the non-irrigated xeric sensor is shown in Table 4. The table also shows the boundaries used for the parameter space searched by the optimization routine. Values for  $s_{fc}$ ,  $K_s$ , and  $b$  were also included in the calibration, but showed no convergence, and are thus not reported here.

As evidenced by the low standard deviations among the final results of the independent optimizations, each parameter showed high convergence to a value not equal

**Table 4:** Summary of ten independent calibrations using data from the non-irrigated xeric sensor.

	<b>Lower Bound</b>	<b>Minimum</b>	<b>Average</b>	<b>Maximum</b>	<b>Upper Bound</b>	<b>Standard Deviation</b>
<b>RMSE</b>	-	0.0171	0.0171	0.0171	-	0.0000
<b>nZ<sub>r</sub> (mm)</b>	20	346.48	347.26	347.51	1600	0.323
<b>s<sub>h</sub></b>	0	0.132	0.133	0.133	0.15	0.0003
<b>s<sub>w</sub></b>	0.15	0.221	0.221	0.221	0.25	0.0001
<b>s*</b>	0.25	0.310	0.310	0.310	0.45	0.0002
<b>E<sub>w</sub> (mm/d)</b>	0.01	0.344	0.346	0.348	0.4	0.0015
<b>s<sub>0</sub></b>	0.15	0.203	0.203	0.203	0.75	0.0000
<b>D<sub>8/28</sub> (mm)</b>	0	67.68	67.84	67.93	100	0.0869

to one of the bounds of the parameter space. Because of this convergence, no further calibrations or iterations were necessary, and the average values in Table 4 were used for further analysis. Figure 10 shows a comparison of the observed and modeled soil moisture time series, as well as the frequency distribution for each (inset), both of which show an excellent fit with a low RMSE of 0.017 in the time series. Model testing used meteorological data from the same source over the 10 months following the calibration period, and resulted in an RMSE of 0.052. The lower performance was likely due to differences between the rain recorded at the AZMET station and that which actually occurred at NDV.

Several features of the observed data are captured well by the simulated response, thereby supporting the model physics. For example, the slopes of the recession limbs in both time series varied according to seasonal PET rates: lower ET demand in winter results in a flatter slope for a given  $s$  value above  $s_w$ , and thus a slower recession limb following storm events in December and February, as compared with the August event. The model also captured the change in soil moisture recession behavior observed during inter-storm periods as a result of the wilting point ( $s_w = 0.22$ ) control on ET, below which



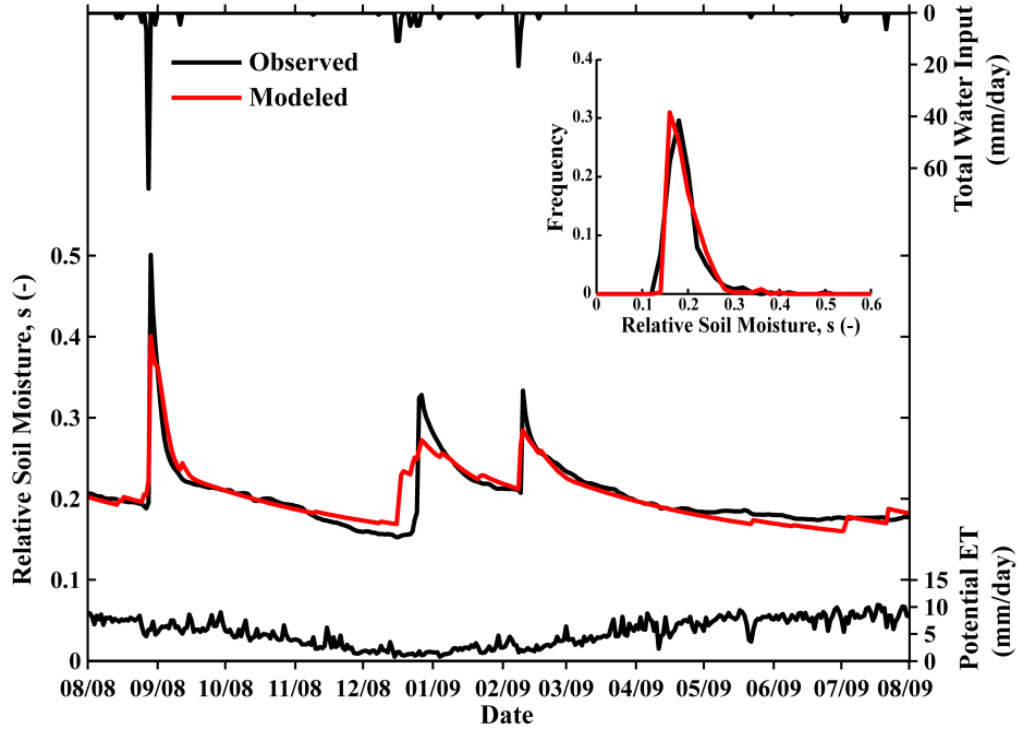


**Figure 10:** Time series and frequency diagram of modeled and observed relative soil moisture at the non-irrigated xeric site. Inset shows frequency distribution in which ordinate values represent frequency of  $s$  within a bin interval of 0.02, relative to the total number of soil moisture values.

soil evaporation ( $E_w = 0.34$  mm/d) becomes dominant. Furthermore, the relatively large response to precipitation events (as compared to the mesic site, to be discussed later) is due to a low  $nZ_r$  value, consistent with the predominantly bare soil and gravel cover at the site, which decreases the area-averaged rooting depth in the area surrounding the sensors.

### 3.1.2 Irrigated Xeric Sensor

Following preliminary optimization runs to determine appropriate bounds for the monthly irrigation depths at the irrigated xeric site, a set of 15 independent optimizations included the summarized results shown in Table 5.

**Table 5:** Partial summarized results of initial 15 independent calibrations using data from the irrigated xeric site. Optimizations also included monthly depths of daily irrigation.

	<b>Lower Bound</b>	<b>Minimum</b>	<b>Average</b>	<b>Maximum</b>	<b>Upper Bound</b>	<b>Standard Deviation</b>
<b>RMSE</b>	-	0.0166	0.0173	0.0206	-	0.00135
<b><math>s_{fc}</math></b>	0.4	0.4	0.420	0.479	0.75	0.0274
<b><math>b</math></b>	1	2.55	3.61	4.55	10	0.585
<b><math>K_s</math> (mm/d)</b>	1	1967	4970	9021	10000	1575
<b><math>s_0</math></b>	0.15	0.451	0.513	0.595	0.75	0.0636

The objective function was found to be highly dependent on  $s_{fc}$ , with the five best-performing final results (lowest objective function) all having  $s_{fc}$  values between 0.428 and 0.430. The next eight best results had  $s_{fc}$  values between 0.40000 and 0.40002, and the two worst between 0.478 and 0.479. To avoid these local minima in the parameter space and allow the routine to more efficiently search for a more precise global minimum by varying other parameters, the bounds on  $s_{fc}$  were narrowed and 15 more independent optimizations were run. These results showed similar patterns for  $K_s$ , prompting a third set of optimizations with narrower bounds on that parameter. A full summary (including irrigation depths) of these results is shown in Table 6.

Average values were used for subsequent analysis for all parameters except  $s_0$ , for which all optimal solutions had values fall within two distinct ranges, 0.459-0.461 and 0.605-0.608. These represent values with and without the leakage loss mechanism being triggered, but resulting in an equivalent  $s$  value after one day. Rather than finding the average value between the two local minima, the average within the lower was used for further analyses.

Figure 11 shows the observed and modeled soil moisture time series at the irrigated xeric sensor, as well as a frequency distribution plot. The calibration period

**Table 6:** Summary of final 15 independent optimizations using data from the irrigated xeric sensor.

	<b>Lower Bound</b>	<b>Minimum</b>	<b>Average</b>	<b>Maximum</b>	<b>Upper Bound</b>	<b>Standard Deviation</b>
<b>RMSE</b>	-	0.0166	0.0166	0.0166	-	0.000
<b><math>s_{fc}</math></b>	0.428	0.428	0.429	0.430	0.43	$2.57 \times 10^{-4}$
<b><math>b</math></b>	1	2.51	2.54	2.56	10	0.0139
<b><math>K_s</math> (mm/d)</b>	1	1905	1942	1964	2000	17.62
<b><math>s_0</math></b>	0.15	0.460	0.548	0.607	0.75	0.0739
<b><math>I_{Jan}</math> (mm/d)</b>	0.1	1.34	1.35	1.35	10	0.00
<b><math>I_{Feb}</math> (mm/d)</b>	0.1	1.87	1.87	1.88	10	0.00
<b><math>I_{Mar}</math> (mm/d)</b>	0.1	5.42	5.42	5.43	10	0.00
<b><math>I_{Apr}</math> (mm/d)</b>	0.1	12.26	12.42	12.51	20	0.07
<b><math>I_{May}</math> (mm/d)</b>	0.1	36.25	36.73	37.28	100	0.30
<b><math>I_{Jun}</math> (mm/d)</b>	0.1	39.70	41.59	42.24	100	0.67
<b><math>I_{Jul}</math> (mm/d)</b>	0.1	43.09	43.82	44.18	100	0.28
<b><math>I_{Aug}</math> (mm/d)</b>	0.1	8.70	8.81	8.90	10	0.05
<b><math>I_{Sep}</math> (mm/d)</b>	0.1	6.05	6.06	6.07	10	0.01
<b><math>I_{Oct}</math> (mm/d)</b>	0.1	4.55	4.55	4.56	10	0.00
<b><math>I_{Nov}</math> (mm/d)</b>	0.1	2.50	2.50	2.51	10	0.00
<b><math>I_{Dec}</math> (mm/d)</b>	0.1	1.04	1.05	1.05	10	0.00

yields an excellent RMSE of 0.017, similar to that from the non-irrigated xeric calibration. A testing period of the preceding seven months had an RMSE of 0.067, with the difference likely being due to inaccuracies in the assumption that the same monthly irrigation factors during the calibration period apply to the testing interval.

The large response to the December storms (again, compared to the mesic site), supports the use of a low  $nZ_r$  value, similar to the previous calibration. Excluding those wetting events, the observed data shows periods of high  $s$  in summer months, indicating that irrigation compensated for increased PET during summer periods to maintain high soil moisture values. The calibrated irrigation is consistent with this seasonality, and with common patterns of outdoor landscape water use in the Phoenix area. While seasonal trends were captured in the simulation, day-to-day variability in  $s$  was overestimated.

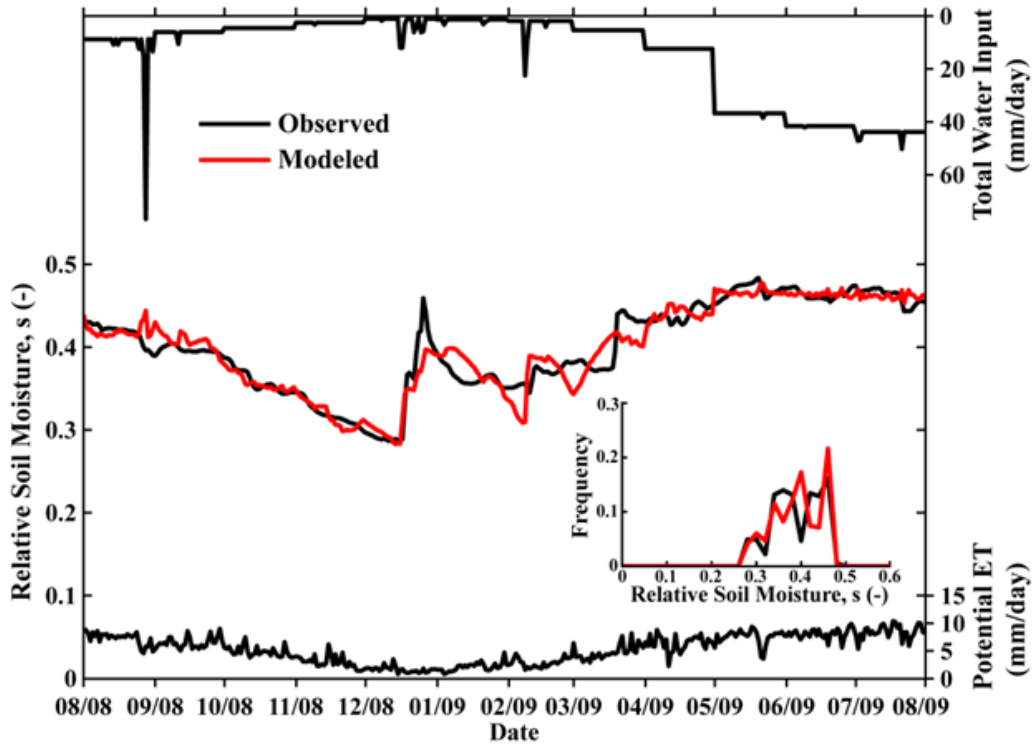


**Figure 11:** Time series and frequency diagram of modeled and observed relative soil moisture at the irrigated xeric site. Inset shows frequency distribution with bin interval of 0.02. Water input reflects precipitation and calibrated irrigation.

Two factors likely contributed to this effect: (1) irrigation was modeled as varying at a monthly scale to maintain computation efficiency, resulting in abrupt changes in water input that might not be seen with an irrigation schedule with finer resolution, and (2) PET, which fluctuates significantly daily, dominated soil moisture losses in the high range of  $s$  observed, creating daily variation in  $s$  that would likely be tempered in time and more evenly distributed in a vertical soil column including the sensor depth. Thus, as shown in the frequency diagram in Figure 11, the model captured well the range and seasonality of  $s$ , but had minor discrepancies in daily variability.

### 3.1.3 Irrigated Mesic Sensor

Similar to the irrigated xeric site, the mesic site required several calibration iterations for parameters to converge to consistent values and yield a parameter set that resulted in a global minimum. A summary of partial initial results are shown in Table 7; Table 8 shows a summary of results (including irrigation depths) after several iterations that sequentially narrowed the bounds on  $s^*$ ,  $s_w$ ,  $s_0$ , and  $nZ_r$ , which was the order of priority of parameters in minimizing the objective function. The RMSE for the final calibration was 0.0094, while a 10-month testing period subsequent to the calibration had an RMSE of 0.039. As at the irrigated xeric sensor, differences in model performance are attributed to variations in inter-annual differences in the monthly irrigation scheduling not captured in the calibration procedure. Estimates obtained from the calibrations for soil and vegetative from all three calibrations are summarized in Table 9.

The observed and modeled soil moisture time series and frequency distribution are presented in Figure 12. Observed  $s$  at the mesic site exhibited significantly smaller response to storm events than at the xeric site, which was reflected in the calibrated parameters by a significantly lower  $nZ_r$  value at the mesic site. The deeper rooting zone at the mesic site is expected since it is comprised primarily of turf grass while the xeric site is predominantly gravel without vegetation, resulting in a greater area-averaged rooting depth. This also accounts for the muted nature of the seasonality of  $I$  and  $s$  at the mesic site as compared with the xeric, though the overall trend of greater  $s$  in the summer was similar at both sites as  $I$  compensated for greater PET demands. Irrigation at the mesic site was of less depth than the xeric site due to the spatial range of the mesic sprinkler system as compared to the smaller drip emitter area at the xeric site.

**Table 7:** Partial summarized results of initial 10 independent calibrations using data from the irrigated mesic site. Optimizations also included monthly depths of daily irrigation.

	<b>Lower Bound</b>	<b>Minimum</b>	<b>Average</b>	<b>Maximum</b>	<b>Upper Bound</b>	<b>Standard Deviation</b>
<b>RMSE</b>	-	0.00950	0.00957	0.00964	-	$5.01 \times 10^{-5}$
<b>s*</b>	0.24	0.243	0.248	0.252	0.428	0.00261
<b>s<sub>w</sub></b>	0.15	0.150	0.184	0.238	0.24	0.0345
<b>nZ<sub>r</sub> (mm)</b>	160	2651	2888	3200	3200	190
<b>s<sub>0</sub></b>	0.15	0.311	0.313	0.316	0.75	0.00598
<b>D<sub>8/28</sub> (mm)</b>	0	65.2	83.3	100.0	100	13.97

**Table 8:** Summary of final 100 independent optimizations using data from the irrigated mesic sensor.

	<b>Lower Bound</b>	<b>Minimum</b>	<b>Average</b>	<b>Maximum</b>	<b>Upper Bound</b>	<b>Standard Deviation</b>
<b>RMSE</b>	-	0.00939	0.00940	0.00942	-	$7.43 \times 10^{-6}$
<b>s*</b>	0.247	0.247	0.248	0.249	0.25	0.00052
<b>s<sub>w</sub></b>	0.23	0.231	0.235	0.239	0.24	0.001565
<b>nZ<sub>r</sub> (mm)</b>	1600	1827	1998	2162	2200	69.90
<b>s<sub>0</sub></b>	0.31	0.311	0.313	0.315	0.315	0.000783
<b>D<sub>8/28</sub> (mm)</b>	30	38.5	47.1	54.3	70	2.83
<b>I<sub>Jan</sub> (mm/d)</b>	0	0.00	0.03	0.07	10	0.0196
<b>I<sub>Feb</sub> (mm/d)</b>	0	1.13	1.54	1.93	10	0.156
<b>I<sub>Mar</sub> (mm/d)</b>	0	4.57	4.70	4.80	10	0.0415
<b>I<sub>Apr</sub> (mm/d)</b>	0	7.94	8.12	8.31	10	0.0740
<b>I<sub>May</sub> (mm/d)</b>	0	8.57	8.65	8.73	10	0.0370
<b>I<sub>Jun</sub> (mm/d)</b>	0	10.14	10.37	10.61	20	0.0892
<b>I<sub>Jul</sub> (mm/d)</b>	0	9.26	9.36	9.47	20	0.0427
<b>I<sub>Aug</sub> (mm/d)</b>	0	5.88	6.13	6.34	10	0.0875
<b>I<sub>Sep</sub> (mm/d)</b>	0	2.67	2.94	3.25	10	0.116
<b>I<sub>Oct</sub> (mm/d)</b>	0	5.01	5.07	5.11	10	0.0176
<b>I<sub>Nov</sub> (mm/d)</b>	0	1.14	1.29	1.14	10	0.0545
<b>I<sub>Dec</sub> (mm/d)</b>	0	0.00	0.00	0.00	10	0.000

The irrigated mesic sensor exhibited higher daily variations in response to storms and sprinkler applications that are not captured in the model, though average soil moisture values and the frequency distribution of  $s$  (inset) were nonetheless well modeled. Still, calibration results should not be seen as precise determinations of site

**Table 9:** Parameter values determined for the three model calibrations, with calibration range used for each. “+” indicates dependence on soil characteristics and applicability to all sites. “#” are dependent on soil and vegetation and applied only within one neighborhood (xeric or mesic).

Parameter	Units	Symbol	Lower Bound	Optimized Value	Upper Bound
<b>Xeric Site, Non-Irrigated</b>					
<b>Porosity*Rooting Depth (#)</b>	[mm]	$nZ_r$	20	347	$3.2 \times 10^3$
<b>Hygroscopic Point (+)</b>	[-]	$s_h$	0	0.133	0.15
<b>Wilting Point (#)</b>	[-]	$s_w$	0.15	0.221	0.25
<b>Stress Threshold (#)</b>	[-]	$s^*$	0.25	0.310	0.45
<b>Bare Soil Evaporation (+)</b>	[mm/d]	$E_w$	0.01	0.347	0.40
<b>Xeric Site, Irrigated</b>					
<b>Field Capacity (+)</b>	[-]	$s_{fc}$	0.4	0.429	0.75
<b>Pore Size Distribution Index (+)</b>	[-]	$b$	1	2.54	10
<b>Saturated Hydraulic Conductivity (+)</b>	[mm/d]	$K_s$	1	$1.94 \times 10^3$	$1 \times 10^4$
<b>Mesic Site, Irrigated</b>					
<b>Porosity*Rooting Depth</b>	[mm]	$nZ_r$	20	$2.0 \times 10^3$	$3.2 \times 10^3$
<b>Wilting Point</b>	[-]	$s_w$	0.15	0.236	0.24
<b>Stress Threshold</b>	[-]	$s^*$	0.24	0.248	0.42

properties and water input, and are rather estimates that reflect observed data and allow for a comparison of average values and seasonal trends between the two sites.

### 3.2 Irrigation Scenarios: Soil Moisture Dynamics and Water Balance Partitioning

Based on the ability of the calibrated model to reproduce soil moisture conditions at the irrigated xeric and mesic sites, simulations were run to investigate the effects of irrigation scheduling on soil water dynamics and water balance partitioning. Figure 13 shows frequency distributions of modeled soil moisture values at the two irrigated sites using calibrated parameter values from Table 9 and five years of precipitation and PET forcing from the Queen Creek AZMET station. Irrigation was included using annual

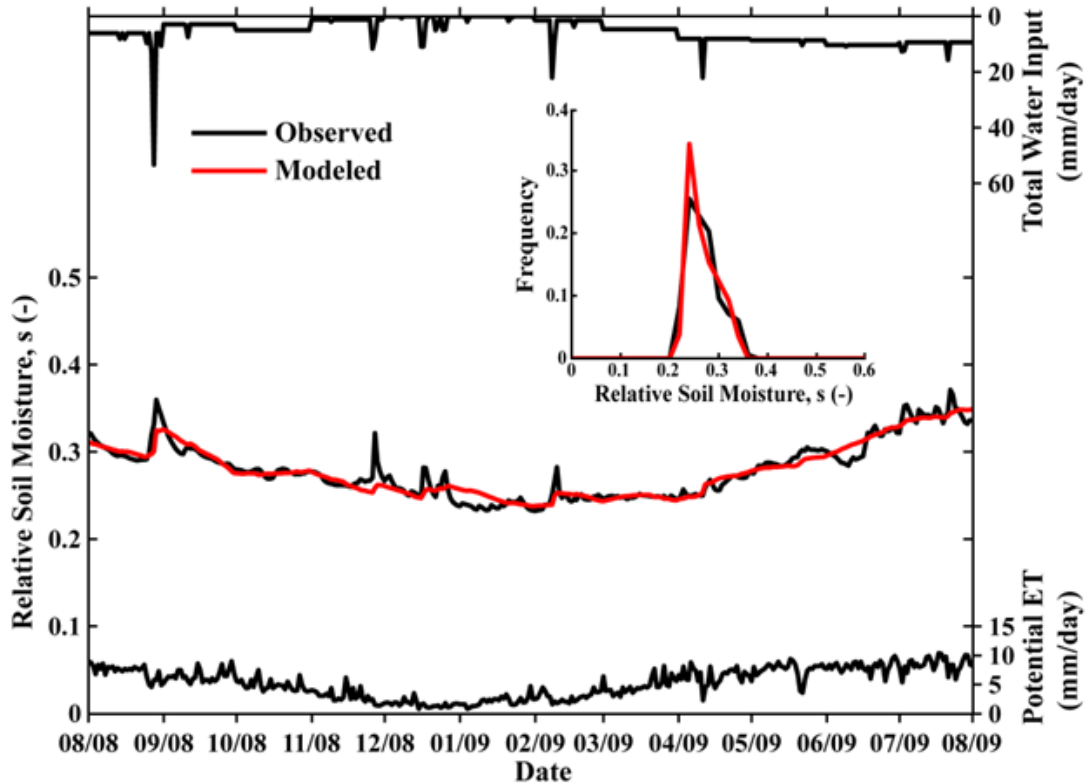


**Figure 12:** Time series and frequency diagram of modeled and observed relative soil moisture at the irrigated mesic site. Inset shows frequency distribution with bin interval of 0.02. Water input reflects precipitation and calibrated irrigation.

totals derived from the calibrations, distributed according to the four scenarios depicted in Figure 9. For seasonal scenarios, the monthly irrigation factors determined in the calibration at each site were used repeatedly for each of the five years.

At the xeric site, monthly (flood-style) irrigation (Scenarios 3 and 4) led to low soil moisture values near the wilting point (0.22), with short periods of high  $s$  near  $s_{fc}$  (0.44) immediately following irrigation pulses. With a low storage capacity in the rooting zone ( $nZ_r$ ), the soil was unable to retain the moisture delivered in large monthly pulses. In this case, varying irrigation seasonally had no appreciable effect on soil moisture conditions. The same annual input distributed at a daily scale resulted in much higher soil moisture values, with a significant impact of seasonality. Scenario 1 (constant daily



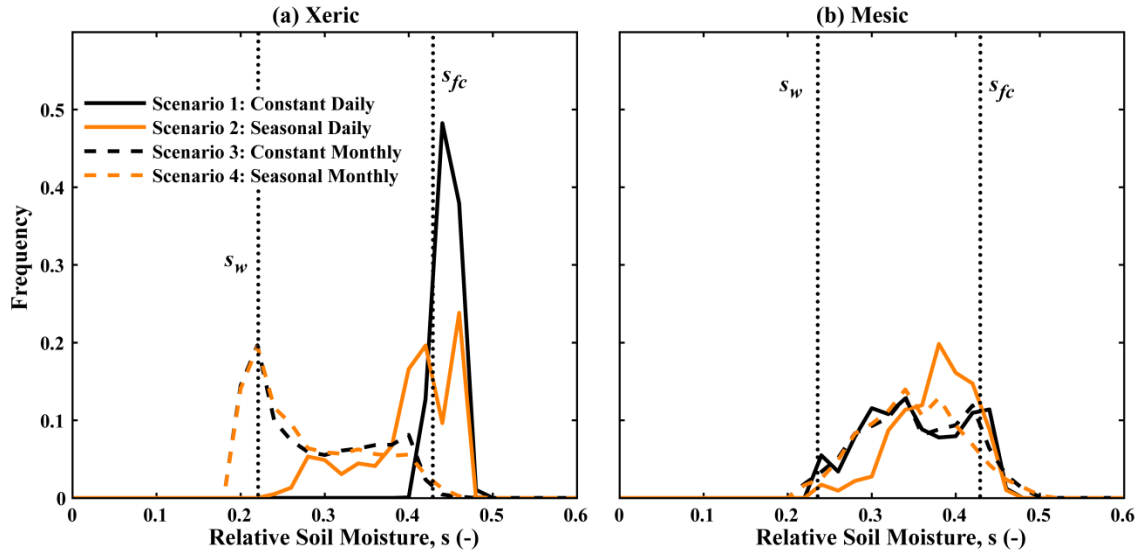


**Figure 13:** Soil moisture frequency distributions for five-year simulations (January 2006–December 2010) for four irrigation scenarios at the irrigated xeric (a) and mesic (b) sites. Ordinate values represent frequency of  $s$  with a bin interval of 0.02, relative to the total number of soil moisture data points.

irrigation) maintained relatively constant soil moisture near the field capacity of the soil (87% of days,  $s \geq 0.43$ ; 0% of days,  $s \leq 0.40$ ). Seasonal irrigation resulted in more variable soil moisture (34% of days,  $s \geq 0.44$ ; 30%  $s \leq 0.40$ ), though in both cases there were no days with moisture below the wilting point. The high frequency of soil moisture above field capacity indicates that leakage losses occurred from the shallow rooting zone, though these losses were reduced with the lower soil moisture values achieved in Scenario 2 (daily seasonal irrigation).

At the mesic site, the greater storage capacity ( $nZ_r$ ) acts as a buffer against changes in irrigation and meteorological conditions. This results in a more uniform frequency distribution of soil moisture in each of the four scenarios, with low sensitivity to irrigation scheduling. While the average soil moisture at the mesic site is comparable among all four irrigation scenarios (0.361, 0.385, 0.362, and 0.359 respectively), there are

noteworthy differences in the distribution of the data. Scenario 1 exhibits bimodality at the mesic site, with high soil moisture values being attained in the winter months due to irrigation in excess of potential evapotranspiration, and low values in the summers when irrigation is insufficient to compensate for the increased rate of PET. However, scenario 2 shows a slightly narrower and more normal distribution, with a greater average value than the other three scenarios. The monthly scenarios show a wider range of soil moisture values than their daily counterparts. Moisture deficits occur during summer months immediately before an irrigation pulse, and surpluses in winter months on dates when pulses are delivered. The bimodality seen in scenario 1 is also exhibited in scenario 3, and for similar reasons, while scenario 4 has a more normal distribution, with a slightly lower average value.

Simulations were then run with varying annual total irrigation in all four scenarios at both sites, using the calibrated model and (in Scenarios 2 and 4) monthly irrigation ratios determined in the calibration. Figure 14 shows the effect of varying annual total on time-averaged soil moisture and its temporal standard deviation for the five-year simulations. At the xeric site, monthly flood irrigation (Scenarios 3 and 4) exhibited lower average  $s$  for annual inputs greater than  $\sim 1000$  mm, but similar values as the daily cases (Scenarios 1 and 2) for lower amounts. Average  $s$  increased with  $I$  for the daily applications, but leveled off for the monthly cases, an indication that the shallow soil (low  $nZ_r$ ) limited the capacity to store water. Seasonal irrigation maintained lower time-averaged  $s$  for large values of  $I$  since additional losses in summer under seasonal irrigation that are the result of the soil-moisture-dependence of ET, are greater than additional losses under constant irrigation in winter when PET rates are lower.

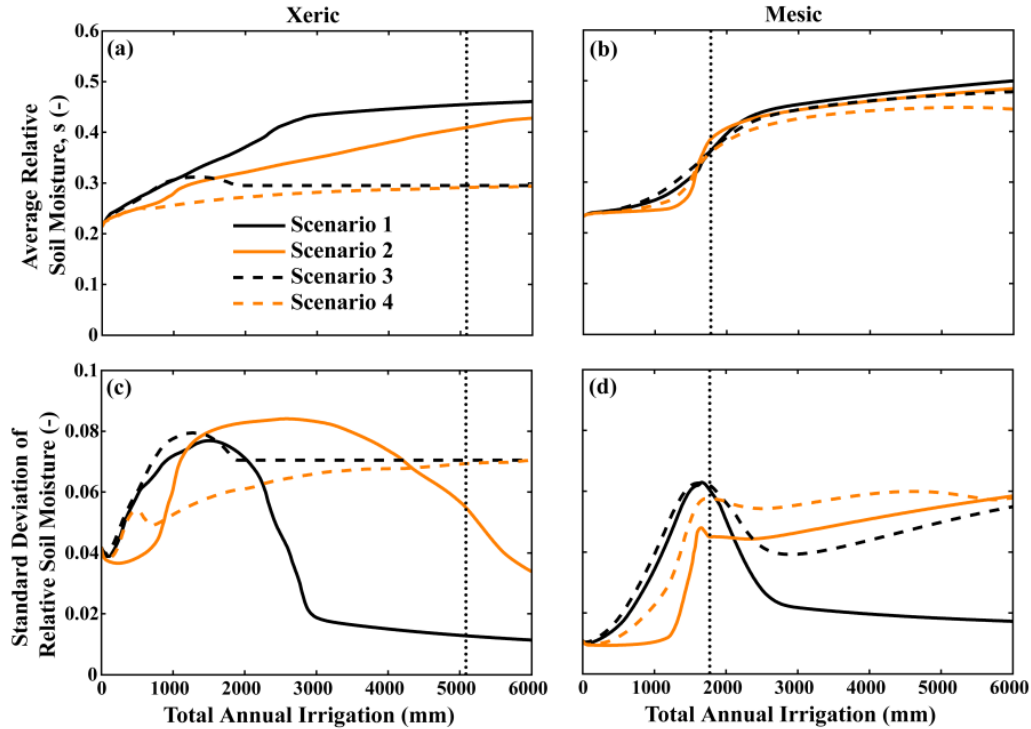


**Figure 14:** Temporal average and standard deviation of relative soil moisture for varying total annual irrigation depths using calibrated model at xeric (a, c) and mesic (b, d) sites. Dotted vertical line indicates base input from calibrations.

Furthermore, since the limiting effects of the soil field capacity are avoided with lower soil moisture in the seasonal cases, they showed greater variability than constant irrigation.

At the mesic site, all four scenarios showed similar behavior with increasing irrigation input, indicating that the deeper soil (high  $nZ_r$ ) buffered the effect of differing irrigation modes. Variability in soil moisture was lower with seasonal irrigation (Scenarios 2 and 4) than with constant (Scenarios 1 and 3) for low irrigation volumes, as irrigation patterns better matched patterns of losses through ET. This relationship reverses with  $I$  greater than  $\sim 2000$  mm as the seasonal input overcompensates for the annual pattern in ET, leading to greater variability in time. As already discussed, monthly

irrigation consistently results in greater variability due to moisture shortages and surpluses immediately preceding and following irrigation pulses, though all four scenarios showed peaks in soil moisture at similar values of  $I$  (~1600 mm).

The causes of the variation of the soil moisture statistics with annual water input for the irrigation scenarios can be discerned from a water balance partitioning analysis (e.g. Laio *et al.*, 2001b). Figure 15 shows how total water input ( $P + I$ ) is partitioned into soil evaporation below the wilting point ( $E_b$ ), stressed evapotranspiration ( $ET_s$ ), unstressed evapotranspiration ( $ET_u$ ), leakage ( $L$ ), and runoff ( $Q$ ) for varying  $I$  and constant  $P$  during a five-year simulation period.

At the xeric site, approximately 60 to 80% of water is lost to  $L$  and  $Q$  using the irrigation determined in the calibration, with greater such losses for higher input, though  $Q$  only occurs with monthly irrigation in the ranges tested for  $I$ . Large  $L$  or  $Q$  implies a sub-optimal use of irrigation water for the purpose of supporting landscape vegetation. Ideally, water is consumed by evapotranspiration that supports plant productivity with the caveat that excessive  $ET_u$  might lead to biomass production requiring higher maintenance (Stabler and Martin, 2004). These losses can be reduced with less irrigation at the xeric site, maximizing evapotranspiration components ( $E_b + ET_s + ET_u$ ) for  $I < 500$  to 1000 mm with  $< 20\%$  of water being lost to  $L$  and  $Q$ .

At the mesic site, only 10% was lost to  $L$  under each of the scenarios using the calibrated input, increasing substantially with greater input, though significant runoff losses were not triggered in the range tested. ET components were maximized for  $I < 1500$  to 1700 mm, which coincides well with the peak in the temporal variability of soil moisture. This indicates that as irrigation input increased beyond this point, loss

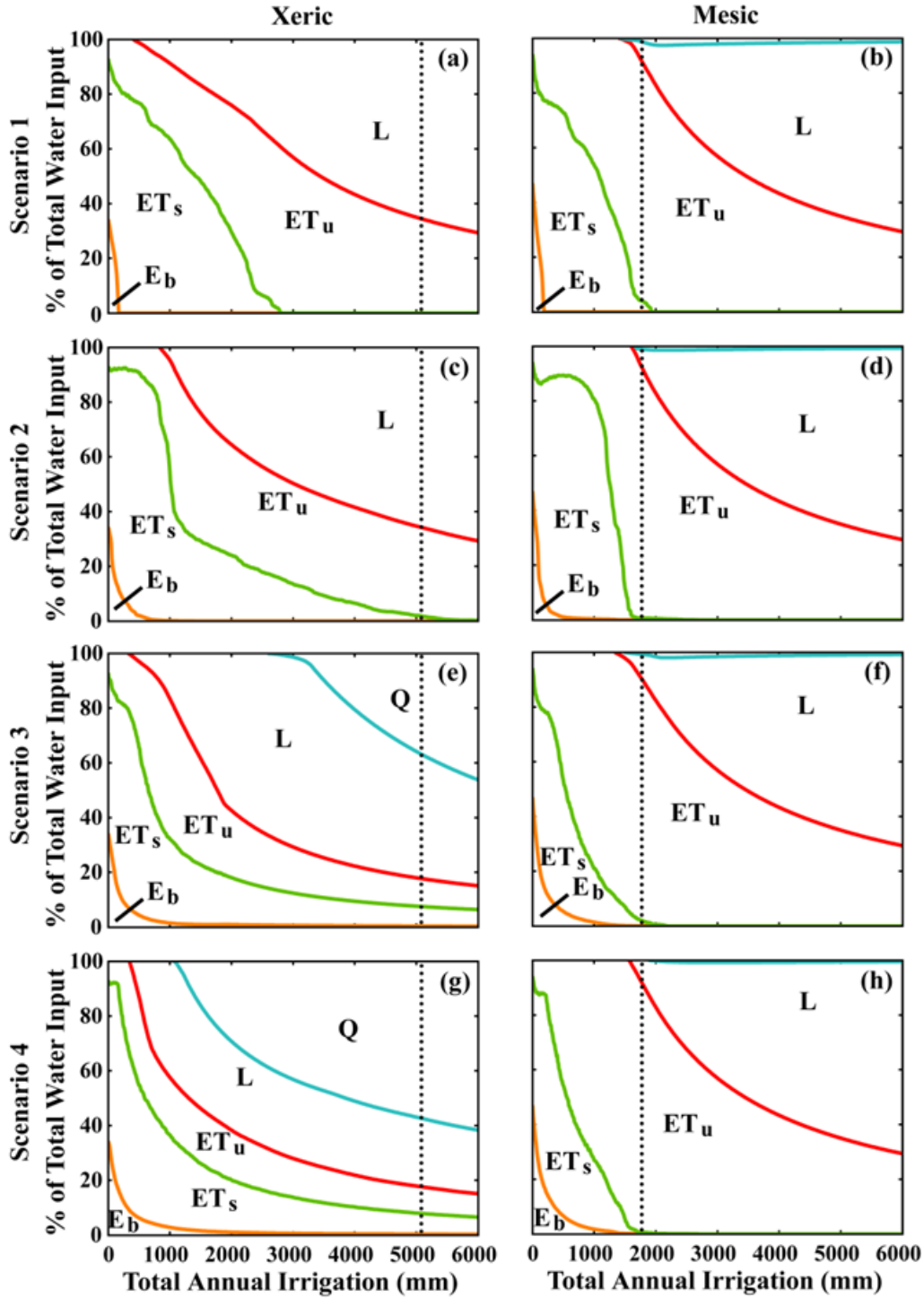


**Figure 15:** Water balance partitioning for varying annual irrigation at xeric (a, c, e, g) and mesic (b, d, f, h) sites.  $Q$  is runoff ( $s > 1$ ),  $L$  is leakage ( $s_{fc} < s \leq 1$ ),  $ET_u$  is unstressed evapotranspiration ( $s^* < s \leq s_{fc}$ ),  $ET_s$  is stressed evapotranspiration ( $s_w < s \leq s^*$ ), and  $E_b$  is bare soil evaporation below the wilting point ( $s \leq s_w$ ). Dotted vertical line indicates calibration input.

mechanisms limited peak  $s$  values and thereby decreased soil moisture variability. However, decreasing irrigation below this point increases  $E_b$ , indicating  $s$  values below the wilting point, especially with monthly irrigation (Scenarios 3 and 4). For daily irrigation, a narrow range exists ( $200 \text{ mm} < I < 1500 \text{ mm}$  for Scenario 1,  $500 \text{ mm} < I < 1500$  for Scenario 2) where both leakage losses and soil moisture values below the wilting point can both be avoided. Such a range does not clearly exist at the xeric site.

Overall, daily scenarios (1 and 2) increase ET components and reduce leakage and runoff, as compared to their monthly counterparts (3 and 4). In contrast, seasonality (Scenarios 2 and 4) has a low overall impact on the water balance as compared to constant input (Scenarios 1 and 3), though it increases stressed evapotranspiration, as explored in the following.

### 3.3 Irrigation Scenarios: Plant Water Stress

The percent of time with  $s$  between  $s_w$  and  $s^*$  provides an indication of conditions that minimize plant wilting ( $s > s_w$ ) and biomass production ( $s < s^*$ ). For non-agricultural purposes, this can be seen as a goal range, as limiting biomass production through small levels of water stress can be advantageous by reducing required maintenance while achieving small water savings. In addition, the dynamic water stress function introduced by Porporato *et al.* (2001, Equation 6 in this document) provides a time-integrated view of vegetation water deficiency. Figure 16 presents both metrics as functions of annual irrigation input for the four scenarios at both irrigated sites, as well as the impact of plant parameters  $q$  and  $k$  for Scenario 2.

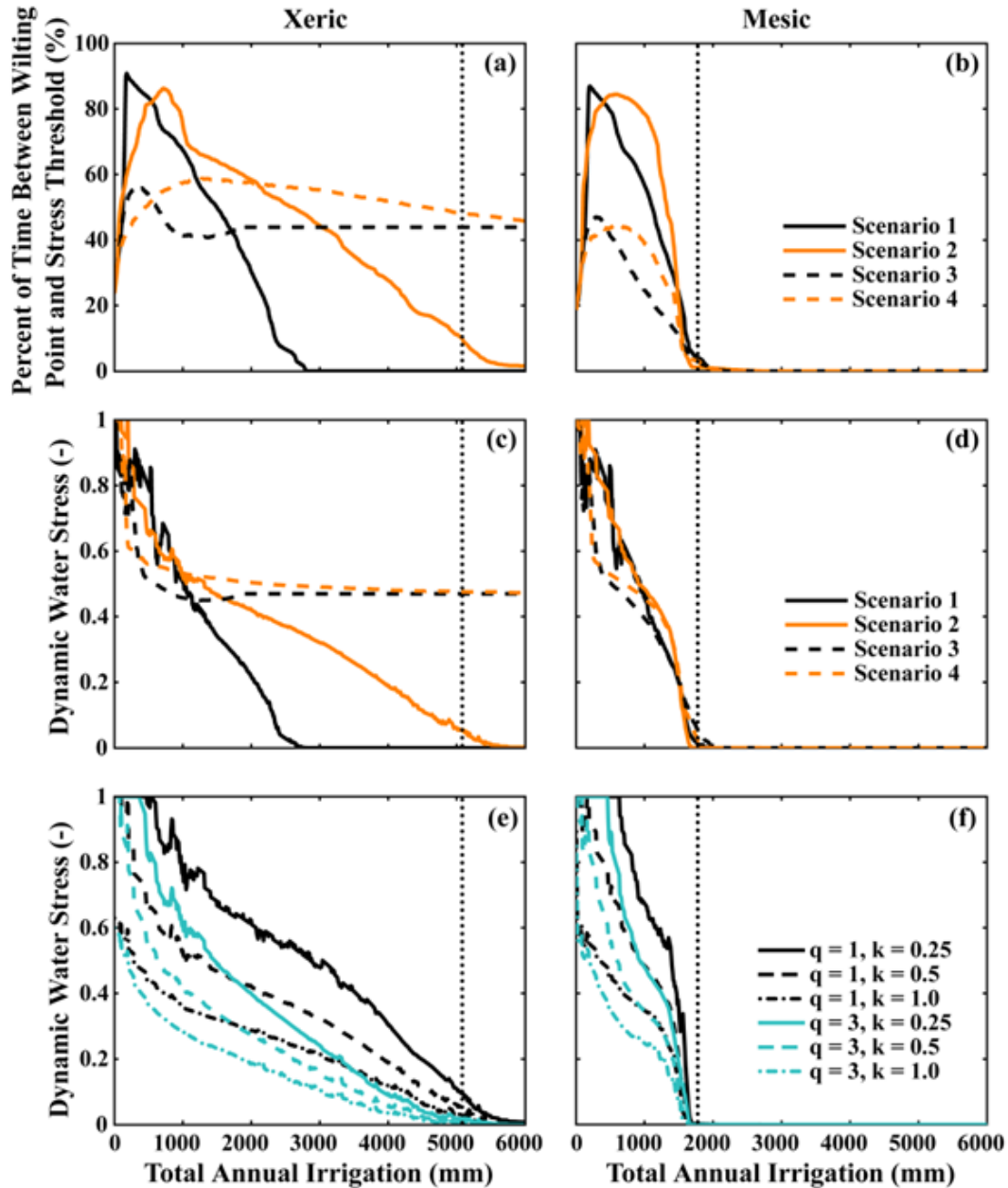


**Figure 16:** Plant water stress for xeric and mesic sites as the percentage of time with  $s_w < s \leq s^*$  (a, b), time-averaged dynamic water stress for  $q = 1$  and  $k = 0.5$  (c, d), and time-averaged dynamic water stress at different  $k$  and  $q$  for Scenario 2 (seasonal daily; e, f). Dotted vertical line indicated calibration irrigation.

At both sites, daily irrigation (Scenarios 1 and 2) provided high percentages of time (60 - 90%) with  $s_w < s \leq s^*$  for annual irrigation between 200 and 1000 mm, consistent with the high values for  $ET_s$  in Figure 15. As annual input increases, relative

soil moisture occurred more often above  $s^*$  and the percentage of time decayed to zero in most cases. Monthly applications (Scenarios 3 and 4) typically achieved lower percentages in the goal range at the mesic site, though it remained constant for high  $I$  at the xeric site due to leakage and runoff losses. Consistent with prior analyses, the higher storage capacity at the mesic site reduced differences among the scenarios, with a decay to zero percent time and  $\bar{\theta} = 0$  at 2000 mm for all cases. Irrigation seasonality at the mesic site showed little impact on dynamic water stress, but seasonal irrigation at the xeric site resulted in substantially higher stress for irrigation exceeding 2000 mm. This suggests that monthly ratios could be adjusted to redistribute annual input and better compensate for losses to ET, since constant irrigation represents a worst-case scenario in terms of plant water stress that should be only improved by tailoring an irrigation schedule to PET demands. Such an analysis is conducted in the following section. At the mesic site, a substantial increase in dynamic water stress should be expected for any decrease in irrigation input under any scenario. However, if a dynamic water stress level of approximately 0.5 or greater is deemed acceptable, water savings of approximately 500 mm could be achieved by using a monthly schedule as compared to a daily irrigation. At the xeric site, water savings of over 3000 mm can be achieved with a similar acceptable water stress under Scenario 2.

For seasonal daily irrigation (Scenario 2; other scenarios, not presented, showed similar effects), the impact of  $q$  and  $k$  on dynamic water stress are presented in Figure 16 (e) and (f). For low levels of irrigation (< 500 mm), a plant's elasticity in response to water stress ( $q$ ) and capacity to withstand prolonged stressed conditions ( $k$ ) have similar effects on dynamic water stress between the two sites. The effects, however, are



significant as plants well adapted to water stress (high  $q$  and  $k$  values) maintain moderate values for dynamic water stress ( $\bar{\theta} = 0.5$ ) even with no irrigation, while low-tolerance plants experience maximum  $\bar{\theta}$  even with as much as 600 mm of irrigation. Irrigation reductions below the calibration value (vertical dotted line) substantially increased  $\bar{\theta}$  at the mesic site regardless of plant characteristics, but impacts at the xeric site largely depended on  $q$  and  $k$ . Thus, while plant characteristics are important for moderating water stress under low irrigation at both sites, their importance dwindles as irrigation increases at the mesic site while still having a significant impact at the xeric site.

The impact of inter- and intra-annual precipitation variability on dynamic water stress was analyzed by comparing different years from the long-term record at Phoenix Sky Harbor Airport. Table 10 shows precipitation from six years selected to represent differences in annual totals at constant seasonality (1974, 1992, 2009), and differences in seasonality at constant annual total (1957, 1958, 1990). Seasonality was determined by comparing winter (October-March) and summer (April-September) precipitation. “Summer” thus includes the typically dry spring months as well as the entire summer “monsoon” season, while “winter” encompasses the moderately wet fall and winter months (see Table 1). Dynamic water stress for each of the six years at both sites is shown in Figure 17 as a function of irrigation input, using Scenario 2 (daily, seasonal input) and  $q$  and  $k$  values of 1 and 0.5, respectively.

As expected, the high  $P$  year (1992) had lower levels of plant water stress than the low  $P$  year (2009), though the difference between the high (1992) and moderate (1974)  $P$  years was small despite a 154 mm variation in  $P$ . This suggests that only extremely dry years effect urban vegetation. At large irrigation totals ( $I > 3500$  mm at xeric and  $I >$

**Table 10:** Precipitation data for years depicted in Figure 17. Summer (April-September) is compared with winter (October-March) precipitation.

<b>Year</b>	<b>Winter Rain (mm)</b>	<b>Summer Rain (mm)</b>	<b>Total Rain (mm)</b>	<b>% of Total Rain During Summer</b>
<b>2009</b>	50	33	83	40
<b>1974</b>	130	78	208	38
<b>1992</b>	213	149	362	41
<b>1957</b>	133	60	193	31
<b>1958</b>	97	110	207	53
<b>1990</b>	64	133	197	68

1200 mm at mesic sites), inter-annual precipitation variability had a negligible effect on  $\bar{\theta}$ , as irrigation instead controls plant response. Interestingly, the difference in  $\bar{\theta}$  for the dry year was more pronounced at the mesic site, suggesting that plants at the xeric site were more adapted (via  $s_w$  and  $s^*$  at constant  $q$  and  $k$ ) to these conditions. The effect of seasonality at a constant annual total illustrates that dynamic water stress was insensitive to intra-annual variations once irrigation exceeded a threshold ( $I = 800$  mm at xeric and  $I = 600$  mm at mesic sites). For low irrigation, a year with high winter (1957) or summer (1990) precipitation led to greater  $\bar{\theta}$  as compared to an even distribution (1958). In fact, the effects of a year with highly seasonal rainfall are comparable to those of a generally dry year at the xeric site. Similar  $\bar{\theta}$  at low and high  $I$  for winter- and summer-dominated years suggested that intra-annual changes were of limited importance, especially at the mesic site.

### 3.4 Optimized Irrigation Schedules

Figure 16 (c) and (d) show cases where a given annual water input (e.g. > 1000 mm at the xeric site for daily application) resulted in higher dynamic stress when applied

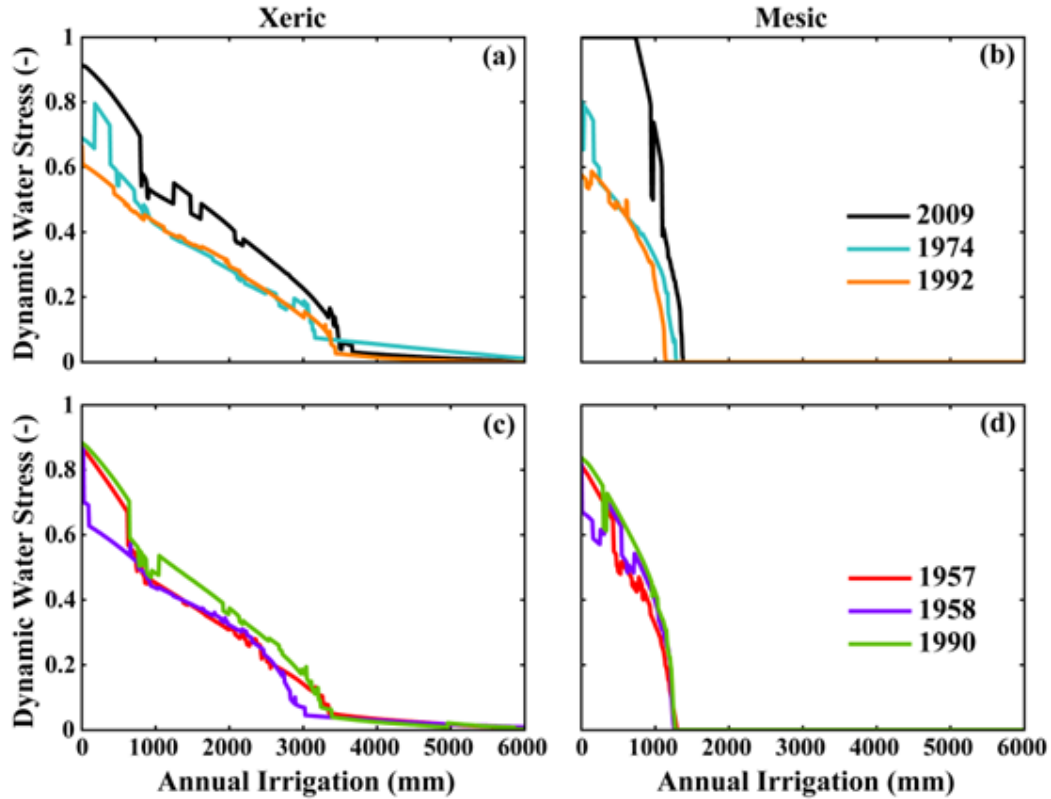


**Figure 17:** Effects of inter- and intra-annual precipitation variability on dynamic water stress for varying irrigation input among years shown in Table 10 for Scenario 2,  $q = 1$ ,  $k = 0.5$  at xeric and mesic sites. (a, b) Varying annual total and constant seasonality. (c, d) Constant annual total and varying seasonality.

at a constant rate (Scenario 1) than when varied seasonally (Scenario 2). This is because the monthly ratios used were determined through the optimization routine using soil moisture observations. Theoretically, seasonally invariant irrigation schedules should represent a worst-case scenario, with any changes to a constant schedule resulting in either less average water stress, or less water input.

The following analyses effectively reverse the previous methodology, by starting with a goal value of dynamic water stress, using the same optimization routine and calibrated model parameter values, and seeking the minimal water input necessary to achieve the target water stress. The analyses start in Scenario 1, finding a depth that can

be applied constantly throughout the year to achieve a stipulated average dynamic water stress level, then continue to find optimal monthly depths of daily input that minimize annual water use. These results show the water savings potential of seasonal irrigation, using a daily application interval. Optimizations were then performed optimizing (for minimal water use) the interval between irrigation events, as well as a single irrigation depth maintained for the entire year. First a single interval for the full year was determined, then seasonality was reintroduced by seeking an optimal irrigation interval for each season. This resulted in a schedule structure comparable to those recommended by Phoenix-area municipalities for residential irrigation. An analysis of the sensitivity of these optimized schedules to plant stress parameters  $q$  and  $k$  was also performed, though initially, respective values of 1 and 0.5 were used. For all analyses in this section, any optimization that resulted in a dynamic stress that differed from the specified value by more than 0.01 was discarded. Also, if a set of optimizations for a given case showed coincidental trends in the objective function and an optimization parameter (e.g. irrigation interval) among independent results, the bounds of that parameter were narrowed to allow for a more precise search of the parameter space to better define the global minimum.

#### 3.4.1 Fixed Interval

Figure 18 shows, for daily application, annual irrigation totals required to achieve acceptable plant water stress values  $\bar{\theta}_A = 0.0, 0.1, 0.25, 0.5, \text{ and } 0.75$ , with greater values representing a higher tolerance for seasonal senescence and potential wilting. With only one calibration parameter (annual irrigation total), the optimization routine returned

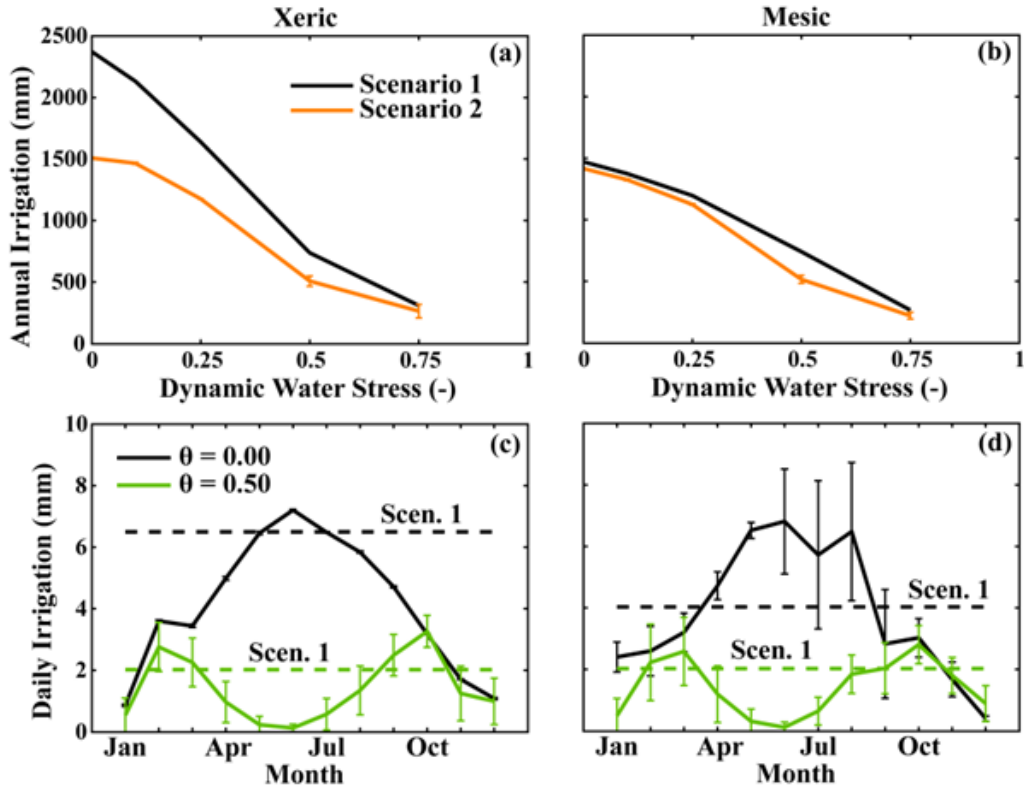


**Figure 18:** Minimized annual irrigation for several values of acceptable dynamic water stress at the xeric (a) and mesic (b) sites under Scenarios 1 and 2 (daily application,  $q = 1$ ,  $k = 0.5$ ). Schedules according to Scenario 2 (solid lines) and Scenario 1 (dashed lines) for  $\bar{\theta}_A = 0$  and 0.5 while minimizing annual input. Error bars show  $\pm$  one standard deviation from several independent optimizations for each case.

consistent results for Scenario 1 with no significant variation among independent optimizations. Annual irrigation was much lower than the calibrated irrigation at the xeric site and similar to calibrated totals at the mesic site. The relative differences from calibrated values was anticipated from the relatively high observed soil moisture (Figure 11), high percentage of water input lost as leakage (Figure 15), and sustained low plant water stress for decreased irrigation (Figure 16c) at the xeric site, as compared with the mesic. As expected, less water was required as tolerable stress increased, with the trivial case of  $\bar{\theta}_A = 1$  requiring no irrigation input.

Since schedules under Scenario 2 required twelve independent optimization parameters, the routine returned results with slight variations, especially for larger  $\bar{\theta}_A$  values. These variations are shown as error bars in Figure 18 that represent  $\pm$  one standard deviation in the annual totals determined in ten independent optimizations. The distance between the two curves represents annual water savings that can be achieved by seasonally varying irrigation. At the xeric site, the water savings is approximately 800 mm for low  $\bar{\theta}$ , though this expectedly decreases with larger  $\bar{\theta}$  as both scenarios converge to zero irrigation at  $\bar{\theta} = 1$ . Mesic landscaping, however, exhibited lower water savings (100 to 500 mm) with a seasonal schedule. This difference was attributed to the greater storage capacity at the mesic site, which allowed it to carryover soil water across seasons, reducing the need for irrigation to match current ET, whereas the xeric site was limited to using soil water within a season.

The annual schedule determined for two  $\bar{\theta}_A$  values at each site is shown in Figure 18 (c) and (d), with  $\pm$  one standard deviation as error bars. Constant daily irrigation (Scenario 1) is shown as a horizontal line for reference, with water savings due to seasonal irrigation represented as the area between the horizontal lines and curves of the same color. As expected, low stress tolerance requires considerably higher irrigation during the summer months, with the mesic site showing more variability due to its greater storage capacity. Variability increases during the summer months at the mesic site as increased PET reduces soil moisture, thereby increasing storage availability. Water can either be applied in winter months and carried over for summer use, or applied to match ET rates, with no difference in losses to either ET or leak. This same reasoning could be used to support the use of less frequent irrigation schedules at the mesic site.

The seasonal schedules for  $\bar{\theta}_A = 0.5$  exhibited an unexpected outcome that is consistent for both sites. The optimized schedule with moderate stress tolerance prescribes decreased input during the winter to match reduced PET rates, but also dictates a decrease in the summer months. Since PET is higher in the summer, applied water is removed from the rooting zone faster, resulting in a greater time-integrated stress value. Thus an increment of applied water is more effective at maintaining soil moisture at or above the stress threshold in the winter months than in the summer. And so, without any stipulation on when the tolerable water stress can be imposed, the most efficient season to reduce water input (in terms of effect on plant water stress) is during the summer months, resulting in the bimodal schedules observed in Figure 18. In short, irrigation is limited in summer when plant health is more difficult to maintain due to greater PET, but matches PET to minimize water stress throughout the rest of the year.

### 3.4.2 Optimized Interval

While the above analysis only considered daily irrigation, it is possible to use the interval between irrigation events as an optimization parameter to determine schedules with a degree of flexibility greater than that found in the idealized schedules, which included only daily or monthly irrigation. However, due to the daily time-step of the model and the necessity of using precise values in the optimization routine to determine a globally minimized objective function, irrigation intervals with decimal values used by the routine posed a challenge. To overcome this, the number of days since the last irrigation event was counted, and the next event was scheduled only when the whole number of days was greater than the appropriate multiple of the irrigation interval. Thus

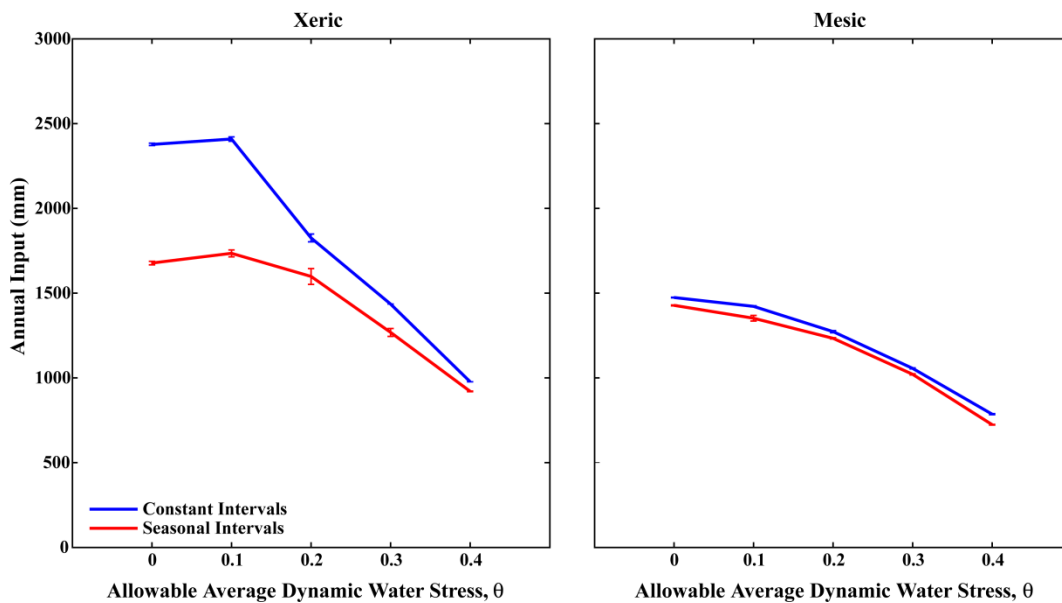
if irrigation was applied on Day 0 and the interval were 2.6 days, watering events would occur on Day 3 ( $2.6 \times 1 = 2.6$ ), Day 6 ( $2.6 \times 2 = 5.2$ ), Day 8 ( $2.6 \times 3 = 7.8$ ), and so on. For seasonally varying irrigation, the first event of the new season was scheduled by comparing the time since the last event to the interval of the new season, or for the first day of the season if the new interval had already elapsed since the last event. For example, if the last event of the winter season had occurred on March 24, the next event would occur on April 1 if the spring interval were eight days or fewer, or one day later for each additional interval day, regardless of the winter interval. This method ensured that the interval of each season was actually observed, rather than encountering legacy effects from seasons with long intervals that happened to have an event scheduled very late in the season.

Table 11 shows the results of optimizations that sought a single irrigation interval and depth to be maintained for the entire year at each site to minimize water input with several levels of acceptable water stress. The annual totals determined from these schedules are compared to similar values determined with seasonally varying irrigation intervals in Figure 19. These results are similar in magnitude and trend to those presented in Figure 18 (a) and (b) from the case of maintaining a constant daily interval while varying only the application depth. A noteworthy exception is the case of  $\bar{\theta}_A = 0.1$  at the xeric site where annual water input increases despite a higher tolerance of water stress. There are two possible explanations for this behavior: (1) inefficiency in searching the parameter space for  $\bar{\theta}_A = 0.1$  as compared to 0.0, and (2) water savings being achieved in the case of  $\bar{\theta}_A = 0.0$  due to the non-negative nature of the stress function, allowing for a wider range of moisture conditions than those necessary to produce a precise positive  $\bar{\theta}$



**Table 11:** Intervals that minimize water use while maintaining an acceptable level of dynamic water stress for seasonally constant application. Results are from ten independent optimizations for each case with  $q = 1$  and  $k = 0.5$ .

$\bar{\theta}_A$	Xeric		Mesic	
	Average Interval (d)	Standard Deviation (d)	Average Interval (d)	Standard Deviation (d)
<b>0</b>	1.01	0.02	1.06	0.07
<b>0.1</b>	4.12	0.54	26.27	4.21
<b>0.2</b>	1.09	0.13	48.72	3.80
<b>0.3</b>	1.33	0.02	66.03	5.44
<b>0.4</b>	1.47	0.02	59.94	6.77



**Figure 19:** Average minimized annual irrigation totals used to achieve various levels of acceptable dynamic water stress, using a constant and seasonally varying irrigation interval ( $q = 1$ ,  $k = 0.5$ ). Error bars show  $\pm$  one standard deviation from several independent optimizations for each case.

value. Future analyses should consider a more thorough search of the parameter space while using an objective function that utilizes only positive values of  $\bar{\theta} - \bar{\theta}_A$ . Such a function would seek irrigation schedules that keep water stress at or below the given value, rather than just equaling it. This would ensure that any water input greater than that for a lower stress value would be due to problems searching the parameter space.


The interval schedules resulting in the annual totals depicted in Figure 19 are shown in Figure 20. As expected from previous analyses, highly frequent irrigation is necessary at the xeric site to maintain low stress levels, with intervals increasing when  $0 \leq \bar{\theta}_A \leq 0.2$ . Interestingly, the seasonal intervals for  $\bar{\theta}_A = 0.3$  are statistically indistinguishable from those for  $\bar{\theta}_A = 0.0$ . This indicates that the decrease in annual total between these values seen in Figure 19 is the result of a decrease in irrigation depth. Since irrigation depth is held constant throughout the year in these scenarios, Figure 20 further indicates moderate stress levels throughout the year for  $\bar{\theta}_A = 0.3$ , which is clearly not the case for  $\bar{\theta}_A = 0.4$ . Similar to results presented in Figure 18 (c), this higher stress value and the accompanying decrease in water input are achieved by severely limiting irrigation during the summer months. The mesic site shows a gradual inversion as  $\bar{\theta}_A$  increases from more frequent irrigation in the spring and summer to more frequent application in the cooler fall and winter months. Here, changes in irrigation interval are a major contributor to decreased water use with increased stress tolerance, as opposed to results seen at the xeric site. When compared with the relatively narrow error bars in Figure 19, the high variation at the mesic site reiterates the scheduling flexibility afforded by the larger storage capacity there.

The irrigation guide shown in Figure 21 is available from the website for the Water – Use It Wisely campaign ([wateruseitwisely.com/region/arizona](http://wateruseitwisely.com/region/arizona)), and is linked to from several local municipal websites (e.g. cities of Phoenix, Gilbert, Scottsdale, Tempe, and Mesa). The intervals recommended for desert-adapted shrubs are similar to those determined for low stress levels at the xeric site ( $\bar{\theta}_A = 0.1$  or  $0.2$ ). (Note that winter season is shown at the left of Figure 20, but at the right of Figure 21.) Interestingly, the

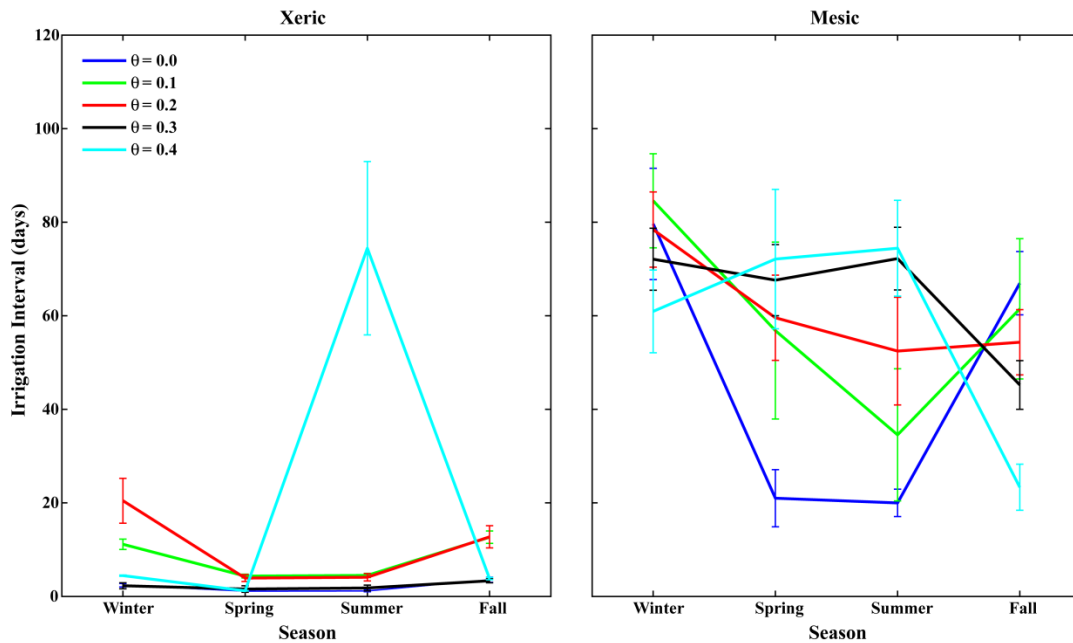


**Figure 20:** Schedule of irrigation intervals that minimize water input for acceptable levels of dynamic water stress. Error bars show  $\pm$  one standard deviation.

annual schedule determined for moderate stress ( $\bar{\theta}_A = 0.4$ ) is comparable to that recommended for cool season grass, which is consistent with the interpretation of such a schedule allowing for high plant stress in summer months while matching PET rates throughout the rest of the year. The intervals determined at the mesic site are generally higher than recommendations for high water-use plants, but similar to those for desert-adapted plants, particularly in the spring and summer seasons. Table 12 converts the recommendation intervals and depths for certain plant types to annual totals by assuming mid-points of the ranges given and 90-day seasons. Though the recommended intervals are comparable to those determined in the above analysis, the event depths are far greater. This results in annual totals far greater than those determined from the model, and even significantly greater than the higher totals calculated from the irrigation depths in the initial model calibrations discussed in Section 3.2. Thus these recommendations may be



## LANDSCAPE WATERING GUIDELINES

How Much & How Often <small>Water to the outer edge of the plant's canopy and to the depth indicated. Watering frequency will vary depending on season, plant type, weather and soil.</small>		Seasonal Frequency — Days Between Waterings				Water This Deeply (Typical Root Depth)
		Spring Mar - May	Summer May - Oct	Fall Oct - Dec	Winter Dec - Mar	
<b>Trees</b>	Desert adapted	14-30 days	7-21 days	14-30 days	30-60 days	24-36 inches
	High water use	7-12 days	7-10 days	7-12 days	14-30 days	24-36 inches
<b>Shrubs</b>	Desert adapted	14-30 days	7-21 days	14-30 days	30-45 days	18-24 inches
	High water use	7-10 days	5-7 days	7-10 days	10-14 days	18-24 inches
<b>Groundcovers &amp; Vines</b>	Desert adapted	14-30 days	7-21 days	14-30 days	21-45 days	8-12 inches
	High water use	7-10 days	2-5 days	7-10 days	10-14 days	8-12 inches
<b>Cacti and Succulents</b>		21-45 days	14-30 days	21-45 days	if needed	8-12 inches
<b>Annuals</b>		3-7 days	2-5 days	3-7 days	5-10 days	8-12 inches
<b>Warm Season Grass</b>		4-14 days	3-6 days	6-21 days	15-30 days	6-10 inches
<b>Cool Season Grass</b>		3-7 days	none	3-10 days	7-14 days	6-10 inches

These guidelines are for established plants (1 year for shrubs, 3 years for trees). Additional water is needed for new plantings or unusually hot or dry weather. Less water is needed during cool or rainy weather. Drip run times are typically 2 hours or more for each watering.

**Figure 21:** Landscape watering guidelines from the Water – Use It Wisely campaign website, referenced by several municipal websites in the Phoenix metropolitan area.

**Table 12:** Conversion of recommendations from Water – Use it Wisely campaign (Figure 21) to annual totals.

Plant Type	# of Irrigation Events				events/yr	mm/event	mm/yr
	Spring	Summer	Fall	Winter			
<b>Desert-Adapted Shrubs</b>	4	6	4	2	16	21	<b>8534</b>
<b>Warm Season Grass</b>	10	20	6	4	40	8	<b>8128</b>
<b>Cool Season Grass</b>	18	0	13	9	40	8	<b>8128</b>

well beyond plant demands as determined by PET rates, and could result in large water losses through deep infiltration beyond the active rooting zone.

Since these results are thought to be highly dependent on the plant stress parameters  $q$  and  $k$ , a sensitivity analysis was performed to investigate their effects, with the results presented in Figure 22. As expected, the analysis showed no difference among different combinations of stress parameters for  $\bar{\theta}_A = 0.0$ , since  $q$  and  $k$  are only used when

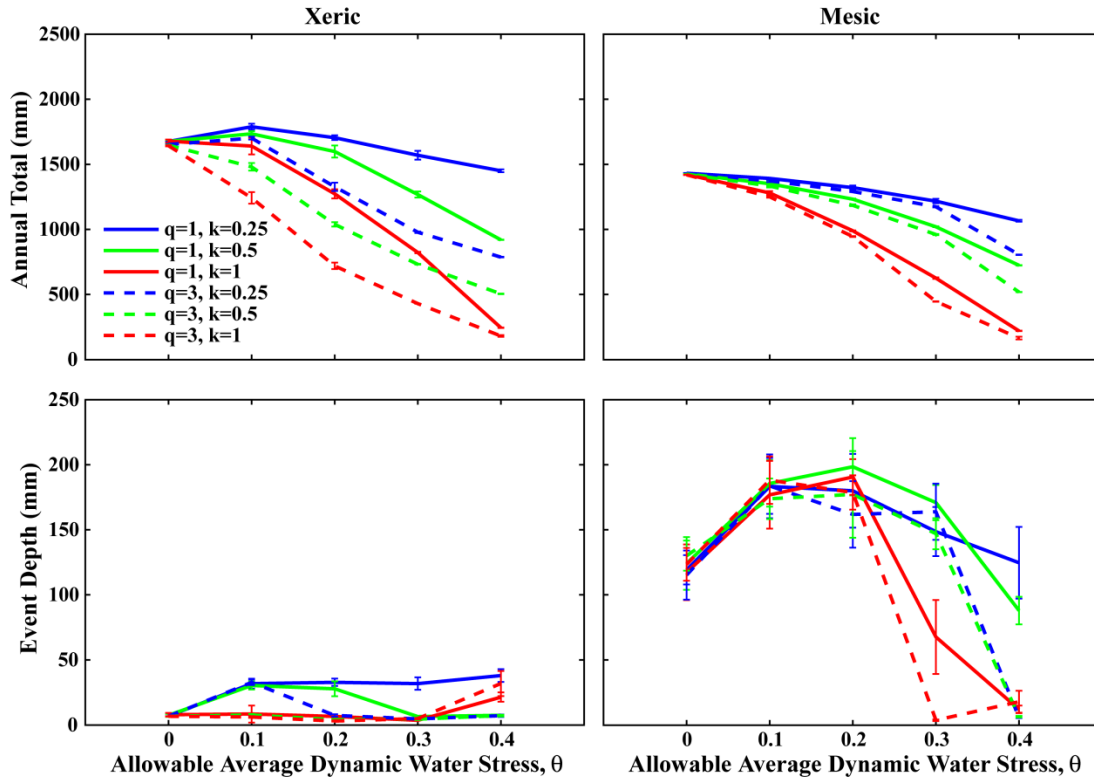


**Figure 22:** Results of sensitivity analysis on plant stress parameters  $q$  and  $k$ . Annual total (a and b) is determined by both event depth (c and d) and irrigation interval (not presented).

soil moisture is below the stress threshold, thereby inducing a positive stress value. The plant stress capacity parameter  $k$  had a large effect on irrigation scheduling at both sites, while the elasticity parameter  $q$  had a pronounced impact at the xeric site, but little at the mesic. This difference between the sites may be due to the relatively small separation between the wilting point and stress threshold at the mesic site. Since  $q$  determines the relative impact of water stress on a plant between the two points, a small range would decrease the sensitivity to  $q$ . Panel (d) shows that for low stress at the mesic site, differences in irrigation input among plant types should be achieved not by varying event depth, but instead by the irrigation interval. This supports the structure of the municipal recommendations in Figure 21 that focus on varying intervals with less variation among

event depths, and none between low and high water-use plants of the same class (tree, shrub, or groundcover). The xeric site, however, shows more sensitivity to  $q$  and  $k$  in event depth, suggesting that schedules carefully tailored to specific plants may be more important with a xeric landscape.

Figure 23 shows the difference in annual water input between irrigation with and without seasonality for several values of  $q$ ,  $k$ , and  $\bar{\theta}_A$ . At the xeric site, potential savings are high for low  $\bar{\theta}_A$  but decrease quickly as  $\bar{\theta}_A$  increases for plants with high  $q$  and  $k$ . This is due to the ability of these plants to withstand low moisture conditions in the non-seasonal case. For poorly adapted plants, however, water savings of several hundred mm are still possible with low positive dynamic stress levels at the xeric site. As  $\bar{\theta}_A$  reaches moderate values, water savings decrease since the ability of the seasonal schedule to match PET rates and stave off water shortages decreases in importance. Water savings at the mesic site were small and relatively constant in  $q$ ,  $k$ , and  $\bar{\theta}_A$ , with little basis for a statistically significant difference among the cases presented. This further supports the conclusion that the greater storage capacity and ability to carryover water across seasons at the mesic decreases the importance of seasonally matching irrigation to PET rates.

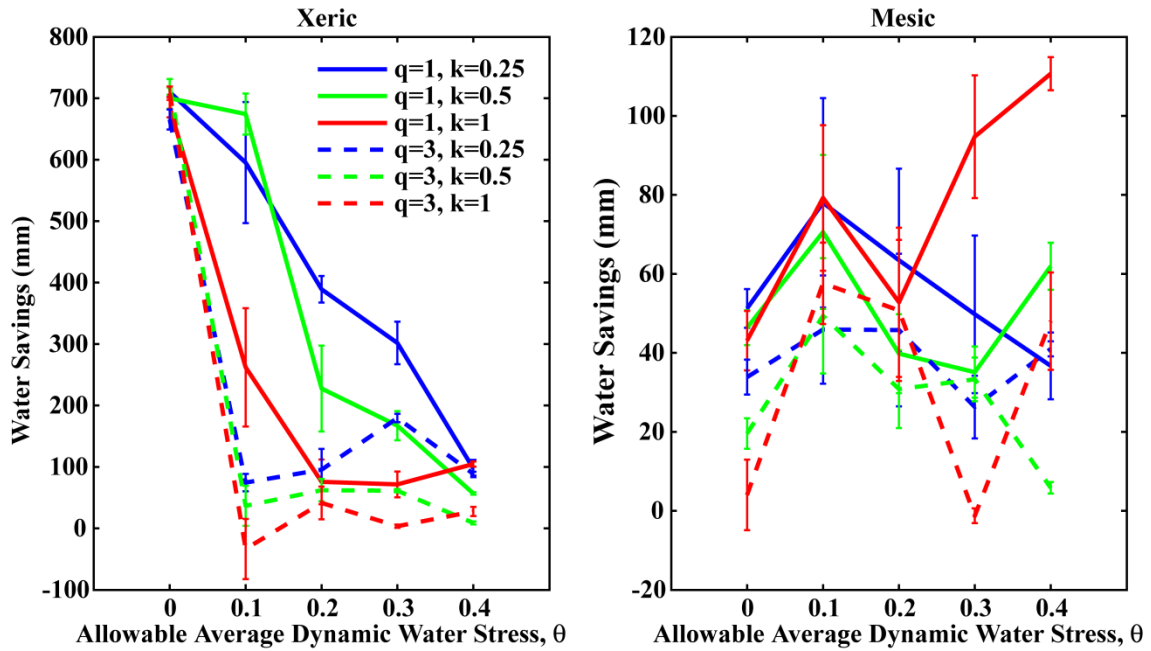


**Figure 23:** Annual water saved with seasonal irrigation compared to seasonally constant for the same plant stress parameters and level of dynamic water stress. Error bars show  $\pm$  one standard deviation.

## 4 CONCLUSIONS AND FUTURE WORK

In this study, a point-scale model of soil moisture dynamics was used to capture a set of observations from non-irrigated and irrigated landscaping treatments in the Phoenix metropolitan area, based on daily precipitation and potential evapotranspiration forcing. An automated routine for parameter calibration was implemented to identify the soil and vegetation conditions that best matched the observed records at each site, including a set of monthly factors describing daily irrigation. The modeled soil moisture time series fit well with observations, evidenced by a low RMSE and good visual fit. Differences in slopes of recession limbs supported the use of model forcing that included seasonally varying PET, an addition made here to the originally published model. The calibration process yielded parameter values within reasonable ranges consistent with site conditions. In particular, the soil storage capacity at the mesic site ( $nZ_r$ ) was found to be larger than at the xeric site, as inferred from a narrower range of observed soil moisture values, and a smaller response to wetting events. This yielded large differences between the two sites in irrigated response.

Four idealized irrigation scenarios were then simulated using the calibrated model at each site, with results explored in terms of soil moisture dynamics, water balance partitioning, and plant water stress. The low storage capacity at the xeric site requires frequent irrigation to avoid large losses to runoff and leakage and maintain moderate levels of plant stress. A seasonal schedule is preferable to reduce annual input while maintaining a tolerable plant water stress level. Inter- and intra-annual precipitation variations have limited impacts for irrigated xeric sites, except during dry years and for



years with no seasonality. The mesic site exhibited less sensitivity to irrigation scheduling in terms of soil moisture levels and plant water stress due to the higher soil storage capacity of the treatment. Small water savings can be achieved using monthly flood-style pulses instead of daily irrigation. The irrigated mesic site was more vulnerable to develop dynamic water plant stress in years with extremely low rainfall but exhibited low sensitivity to precipitation seasonality. Overall, the seasonal scheduling of daily irrigation input was found to be more important at the xeric site than at the mesic site to minimize water losses, while maintaining an optimal soil moisture range.

The optimization routine was then used to determine irrigation schedules that minimized water input for a range of tolerable values of dynamic water stress. Initial simulations using constant daily irrigation were found to require less water than was determined in the original model calibration, and much less than annual totals recommended by local municipalities. Further optimizations using seasonally varying irrigation depths found opportunity for substantial water savings at the xeric site only, with little potential for decreased irrigation at the mesic for comparable values of water stress. For low stress tolerance, high summer irrigation of  $\sim 7$  mm/d and low winter irrigation of  $\sim 1$  mm/d fulfills minimizes water input at each site. For moderate stress tolerance, a bimodal irrigation pattern was found, with less daily irrigation in the summer and winter and higher irrigation in the transition periods. This novel irrigation strategy is a result of accepting some water stress while evaporative demands peak, while only supplementing precipitation to match PET through the rest of the year.

Another set of irrigation schedules was determined by instead varying the irrigation interval while maintaining a constant depth throughout the year; local

municipalities use such a structure in their irrigation recommendations. Results were similar to the previous analysis in that seasonal scheduling was more beneficial at the xeric site than the mesic. Also, for moderate stress levels, reduced irrigation in the warmer summer months was found to minimize water input at both sites. For low stress levels, water savings through increased allowable plant water stress were found to be achieved at the xeric site through decreased event depth, but at the mesic site an increased event depth, combined with an increased interval between irrigation events was found to be preferable. The xeric site showed greater potential for water savings through optimized irrigation scheduling that considers seasonally varying PET rates. These results were highly dependent on plant stress parameters, with such schedules showing greater benefit to plants poorly adapted to conditions of water shortage.

These results are limited by the relatively small sample size of sensor locations used, and by the limited forcing data available (particularly irrigation) that instead needed to be determined from the soil moisture time series. If the experiment were repeated, rain gauges should be placed at each neighborhood, and irrigation schedules should be recorded at a daily or perhaps hourly scale. Additional soil moisture sensors along vertical profiles would also improve understanding of water fluxes in the active rooting zone. The point-scale model does not account for spatial heterogeneities, but does allow for the consideration of irrigation depths at points where plants are located. A spatially distributed model would allow for spatial heterogeneities in water distribution and plant life. Additionally, as discussed in section 2.1, the daily time step disallows for the investigation of interactions between fluxes (e.g. irrigation and evapotranspiration) at sub-daily time scales. A study of such interactions would require ET data of higher

resolution, potentially using actual ET rates from eddy-covariance techniques. Plant growth dynamics and plant mortality are not modeled, though this could be corrected by adjusting the optimization function for the alternative irrigation schedules by weighting seasons differently to prioritize low static water stress values during times of the year when plants experience active growth. This work could also be improved by a better understanding of how plant stress parameters  $k$  and  $q$  relate to ecophysiological processes such as plant conductance, cavitation, and plant water storage. Finally, the precise numerical results found here are specific to the study site, though optimized irrigation schedules could be determined for another site using similar methods if soil and vegetative parameters are known.

The current results can also serve as a basis for several possible avenues of further research. One possibility is to adjust the climatic forcing to investigate the effects of climate change on urban irrigation demands. A second would be to test the optimized irrigation schedules in the field, observing the effects on plant health. Additionally, an understanding of the effective areas of the irrigation systems at the two sites could be used with the results of this study to allow for a comparison of xeric and mesic irrigation in volumetric terms. Finally, the methods described here could also be the basis for a public-access tool that determines optimal irrigation schedules for a given soil type, landscape design, climate, and acceptable plant water stress level.

Despite the limitations in the precision of the data and model in this study, the consistencies in the data within each neighborhood and the differences in data between neighborhoods still allow for several recommendations for homeowners and landscape managers in desert urban areas. First, a xeric landscape with irrigation that does not vary

seasonally is highly susceptible to either lose considerable water to leakage or even runoff in the winter months, or else experience significant and potentially permanent damaging effects due to water shortages in the summer months. Second, municipal recommendations should be seen as representing a high estimate of plant water needs. For a xeric site, water conservation is better achieved by decreasing event depth from these recommendations, while for a mesic site, it may be preferable to instead increase the interval between irrigation events. Finally, for either type of landscape design, if moderate levels of plant water stress are deemed acceptable, it may be beneficial to not only decrease irrigation input in the winter to match decreased rates of PET, but also during summer months when PET rates are high. Such a bimodal irrigation schedule essentially allows for higher stress levels in months when high PET rates require much greater water input in order to maintain low stress levels.

These results could have substantial implications for residential outdoor water use in desert cities. According to these results, urban landscape irrigation could be reduced to approximately a quarter of municipal recommendations under certain circumstances. By emphasizing irrigation schedules based on rates of PET, landscape managers could not only achieve substantial water savings, but also link water usage rates to local climatic conditions, which are largely uncoupled currently in the Phoenix area. This would decrease dependence on the buffering capacity of distant water sources, enhancing water security. Furthermore, increased promotion of the potential savings that can be achieved through more carefully designed irrigation schedules may increase the water consciousness of the general public, which may help foster a culture of more responsible

water use, and a water policy that ensures continued benefit from water resources for future generations.

## REFERENCES

Balling RC, Gober P. 2007. Climate variability and residential water use in the city of Phoenix, Arizona. *Journal of Applied Meteorology and Climatology* 46: 1130-1137. DOI: 11.1175/JAM2518.1.

Balling RC, Gober, P, Jones N. 2008. Sensitivity of residential water consumption to variations in climate: An intraurban analysis of Phoenix, Arizona. *Water Resources Research* 44: W10401. DOI: 10.1029/2007WR006722.

Brown PW. 2005. *Standard reference evapotranspiration: A new procedure for estimating reference evapotranspiration in Arizona*. Cooperative Extension Publication AZ1324, University of Arizona, Tucson. 12 pp.

Campbell HE, Johnson RM, Larson EH. 2004. Prices, devices, people, or rules: The relative effectiveness of policy instruments in water conservation. *Review of Policy Research* 5: 637-662.

Caylor KK, Manfreda S, Rodríguez-Iturbe I. 2005. On the coupled geomorphological and ecohydrological organization of river basins. *Advances in Water Resources* 28: 69-86. DOI: 10.1016/j.advwatres.2004.08.013.

Chow WTL, Brazel AJ. 2012. Assessing xeriscaping as a sustainable heat island mitigation approach for a desert city. *Building and Environment* 47: 170-181. DOI: 10.1016/j.buildenv.2011.070.27

Clapp RB, Hornberger GM. 1978. Empirical equations for some soil hydraulic properties. *Water Resources Research* 14: 601-604.

Coates D, Connor R, Leclerc L, Rast W. 2012. Water demand: What drives consumption? In: *The United Nations World Water Development Report 4: Managing Water under Uncertainty and Risk*. Paris, UNESCO. 44-76.

Drought in Perspective. 2013. Retrieved July 6, 2013, from <http://phoenix.gov/waterservices/wrc/yourwater/climchange/perspective>

Duan QY, Gupta VK, Sorooshian S. 1993. Shuffled complex evolution approach for effective and efficient global minimization. *Journal of Optimization Theory and Applications* 76: 501-521. DOI: 10.1007/BG00939380

Grimm NB, Foster D, Groffman P, Grove JM, Hopkinson CS, Nadelhoffer K, Peters D, Pataki DE. 2008. The changing landscape: Ecosystem responses to urbanization and pollution across climatic and societal gradients. *Frontiers in Ecology and the Environment* 6: 264-272. DOI: 10.1890/070147

Grimmond CSB, Roth M, Oke TR, Au YC, Best M, Betts R, Carmichael G, Cleugh H, Dabberdt W, Emmanuel R, Freitas E, Fortuniak K, Hanna S, Klein P, Kalkstein LS, Liu

- CH, Nickson A, Pearlmutter D, Sailor D, Voogt J. 2010. Climate and more sustainable cities: climate information for improved planning and management of cities (producers/capabilities perspective). *Procedia Environmental Sciences* 1: 247-274. DOI: 10.1016/j.proenv.2010.09.016.
- Hirt P, Gustafson A, Larson KL. 2008. The mirage in the Valley of the Sun. *Environmental History* 13: 482-514.
- Jacobs KL, Holway JM. 2004. Managing for sustainability in an arid climate: Lessons learned from 20 years of groundwater management in Arizona, USA. *Hydrogeology Journal* 12: 52-65.
- King EG, Caylor KK. 2011. Ecohydrology in practice: strengths, conveniences, and opportunities. *Ecohydrology* 4: 608-612. DOI: 10.1002/eco.248.
- Laio F, Porporato A, Fernández-Illescas CP, Rodríguez-Iturbe I. 2001a. Plants in water-controlled ecosystems: active role in hydrologic processes and response to water stress IV. Discussion of real cases. *Advances in Water Resources* 24: 745-762.
- Laio F, Porporato A, Ridolfi L, Rodríguez-Iturbe I. 2001b. Plants in water-controlled ecosystems: active role in hydrologic processes and response to water stress II. Probabilistic soil moisture dynamics. *Advances in Water Resources* 24: 707-723.
- Laio F, Porporato A, Ridolfi L, Rodríguez-Iturbe I. 2002. On the seasonal dynamics of mean soil moisture. *Journal of Geophysical Research* 107: D15, 4272. DOI: 10.1029/2001JD001252.
- Larsen L, Harlan S. 2005. Desert dreamscapes: Residential landscape preference and behavior. *Landscape and Urban Planning* 78: 85-100.
- Larson KL, Casagrande D, Harlan SL, Yabiku ST. 2009. Residents' yard choices and rationales in a desert city: Social priorities, ecological impacts, and decision tradeoffs. *Environmental Management* 44: 921-937. DOI: 10.1007/s00267-009-9353-1.
- Logan MF. 2006. *Desert Cities: The Environmental History of Phoenix and Tucson*. University of Pittsburgh Press: Pittsburgh, PA. 228 pp.
- Manfreda S, Scanlon TM, Caylor KK. 2010. On the importance of accurate depiction of infiltration processes on modeled soil moisture and vegetation water stress. *Ecohydrology* 3: 155-165. DOI: 10.1002/eco.79.
- Martin, CA. 2001. Landscape water use in Phoenix, Arizona. *Desert Plants* 17: 26-31.
- Martin, CA, Stabler LB. 2002. Plant gas exchange and water status in urban desert landscapes. *Journal of Arid Environments* 51: 235-254. DOI: 10.1006/yjare.2001.0946.

Martin CA, Peterson KA, Stabler L. 2003. Residential landscaping in Phoenix, Arizona, U.S.: Practice and preferences relative to covenants, codes, and restrictions. *Journal of Arboriculture* 29: 9-16.

Martin, CA, Busse K, Yabiku S. 2007. North Desert Village: The effect of landscape manipulation on microclimate and its relation to human landscape preferences. *HortScience* 42: 853.

Martin, CA. 2008. Landscape sustainability in a Sonoran Desert city. *Cities and the Environment* 1(2): 1-16.

Mayer PW, DeOreo WB (Eds.). 1999. *Residential End Uses of Water*. American Water Works Association Research Foundation: Denver, CO. 352 pp.

McCarthy HR, Pataki DE. 2010. Drivers of variability in water use of native and non-native urban trees in the greater Los Angeles area. *Urban Ecosystems* 13: 393-414. DOI: 10.1007/s11252-010-0127-6.

Mitchell VG, Cleugh HA, Grimmond CSB, Xu J. 2008. Linking urban water balance and energy balance models to analyse urban design options. *Hydrological Processes* 22: 2891-2900. DOI: 10.1002/hyp.6868.

Pataki DE, Boone CG, Hogue TS, Jenerette GD, McFadden JP, Pincetl S. 2011. Socio-ecohydrology and the urban water challenge. *Ecohydrology* 4: 341-347. DOI: 10.1002/eco.209.

Porporato A, Laio F, Ridolfi L, Rodríguez-Iturbe I. 2001. Plants in water-controlled ecosystems: active role in hydrologic processes and response to water stress III. Vegetation water stress. *Advances in Water Resources* 24: 725-744.

Porporato A, Laio F, Ridolfi L, Caylor KK, Rodríguez-Iturbe I. 2003. Soil moisture and plant stress dynamics along the Kalahari precipitation gradient. *Journal of Geophysical Research* 108(D3): 4127. DOI: 10.1029/2002JD002448.

Rodríguez-Iturbe I, Porporato A. 2004. *Ecohydrology of Water-Controlled Ecosystems: Soil Moisture and Plant Dynamics*. Cambridge University. 442 pp.

Sadler J, Bates A, Hale J, James P. 2010. Bringing cities alive: The importance of urban green spaces for people and biodiversity. In: Gaston K (ed). *Urban Ecology*. Cambridge University Press, Cambridge. 230-260.

SRP: Canal origins. 2013. Retrieved April 27, 2013, from <http://www.srpnet.com/water/canals/origins.aspx>

Stabler LB, Martin CA. 2004. Irrigation and pruning affect growth water use efficiency of two desert-adapted shrubs. *Acta Horticulturae* 638: 255-258.



U.S. Census Bureau. 2010. *2010 Demographic profile AZ – Maricopa County and AZ – Pinal County*. Retrieved July 26, 2013 from [www.census.gov/popfinder](http://www.census.gov/popfinder)

Vico G, Porporato A. 2011. From rainfed agriculture to stress-avoidance irrigation: II. Sustainability, crop yield, and profitability. *Advances in Water Resources* 34: 272-281. DOI: 10.1016/j.advwatres.2010.11.011.

Walker JS, Grimm NB, Briggs JM, Gries C, Dugan L. 2009. Effects of urbanization on plant species diversity in central Arizona. *Frontiers in Ecology and the Environment* 7: 465-470. DOI: 10.1890/080084

White R, Havlak R, Nations J, Pannkuk T, Thomas J, Chalmers D, Dewey D. 2004. *How Much Water is Enough? Using PET to Develop Water Budgets for Residential Landscapes*. Texas Water Resources Institute: College Station, TX. 8 pp.

Yabiku ST, Casagrande DG, Farley-Metzger E. 2008. Preferences for landscape choice in a Southwestern desert city. *Environment and Behavior* 40: 382-400. DOI: 10.1177/0013916507300359.

APPENDIX A

NORTH DESERT VILLAGE IMAGES

This appendix describes images of and information on the North Desert Village (NDV) landscape experiment at the Arizona State University Polytechnic campus in East Mesa, Arizona. Data from the site are included in a separate appendix. Images are stored on an external hard drive entitled Volo\_Thesis\_Appendices in the folder AppendixA. There are four folders within AppendixA.

Volo\_Thesis\_Appendices/AppendixA/vegetation contains two files, provided by Dr. Chris Martin, with information on vegetation at NDV. NDV Tree List.doc contains a list of all trees at each of the four landscaped neighborhoods: mesic, oasis, xeric, and native. The number of each species in the yards of each of the houses is shown, as well as in the common area within each neighborhood. Species totals for each neighborhood are also provided. NDV\_vegetation.xlsx lists all trees and shrubs at NDV as of the 2005 installation of the four neighborhoods. The spreadsheet contains fields to keep track of whether the plants are still alive at the site, though this has not been updated since 2009. It is possible that Dr. Martin has an updated version, though this nonetheless provides a useful list of the species present at each of the neighborhoods. The eight fields in the spreadsheet are described below:

**site\_id:** a single letter to denote neighborhood (C: control, M: mesic, N: native, O: oasis, X: xeric), followed by either the 4-digit address of the house whose yard the specimen is in, or “common” to denote the common area of the neighborhood.

**plant\_id:** 3-digit unique identifier

**taxon\_id:** 4-letter code to identify species

**existing:** Y/N to denote if plant still exists as of most recent update

**date\_missing:** date plant identified as missing

**notes:** miscellaneous historical information

**assigned\_plant\_id:** a unique identifier comprised of three parts: a single letter to denote neighborhood (see **site\_id**), a single letter to denote tree (T) or shrub (S), and a 2-digit number.

**scientific\_name:** genus and species of plant specimen

The folder Volo\_Thesis\_Appendices/AppendixA/diagrams contains a diagram for each of the four designed neighborhoods (mesic.jpg, native.jpg, oasis.jpg, xeric.jpg).

These show the locations of the houses, streets, and walkways at each neighborhood, as well the locations of all the trees. Also shown are the locations of the micrometeorological stations that included sensors for air temperature and wind speed. The micrometeorological stations also contain solar panels and batteries, as well as the data loggers used for the sensors at the station and in the ground. The diagrams also show the locations of the soil moisture sensors, which are accompanied by thermocouples to measure soil temperature.

The folder Volo\_Thesis\_Appendices/AppendixA/images2006 contains images provided by Dr. Stevan Earl relating to the installation of the micrometeorological stations in the four NDV neighborhoods in 2006. All three show the xeric site. Two show the channels dug for the cables from the soil moisture sensor locations to the micrometeorological station. The third shows one of the two CS-616 soil moisture sensors placed in the soil at 30 cm before being buried. Thermocouples to determine soil temperatures, as well as heat flux sensors, can also be seen.

The folder Volo\_Thesis\_Appendices\_AppendixA/images2011 contains a folder for each of the four designed neighborhoods with images taken by the author in November 2011:

images2011/mesic: 3 images of the common area with houses in the background. mesic1.jpg faces north from the southern end of the common area. mesic2.jpg is taken from the same location but faces east. mesic3.jpg faces south from the north end of the common area. The micrometeorological station can be seen in mesic1.jpg and mesic3.jpg.

images2011/native: 3 images of the common area. native1.jpg faces south and shows the central saguaro cactus with homes in the background. The micrometeorological station can be seen through the creosote bush in the foreground left. native2.jpg faces north and shows the saguaro and micrometeorological station. The golf course to the north of NDV can be seen in the background. native3.jpg faces northeast and again shows the common area with the golf course in the background.

images2011/oasis: 3 images of the common area (oasis1.jpg through oasis3.jpg) showing turf grass islands within area of gravel base, with the first two also showing the micrometeorological station. Two additional images show examples of the irrigation system: drip irrigator at the base of a tree (oasis4.jpg) and the piping for the sprinkler system that indicates the boundary of the turf grass island (oasis5.jpg).

images2011/xeric: 2 images looking south from the north side of the common area. xeric1.jpg faces southwest, and xeric2.jpg faces southeast and shows the micrometeorological station.

APPENDIX B

NORTH DESERT VILLAGE DATA

This appendix describes data collected from the micrometeorological stations at the North Desert Village (NDV) landscape experiment. The actual data files are stored on an external hard drive entitled Volo\_Thesis\_Appendices in the folder AppendixB. While this thesis only used soil moisture data from the xeric and mesic neighborhoods, data is also included from the oasis and native sites, as well as other datasets (e.g. air temperature, soil heat flux) collected at all four neighborhoods. There are three folders, plus two additional files within AppendixB.

Volo\_Thesis\_Appendices/AppendixB/climate contains the full data collected from the micrometeorological stations at NDV, stored as one .xlsx file for each of the four neighborhoods. In addition to above-ground temperature measurements, each station included two sets of sensors at 30 cm depth, with each set consisting of a soil heat flux sensor, a soil moisture sensor, and a thermocouple. The relative locations of the stations and the soil sensors can be seen in the diagrams folder described in Appendix A. Data is available from April 10, 2006 to June 15, 2010, though there are gaps in the data that vary among the four sites. Data was recorded at hourly intervals. The spreadsheet contains the following fields, with units in parentheses where applicable:

**sample\_date:** date of data entry

**sample\_time:** time of data entry

**battery\_voltage:** voltage of battery at time data entry was taken (V)

**panel\_temp:** temperature within the data logger enclosure (° C)

**air\_temp:** air temperature 2 m above the soil (° C)

**soil\_temp1:** first soil temperature at 30 cm (° C)

**soil\_temp2:** second soil temperature at 30 cm (° C)

**volum\_water1:** first volumetric water content at 30 cm ( $\text{m}^3_{\text{water}}/\text{m}^3_{\text{soil}}$ )

**volum\_water2:** second volumetric water content at 30 cm ( $\text{m}^3_{\text{water}}/\text{m}^3_{\text{soil}}$ )

**soil\_heat\_flux1:** first heat flux at 30 cm (mW)

**soil\_heat\_flux2:** second heat flux at 30cm (mW)

**surf\_temp\_mean:** average surface temperature measured by an infrared sensor at 2 m pointing down at 45° (° C)

**surf\_temp\_max:** maximum surface temperature measured by an infrared sensor at 2 m pointing down at 45° (° C)

**surf\_temp\_min:** minimum surface temperature measured by an infrared sensor at 2 m pointing down at 45° (° C)

The units of milliwatt for the soil heat flux may be in error, since heat fluxes are typically expressed as a rate of energy transfer per unit area. The magnitude of the measurements suggests the proper units may be  $\text{W}/\text{m}^2$ .

Volo\_Thesis\_Appendices/AppendixB/sm\_hourly contains hourly soil moisture data from each of the four neighborhoods at NDV. The same data is included in the spreadsheets in the climate folder described above, though here it is in .csv format. The fields are unlabeled, but are ordered as follows:

**year:** 4-digit year

**month:** 1-12

**day:** 1-31

**hour:** 0-23

**volumetric soil moisture 1:** first soil moisture sensor

**volumetric soil moisture 2:** second soil moisture sensor



The file hourly2daily.m is a MATLAB aggregating script used to convert hourly soil moisture data from the above files to daily averages. It also inputs lines for dates without data, showing “NaN” for both soil moisture values on such days. The script pulls data from one of the .csv files described above and outputs a .txt file similar to those described below.

The folder Volo\_Thesis\_Appendices/AppendixB/sm\_daily contains daily soil moisture data from each of the four neighborhoods at NDV. The fields are unlabeled, but are ordered as follows:

**datenum:** a 6-digit number used by MATLAB to represent a date

**volumetric soil moisture 1:** first soil moisture sensor

**volumetric soil moisture 2:** second soil moisture sensor

**year:** 4-digit year

**month:** 1-12

**day:** 1-31

Subsets of these data files with shorter periods used for calibration purposes are pulled from these files and described in Appendix E.

The file water\_meter.xlsx contains monthly water meter readings for the irrigation systems at the xeric, oasis, and mesic sites. Dates of readings are shown with cumulative gallons used at each site. These readings apply only to the outdoor irrigation systems, and not indoor use within the homes at NDV. However, the irrigation systems at the mesic and oasis sites are comprised of different types of outlets (e.g. sprinkler heads of differing capacity or a combination of sprinkler heads and drip irrigators). Furthermore, changes to the frequency and duration of irrigation events were not documented and so a higher

resolution of irrigation scheduling cannot be determined. Finally, in order to convert these volumetric data to measures of depth would require the effective area of each irrigation system.

## APPENDIX C

### PRECIPITATION AND POTENTIAL EVAPOTRANSPIRATION DATA

This appendix describes data used in this thesis and stored on an external hard drive entitled Volo\_Thesis\_Appendices in the folder AppendixC. Precipitation and potential evapotranspiration (PET) data for the duration of the NDV landscape experiment (2006-2010) was taken from the Arizona Meteorological Network (AZMET) stations at Queen Creek and Mesa. Long-term precipitation and PET data from Phoenix Sky Harbor Airport and the AZMET Phoenix Encanto station, respectively, were used for the optimized irrigation schedules discussed in section 3.4. The AppendixC folder contains one folder for each of the two data sources: AZMET and SkyHarbor.

### **C.1 Arizona Meteorological Network**

Data was accessed through the AZMET website: <http://ag.arizona.edu/azmet/az-data.htm>. “Daily Raw Data” (as labeled on the website) was obtained for years 2006-2011 at the Queen Creek and Mesa stations. The .txt files containing these data are included in the respective station folders in the AppendixC folder on the external hard drive. These files have been processed to remove repeated days (duplicative data entries). Full documentation for these days can be found through the AZMET website at <http://ag.arizona.edu/azmet/raw2003.htm>. The only AZMET data used for this thesis were daily precipitation and PET records. The file AZMET\_formatting.m in the AppendixC/AZMET folder has three purposes: it compiles several years of data into a single file, extracts only precipitation and PET values, and enters an additional for any missing dates with “NaN” as data entries. The output is a .txt file that contains the following fields:

**year:** 4-digit year

**month:** 1-12

**day:** 1-31

**daily precipitation:** (mm)

**daily PET:** (mm)

These files are also included in the respective station folders with the names QC\_compiled\_ET-P.txt and MESA\_compiled\_ET-P.txt.

Days with missing data at the Queen Creek station were filled in with data from the Mesa station to complete a full 5-year record, included as AZMET/QC/QC\_ET-P\_5yr.txt. Data files of shorter duration used for model calibration and testing are subsets of this file.

PET data in the Phoenix area is generally inaccessible before the 1990's. Thus, daily averages from recent data were used to coincide with long-term precipitation data from Phoenix Sky Harbor Airport. Thirteen years of data from the Phoenix Encanto AZMET station were used, accessed from <http://ag.arizona.edu/azmet/15.htm> under "ETo Special Reports". The file AZMET/Encanto/LT\_ET.xlsx includes daily PET data, in inches, from the Encanto station for the years 1999-2011. The first two columns show daily averages from those 13 years, in mm, for 365- and 366-day years, respectively. These averages were used as a proxy for actual PET records in the precipitation sensitivity analysis in section 3.3. These averages were also repeated in an appropriate pattern of 365- and 366-day years to determine a 61-year schedule of averaged daily PET values, used in the long-term irrigation studies described in section 3.4.

## **C.2 Phoenix Sky Harbor Airport**

Long-term daily precipitation data was obtained from the National Climatic Data Center (NCDC) station 023183: Phoenix Sky Harbor International Airport. A 61-year record is included in SkyHarbor/SH\_ET-P\_61yr.txt, with the 61-year PET schedule described in the previous section. The file includes fields for 4-digit year, month, date, precipitation (mm), and PET (mm).

APPENDIX D

GIS DATA

This appendix describes a repository of GIS data used in the creation of Figure 2 of this thesis, stored on an external hard drive entitled Volo\_Thesis\_Appendices in the folder AppendixD.

The following shapefiles were used to create Figure 2a, the map of Arizona and its surrounding states.

NA\_CEC\_Sonoran.shp: Sonoran desert

usa\_state\_boundaries.shp: detailed state boundaries within the U.S.

phoenix.shp: location of the city of Phoenix, Arizona

dtl\_cntry\_ln.shp: detailed outline of countries of the world (used for Mexican coasts)

The following shapefiles were used to create Figure 2b, the map of the Phoenix metropolitan area:

generalized\_cities.shp: Phoenix area generalized city boundaries, with small plots outside city limits and fine details smoothed out

AZMET.shp: locations of Queen Creek and Mesa AZMET stations

Airport.shp: location of Phoenix Sky Harbor Airport

NDV.shp: location of North Desert Village landscape experiment

Additionally, a geo-referenced image of the Phoenix area from Google Earth was used.

The image is included as georefphx.jpg and the coordinates of the four points marked on the image for geo-referencing are listed in the file controlpoints.txt. The coordinate system used is GCS\_WGS\_1984.

Figure 2c of NDV and its immediate surroundings was created from a simple image from Google Earth and is not geo-referenced. The original image is included as NDV.jpg.



## APPENDIX E

### SOIL MOISTURE BALANCE AND OPTIMIZATION SCRIPTS

This appendix describes the MATLAB scripts used in this thesis and stored on an external hard drive entitled Volo\_Thesis\_Appendices in the folder AppendixE.

### **E.1 Model Calibration and Testing**

The Shuffled Complex Evolution automated optimization routine by Duan *et al.* (1993), as written for MATLAB, contains two optimization scripts, plus an initializing script. The optimization scripts sceua.m and cceua.m work together to minimize an objective function in multi-dimensional parameter space. They both call a function functn.m that returns a single value that is to be minimized. In the case of these model calibrations, the objective function to be minimized is the RMSE between the observed and modeled soil moisture time series. The initialization of the optimization script will be described below, followed by a description of the soil moisture balance model scripts. Results of the model calibration and testing will also be discussed.

The initialization script optim\_swb.m requires several user-specified inputs, described below and identified in italics. The optimization script requires the bounds for the parameter space, contained in the arrays *bl* and *bu* (for lower and upper bounds), with each column representing a different variable parameter. Sets of parameter values are chosen from within the parameter space, and passed to the objective function as *x* (determined by the script from the parameter space, not user-specified). The script uses *ngs* complexes, or groups of sets of parameter values (multiple *x*'s). More complexes will more thoroughly search the parameter space, but will increase computation time. The routine works in loops, with each loop consisting of many trials of the objective function while competitively evolving the parameter values to achieve minimum objective values

within each complex. Between loops, sets of parameter values are shuffled to form new complexes, then the new complexes are re-evolved in the next loop to search for global, as opposed to merely local, minima in the parameter space. The routine will discontinue searching the space when one of three conditions is met: the number of trials reaches the specified *maxn*, the normalized geometric range of the parameter space being searched is smaller than the specified *peps*, or the objective function fails to improve by *pcento* percent in *kstop* loops. Throughout this thesis, use of the routine was designed such that the third of these conditions was the exclusive reason for an end to an optimization run. Repeated results can be achieved by setting an initial seed *iseed* and setting *seedflg* to 1. A *seedflg* of zero will begin with a random seed, which is useful when running several consecutive optimizations to test for parameter convergence and sensitivity, as was done repeatedly in this thesis. An initial parameter set *x0* can be used by setting *iniflg* to 1.

Additional user-specified variables used here include the number of calibration runs to be performed *opt\_runs*, and *sensor* (1, 2, or 3, for non-irrigated xeric, irrigated xeric, or mesic, respectively). The latter of these two is passed from the initialization script through the optimization scripts to the objective function script, which uses the variables to obtain the correct soil moisture record. After *opt\_runs* optimizations are performed, the final values for the objective function and the parameter set used to reach that minimum, for each of the *opt\_runs* optimizations, are exported into a .txt file.

The objective function script *functn.m* pulls the appropriate meteorological forcing and soil moisture data based on the *sensor* variable. (Different precipitation records were used between the xeric and mesic sites, as described in section 2.3.) Model parameters are established from the parameter set *x* and, for irrigated sensors, irrigation is

added to precipitation according to the monthly values in  $x$ . The combined water input and model parameters are then passed to the `soil_loop.m` function to determine the modeled soil moisture time series. The `soil_loop.m` function calls the `et_func.m` and `leak_func.m` functions to determine losses to ET and leakage. After the modeled soil moisture time series is determined, the RMSE between that and the observed series is computed and returned to the optimization script.

Results on which this thesis is based are included in the “calibrations/thesis\_results” folder. These results can be repeated by entering the appropriate parameter bounds from Tables 4, 6, and 8 for  $bl$  and  $bu$  and using an  $ngs$  of approximately 20. Results will not be identical due to the random seed, but averages among several optimization runs should be similar. All scripts necessary for the calibrations are properly positioned within the AppendixE folder to allow for a calibration to be run by executing an `optim_swbX.m` script ( $X = 1, 2, \text{ or } 3$  for the three sensors) from the AppendixE/calibrations folder in a MATLAB terminal. Data is pulled from the calibrations/data folder, which contains appropriate subsets of the data described in Appendix B and Appendix C. Results are output into the calibrations/results folder. For the irrigated sensors, a series of calibration exercises, each consisting of multiple runs, would need to be performed as described in section 3.1.2 and 3.1.3. Each exercise would decrease the size of the parameter space from the bounds in Tables 5 and 7. Bounds on irrigation parameters found in Tables 6 and 8 can be maintained through the entire process. In this manner, the results shown below can be shown from the optimization process, using the specified parameter bounds:

Parameter	Units	Symbol	Lower Bound	Optimized Value	Upper Bound
<b>Xeric Site, Non-Irrigated</b>					
Porosity*Rooting Depth (#)	[mm]	$nZ_r$	20	347	$3.2 \times 10^3$
Hygroscopic Point (+)	[-]	$s_h$	0	0.133	0.15
Wilting Point (#)	[-]	$s_w$	0.15	0.221	0.25
Stress Threshold (#)	[-]	$s^*$	0.25	0.310	0.45
Bare Soil Evaporation (+)	[mm/d]	$E_w$	0.01	0.347	0.40
Depth of 8/28 Storm (#)	[mm]	$D_{8/28}$	0	67.84	100
Initial Soil Moisture	[-]	$s_0$	0.15	0.203	0.75
<b>Xeric Site, Irrigated</b>					
Field Capacity (+)	[-]	$s_{fc}$	0.4	0.429	0.75
Pore Size Distribution Index (+)	[-]	$b$	1	2.54	10
Saturated Hydraulic Conductivity (+)	[mm/d]	$K_s$	1	$1.94 \times 10^3$	$1 \times 10^4$
Initial Soil Moisture	[-]	$s_0$	0.15	0.460	0.75
<b>Mesic Site, Irrigated</b>					
Porosity*Rooting Depth	[mm]	$nZ_r$	20	$2.0 \times 10^3$	$3.2 \times 10^3$
Wilting Point	[-]	$s_w$	0.15	0.236	0.24
Stress Threshold	[-]	$s^*$	0.24	0.248	0.42
Depth of 8/28 Storm	[mm]	$D_{8/28}$	0	47.1	100
Initial Soil Moisture	[-]	$s_0$	0.15	0.313	0.75

“+” indicates applicability to all sites. “#” are applied only at one site (xeric or mesic).

	Xeric			Mesic		
	Lower Bound	Average	Upper Bound	Lower Bound	Average	Upper Bound
$I_{Jan}$ (mm/d)	0.1	1.35	10	0	0.03	10
$I_{Feb}$ (mm/d)	0.1	1.87	10	0	1.54	10
$I_{Mar}$ (mm/d)	0.1	5.42	10	0	4.70	10
$I_{Apr}$ (mm/d)	0.1	12.42	20	0	8.12	10
$I_{May}$ (mm/d)	0.1	36.73	100	0	8.65	10
$I_{Jun}$ (mm/d)	0.1	41.59	100	0	10.37	20
$I_{Jul}$ (mm/d)	0.1	43.82	100	0	9.36	20
$I_{Aug}$ (mm/d)	0.1	8.81	10	0	6.13	10
$I_{Sep}$ (mm/d)	0.1	6.06	10	0	2.94	10
$I_{Oct}$ (mm/d)	0.1	4.55	10	0	5.07	10
$I_{Nov}$ (mm/d)	0.1	2.50	10	0	1.29	10
$I_{Dec}$ (mm/d)	0.1	1.05	10	0	0.00	10

These parameter values have been saved in the file AppendixE/parameters.m and are used for the remainder of the analysis. The function model\_test.m can be used with one input parameter (sensor number 1, 2, or 3) to output the RMSE for the model testing period for each sensor, as defined in each of subsection of section 3.1. The calibration figures in this thesis (10, 11, and 12, with insets) can be created using the function AppendixE/calibrations/calibration.m with a single input parameter of 1, 2, or 3 to indicate the sensor (non-irrigated xeric, irrigated xeric, or mesic, respectively).

## **E.2 Idealized Irrigation Scenarios**

The folder AppendixE/scenarios contains several MATLAB scripts used to create the figures contained in this thesis relating to the idealized irrigation scenarios presented in sections 3.2 and 3.3. The files are listed below, with the corresponding figure it creates, and information on embedded functions. All are written to be executable from a MATLAB terminal in the “scenarios” folder. None require any input arguments. Data for these simulations, which generally use different time periods than the calibrations, is pulled from the folder AppendixE/scenarios/data. All meteorological forcing data found therein are subsets of data found in Appendix C

**fig\_schematic.m:** Figure 9.

**fig\_freqdist.m:** Figure 13. Calls the function soilmoist.m, which returns the modeled soil moisture time series using any of the four irrigation scenarios and the annual irrigation totals determined in the calibrations.

**fig\_sm\_stats:** Figure 14. Calls the function `sm_scale.m`, which is similar to `sm_irr.m`, but scales irrigation input according to the ratio between the annual total from the calibrations and a specified value.

**fig\_partition:** Figure 15. Calls the function `part_scale.m`, which returns the partitioning of the water balance among loss functions, based on a specified irrigation scenario and annual irrigation total

**fig\_stress:** Figure 16. Calls the function `zeta_scale.m`, which is similar to `sm_scale.m` and `part_scale.m`, but returns the time series of static plant water stress for a given  $q$  value. Also calls the function `dyn_stress.m`, which determines an average dynamic water stress value based on a time series of static water stress and a given  $k$  value.

**fig\_precip\_sens:** Figure 17. Calls the function `zeta_histyr.m`, which determines a static plant water stress time series using the precipitation record from a specific year.

### **E.3 Optimized Irrigation Schedules**

This section discusses optimizations for four different schedule structures. Two maintain daily irrigation, while two use longer irrigation intervals. One of the daily schedule structures uses the same irrigation depth throughout the year while the other varies that depth each month. Of the other two, one maintains the irrigation interval while the other varies it seasonally, though both of these latter two maintain a constant irrigation depth throughout the year. The differences among the structures of the model forcing necessitate different scripts to compute the soil moisture time series and the objective function. They are therefore stored in separate folders within AppendixE/opt\_

sched, each with its own optimization scripts. The following summarizes the differences among the four types of optimizations:

<b>Folder</b>	<b>Interval</b>	<b>Event Depth</b>
<b>opt_sched1</b>	daily	constant (optimized)
<b>opt_sched2</b>	daily	vary monthly
<b>opt_sched3</b>	constant (optimized)	constant (optimized)
<b>opt_sched4</b>	vary seasonally	constant (optimized)

As described in section 2.6, the objective function for these optimizations is different than in the calibrations, and the scripts are accompanied by an additional irr\_stats.m function. This function reports, for the final optimized parameter set in each optimization run, the total annual irrigation input and dynamic water stress value, in addition to the objective function that is a combination of the two. Otherwise, these optimization scripts work similar to those in the calibrations, and can be run by executing the optim\_swb.m script in a MATLAB terminal within one of the opt\_sched# folders.

For the daily schedules, results are stored in an Excel spreadsheet in the appropriate opt\_sched# folder. The sheets of the spreadsheet follow the following naming convention:

A.##, where

A represents the site, X for xeric or M for mesic, and

## represents the acceptable dynamic plant water stress value  $\bar{\theta}_A$ .

Results are summarized below in tabular form, but are presented graphically in Figure 18, with standard deviations among several independent optimizations. The script fig\_daily\_irr.m in the AppendixE/opt\_sched folder can be executed to create Figure 18.



<b>Site:</b>	<b>Xeric</b>					<b>Mesic</b>				
$\bar{\theta}_A$ :	<b>0.00</b>	<b>0.10</b>	<b>0.25</b>	<b>0.50</b>	<b>0.75</b>	<b>0.00</b>	<b>0.10</b>	<b>0.25</b>	<b>0.50</b>	<b>0.75</b>
<i>Constant Event Depth</i>										
<b>Total (mm/yr)</b>	2371	2131	1638	738	310	1471	1374	1196	740	266
<i>Depth Varied Monthly</i>										
<b>Jan (mm/d)</b>	0.86	0.69	0.86	0.54	1.17	2.4	2.73	3.06	0.5	1.01
<b>Feb (mm/d)</b>	3.6	2.97	3.33	2.76	3.64	2.6	3.64	3.02	2.23	0.63
<b>Mar (mm/d)</b>	3.44	2.84	3.1	2.26	0.27	3.21	3.33	3.26	2.59	0.45
<b>Apr (mm/d)</b>	4.99	5.42	5.24	0.97	0.16	4.72	4.86	3.85	1.2	0.47
<b>May (mm/d)</b>	6.46	6.56	6.5	0.23	0.4	6.52	4.41	4.14	0.32	0.84
<b>Jun (mm/d)</b>	7.2	6.59	1.11	0.12	0.24	6.81	5.59	1.06	0.12	0.75
<b>Jul (mm/d)</b>	6.48	6.26	1	0.57	0.32	5.72	2.18	0.1	0.65	0.56
<b>Aug (mm/d)</b>	5.84	6.29	7.27	1.35	0.08	6.48	2.82	3.96	1.85	0.35
<b>Sep (mm/d)</b>	4.71	4.68	4.31	2.49	0.12	2.83	6.54	7.13	2.04	0.25
<b>Oct (mm/d)</b>	3.18	3.22	3.12	3.27	0.22	3.03	3.56	2.89	2.81	0.18
<b>Nov (mm/d)</b>	1.71	1.38	1.71	1.25	1.14	1.68	1.8	2.76	1.81	0.68
<b>Dec (mm/d)</b>	1.08	1.2	1.09	0.99	1.14	0.41	2.21	1.78	0.89	1.15
<b>Total (mm/yr)</b>	1508	1465	1176	508	264	1415	1325	1125	515	223

The optimizations using a variable irrigation interval were conducted using several combinations of values for plant stress parameters  $q$  and  $k$ . Results are stored in Excel spreadsheet in the appropriate opt\_sched# folder, with one spreadsheet for each site (Xeric.xlsx, Mesic.xlsx). The sheets of the spreadsheet follow the following naming convention:

qXkYtZ, where

X is the value for  $q$  (1 or 3),

Y is 100x the value for  $k$  (25, 50, or 100 for  $k = 0.25, 0.50, \text{ or } 1.00$ )

Z is 10x the value for  $\bar{\theta}_A$  (0, 1, 2, 3, or 4, for  $\bar{\theta}_A = 0.0, 0.1, \text{ etc.}$ ).

Results for  $q = 1$  and  $k = 0.5$  are shown in Figures 19 and 20 and in tabular form below.

These figures can be re-created for any combination of  $q$  and  $k$  values using the

MATLAB scripts AppendixE/opt\_sched/fig\_ann\_2site.m and AppendixE/opt\_sched/fig\_

int\_2site.m, respectively (enter  $k$  and  $q$  values in the first few lines of code where designated). Alternatively, six-panel figures showing results for all  $q$  and  $k$  values at one site can be produced using the scripts fig\_ann\_1site.m and fig\_int\_1site.m in the same folder. These scripts access .txt files in the opt\_sched/opt\_sched4 folder that contain the data from Excel files necessary for the figures. The .txt files use the same naming convention as the Excel worksheets, excluding the  $\bar{\theta}_A$  value, since all five values are included in the same file.

<b>Xeric, <math>q = 1, k = 0.50</math></b>						
$\bar{\theta}_A:$		<b>0.0</b>	<b>0.1</b>	<b>0.2</b>	<b>0.3</b>	<b>0.4</b>
<i>Constant (Optimized) Interval</i>						
<b>Interval (d)</b>		1.01	4.12	1.09	1.33	1.47
<b>Event Depth (mm)</b>		6.57	27.2	5.46	5.22	3.93
<b>Total (mm/yr)</b>		2377	2408	1825	1435	976
<i>Interval Varies Seasonally</i>						
<b>Intervals (d)</b>	<b>Winter</b>	2.37	11.13	20.43	2.25	4.41
	<b>Spring</b>	1.1	4.32	3.9	1.56	1.18
	<b>Summer</b>	1.15	4.46	4.07	1.78	74.42
	<b>Fall</b>	3.53	12.64	12.71	3.31	3.77
	<b>Event Depth (mm)</b>	7.41	30.37	27.78	6.46	7.44
<b>Total (mm/yr)</b>		1677	1734	1598	1268	920

<b>Mesic, <math>q = 1, k = 0.50</math></b>						
$\bar{\theta}_A:$		<b>0.0</b>	<b>0.1</b>	<b>0.2</b>	<b>0.3</b>	<b>0.4</b>
<i>Constant (Optimized) Interval</i>						
<b>Interval (d)</b>		1.06	26.27	48.72	66.03	59.94
<b>Event Depth (mm)</b>		4.27	102.25	169.54	190.56	128.73
<b>Total (mm/yr)</b>		1473	1422	1272	1055	785
<i>Interval Varies Seasonally</i>						
<b>Intervals (d)</b>	<b>Winter</b>	79.63	84.56	78.41	72.08	60.93
	<b>Spring</b>	20.96	56.82	59.55	67.6	72.11
	<b>Summer</b>	19.97	34.52	52.43	72.2	74.43
	<b>Fall</b>	66.95	61.45	54.31	45.19	23.32
	<b>Event Depth (mm)</b>	7.41	7.41	124.12	185.61	198.42
<b>Total (mm/yr)</b>		1677	1677	1427	1351	1233

Figure 22, which shows the sensitivity in irrigation event depth and annual total to  $k$  and  $q$ , can be created using the script AppendixE/opt\_sched/fig\_qk\_sens.m. Figure 23, which shows the potential water savings of seasonal irrigation, can be created using fig\_savings.m in the same folder. Both of these scripts access similar .txt files in the opt\_sched4 folder, and potential water savings are calculated in the final worksheet of the two Excel files in that folder. Results are summarized in tabular form below.

<b>Annual Irrigation Total, Xeric Site (mm/yr)</b>						
$\bar{\theta}_A$	$q = 1$			$q = 3$		
	$k = 0.25$	$k = 0.50$	$k = 1.00$	$k = 0.25$	$k = 0.50$	$k = 1.00$
<b>0.0</b>	1676	1677	1678	1652	1647	1643
<b>0.1</b>	1789	1734	1640	1701	1480	1242
<b>0.2</b>	1705	1598	1273	1327	1039	720
<b>0.3</b>	1569	1268	822	978	732	429
<b>0.4</b>	1450	920	244	787	505	181

<b>Annual Irrigation Total, Mesic Site (mm/yr)</b>						
$\bar{\theta}_A$	$q = 1$			$q = 3$		
	$k = 0.25$	$k = 0.50$	$k = 1.00$	$k = 0.25$	$k = 0.50$	$k = 1.00$
<b>0.0</b>	1482	1473	1465	1461	1444	1423
<b>0.1</b>	1470	1422	1359	1418	1382	1308
<b>0.2</b>	1385	1272	1041	1337	1216	995
<b>0.3</b>	1267	1055	720	1200	994	445
<b>0.4</b>	1103	785	331	846	523	212

<b>Water Savings with Seasonal Irrigation, Xeric Site (mm/yr)</b>						
$\bar{\theta}_A$	$q = 1$			$q = 3$		
	$k = 0.25$	$k = 0.50$	$k = 1.00$	$k = 0.25$	$k = 0.50$	$k = 1.00$
<b>0</b>	710	700	685	665	719	708
<b>0.1</b>	595	674	262	74	37	-34
<b>0.2</b>	389	227	76	95	62	41
<b>0.3</b>	302	167	18	180	61	3
<b>0.4</b>	97	57	105	89	9	27

<b>Water Savings with Seasonal Irrigation, Mesic Site (mm/yr)</b>						
$\bar{\theta}_A$	$q = 1$			$q = 3$		
	$k = 0.25$	$k = 0.50$	$k = 1.00$	$k = 0.25$	$k = 0.50$	$k = 1.00$
<b>0.0</b>	51	46	43	34	20	4
<b>0.1</b>	78	71	79	46	49	58
<b>0.2</b>	63	39	53	46	31	51
<b>0.3</b>	50	35	95	26	33	-1
<b>0.4</b>	37	62	111	41	6	48

